THE UNIVERSITY OF ALBERTA

LAMINAR FREE CONVECTION FROM A RADIAL ROTATING FIN

by

© RU-SAN R. KO, M.Sc.

A THESIS

SUBMITTED TO THE FACULTY OF GRADUATE STUDIES AND RESEARCH

IN PARTIAL FULFILMENT OF THE REQUIREMENTS FOR THE DEGREE

OF MASTER OF SCIENCE

DEPARTMENT OF MECHANICAL ENGINEERING

EDMONTON, ALBERTA

FALL, 1971

THE UNIVERSITY OF ALBERTA

FACULTY OF GRADUATE STUDIES AND RESEARCH

The undersigned certify that they have read, and recommend to the Faculty of Graduate Studies and Research for acceptance, a thesis entitled, "LAMINAR FREE CONVECTION FROM A RADIAL ROTATING FIN" submitted by RU-SAN R. KO in partial fulfilment of the requirements for the degree of Master of Science.

ABSTRACT

This thesis presents a theoretical investigation of the coupled heat transfer problem of conduction through, and laminar free convection from, a radial triangular fin rotating synchronously with its surroundings at a constant high speed about a horizontal axis.

When the Biot number is assumed to be small and the Prandtl number is of order one, two essential parameters are revealed through an order-of-magnitude analysis. These are the ratio of the fin length to the distance from the fin tip to the center of rotation (γ); and the product of the fin slenderness ratio, the thermal conductivity ratio and the Rayleigh number to the fourth power (C).

The overall problem was solved numerically after a transformation favored by a "local similarity" technique had been applied. The interfacial temperature and heat flux between solid fin and the fluid were successfully matched to a satisfactory degree.

The effects of parameters C and γ on the validity of similarity solutions, Nusselt number, fin effectiveness, and the corresponding boundary layer profiles were studied over the ranges of $0.01 \leq C \leq 10$ and $0 \leq \gamma \leq 0.3$. All the results appear to be interesting and reasonable.

ACKNOWLEDGEMENTS

The author wishes to express the sincere appreciation to the following:

- Prof. G.S.H. Lock for his patient supervision and assistance during the course of this thesis.
- the National Research Council for financial support under grant no. A-1672.
- my wife, Lily, for her understanding during my thesis writing and her patience in typing this thesis.

TABLE OF CONTENTS

		PAGE
CHAPTER I	INTRODUCTION	1
CHAPTER II	THEORETICAL ANALYSIS	5
2.1	BOUNDARY LAYER PROBLEM	5
	2.1-1 MATHEMATICAL FORMULATION	5
	2.1-2 LOCAL SIMILARITY TRANSFORMATION	9
2.2	CONDUCTION PROBLEM OF FIN	10
2.3	MATCHING OF THE COUPLED CONDUCTION AND CONVECTION SYSTEMS	14
CHAPTER III	RESULTS AND DISCUSSION	17
3.1	SOLUTIONS OF CONVECTION PROBLEM	17
	3.1-1 DEPARTURE FROM SIMILARITY	17
	3.1-2 EFFECT OF PARAMETER γ	19
	3.1-3 EFFECT OF PARAMETER C	21
	3.1-4 NUSSELT NUMBER	23
	3.1-5 FIN EFFECTIVENESS ε	27
3.2	SOLUTIONS OF CONDUCTION EQUATION	30
CHAPTER IV	CONCLUSIONS AND RECOMMENDATIONS	39
4.1	CONCLUSIONS	39
4.2	RECOMMENDATIONS	42

PAGE

REFERENCES 44

APPENDIX A NORMALIZATION 46

APPENDIX B LOCAL SIMILARITY TRANSFORMATION 52

APPENDIX C QUASI-ONE-DIMENSIONAL PROBLEM OF FIN 63

APPENDIX D FORMULATION OF THE LIMITING CASE $\gamma = 0$ 69

APPENDIX E NUMERICAL TECHNIQUE 75

LIST OF ILLUSTRATIONS

FIGURE		PAGE
2.1	SYSTEM OF RADIAL ROTATING FIN	6
2.2	DIMENSIONS OF TRIANGULAR FIN	11
3.1	DEPARTURE FROM SIMILARITY	18
3.2	EFFECT OF γ	20
3.3	EFFECT OF C	22
3.4	HEAT TRANSFER RELATION WITH γ AS THE PARAMETER	25
3.5	HEAT TRANSFER RELATION WITH C AS THE PARAMETER	26
3.6	FIN EFFECTIVENESS	28
3.7	EFFECT OF C ON INTERFACIAL TEMPERATURE	31
3.8	EFFECT OF γ ON INTERFACIAL TEMPERATURE	33
3.9	RATE OF CONVERGENCE	35
3.10	INTERFACIAL TEMPERAUTRE PROFILES FOR CHECKING THE POSSIBILITY OF POWER LAW ASSUMPTION, $\phi_0 = x^n$	36
3.11	INTERFACIAL TEMPERATURE PROFILES FOR CHECKING THE POSSIBILITY OF EXPONENTIAL ASSUMPTION, $\phi_0 = e^{mx}$	37

NOMENCLATURE

ξ, x, X	radial distance from fin tip
p, P_d	pressure departure
R	radial distance from axis of rotation
y, Y	lateral distance from fin surface
ξ, η	local similarity variable
u, U	radial velocity
v, V	circumferential velocity
f, ψ	stream function
Φ, ϕ, Θ, T	temperature
ω	angular velocity
A	cross sectional area of fin
L	fin length (radially)
W	root half-width of fin
g	gravitational acceleration
k	thermal conductivity
β	thermal expansion coefficient
ν	momentum diffusivity
κ	thermal diffusivity
c_p	constant pressure specific heat
h	heat transfer coefficient
D	span of fin

t,τ	time
α	angle from vertical line to radial axis in counterclockwise direction
Nu	Nusselt number (hL/k_f)
Ra	Rayleigh number ($\beta\omega^2 R_t \Theta_r L^3/\nu\kappa$)
Pr	Prandtl number (ν/κ)
Bi	Biot number (hW/k_s)
Ek	Ekman number ($\nu/\omega L^2$)
Fr	Froude number ($R_t\omega^2/g$)
Os	Ostrach number ($\beta R_t \omega^2 L/c_p$)
γ	length-radius ratio (L/R_t)
C	dimensionless group ($Ra^{1/4} Lk_f/Wk_s$)

SUBSCRIPTS

0	fin
r,t	fin root, tip
∞	outside boundary layer
f,s	fluid, solid
y,x	differentiation with respect to y, x
'	differentiation with respect to η

CHAPTER I

INTRODUCTION

Free convection phenomena arise in a non-isothermal fluid because of body forces which generate a density difference. For example, when a vertical surface generates a lateral temperature gradient in its surrounding fluid, a boundary layer forms adjacent to the surface.

Although many papers have dealt with steady laminar free convection from a vertical wall subjected to a parallel uniform body force field, only those solutions with similarity characteristics have been intensively worked out, e.g., references [1-5]*. It was analyzed in Yang's work [4] that similarity solutions are possible only when the wall temperature distribution satisfies some prescribed forms. In fact, similarity solutions are very special cases in the physical world. When the wall temperature profile does not exhibit similarity forms, the partial differential equations governing the boundary layer system can no longer be transformed into ordinary differential forms. Hence non-similar problems, which are much more difficult to solve, are encountered.

Obviously, instead of a uniform body force (such as gravity), free convection can also be induced by centrifugal and Coriolis forces. Although Kreith [6] gave a detailed review of many papers on convective heat transfer in rotating systems, very few publications of laminar free convection problems on a vertical surface rotating synchronously with

---

* Numbers designate references given on page 44

surroundings are available. In 1963 and 1964, Lemlich and co-workers [7-9] investigated the problem of an isothermal cold plate rotating with its leading edge at the center of rotation. Meanwhile, Catton [10] applied an integral technique to the rotating isothermal plate problem (with large Prandtl number) but shifting the leading edge to a certain distance from the center of rotation. It was not until 1969, that a similarity solution of the former cold plate problem was presented by Manoff and Lemlich [11].

It should be noticed that these cold rotating plate problems contain a tacit assumption, i.e., the gravitational field does not exist. Without this assumption, the gravitational force will periodically affect the system in the vicinity of the center of rotation, a horizontal axis, and no leading edge of a steady boundary layer can take place. Hence, only Catton's attempt of shifting the leading edge from the center of rotation appears justifiable to the problems under the simultaneous influence of gravitational force.

From the practical viewpoint, the heat transfer from a hot surface is more significant than from a cold surface. The application of thermal fins to increase the cooling rate of a heated body is a good example. In a uniform body force field parallel to the vertical surface, the physical phenomenon of a hot plate can easily be simulated from the study of a cold plate (and vise versa) by choosing the opposite end of the plate as the leading edge and reversing the longitudinal axis. However, when the body force is non-uniform, this "reversibility" can

not hold anymore. As an example, a heated radial fin spinning together with its surroundings about a horizontal axis in a gravitational field is somewhat different from the aforementioned cold rotating plate problem. Besides the fact that a stable leading edge can now form at the tip of the thermal fin, two substantial differences are:

(1) the centrifugal force decreases linearly along the flow direction, whereas it increases in the cold rotating plate problem.

(2) the similarity assumption of the cold plate temperature distribution may not satisfy the surface temperature of a rotating fin heated at the root, since the boundary layer problem is always coupled with the conduction problem in the fin.

The first difference between these two problems results in a radical difference in the equations of motion, while the second gives rise to a problem of interfacial temperature and heat flux matching.

In 1968, when Lock and Gunn [12] presented the similarity solution of a tapered fin parallel with uniform body force, the interfacial temperature between the solid and liquid was matched by imposing the similarity assumption of the boundary layer problem upon the quasi-one-dimensional conduction equation of the fin. The matched solutions were still constrained to the limited case of power law temperature distributions along the fin. A coupled heat transfer problem without power law restriction on the solution was studied by Kelleher and Yang [13].

In that work, the two-dimensional conduction problem was treated analytically with Fourier transforms and the boundary layer problem was solved with Görtler-type series. Though the interfacial temperature and heat flux were formally matched by comparing the series solutions, their non-similarity results were stated to be valid only near the leading edge.

In the present analysis, the steady coupled heat transfer problem of a heated radial fin rotating simultaneously with the ambient air is studied. The fin is located at a certain distance from the center of rotation so that the centrifugal acceleration can override the periodically changing effect of gravitational force. One can verify with an order of magnitude that the Coriolis force effect along the flow direction becomes negligible when the rotating speed is high, and hence the centrifugal force dominates the overall region of interest.

A suitable transformation is then introduced so that the coupled governing equations can be solved numerically with a "local similarity" technique [17]. The matching problem of interfacial temperature and heat flux is thoroughly resolved in a few iterative loops.

CHAPTER II

THEORETICAL ANALYSIS

2.1 BOUNDARY LAYER PROBLEM

Laminar free convection from an outward-projecting fin in a centrifugal force field is studied theoretically for an arbitrary surface temperature increasing monotonically from the tip to the root.

2.1-1 MATHEMATICAL FORMULATION

The system of coordinates is displayed in figure (2.1). To make the problem mathematically tractable, the following assumptions were made:

(1) The fluid is Newtonian.

(2) The flow is laminar.

(3) The fluid is mechanically incompressible.

(4) The flow is two dimensional.

(5) Fluid properties, except density in the buoyancy effect, are constant.

(6) There is no heat generation.

(7) The fluid is assumed to be of sufficient extent that wall effects are insignificant.

(8) Radiation is neglected.

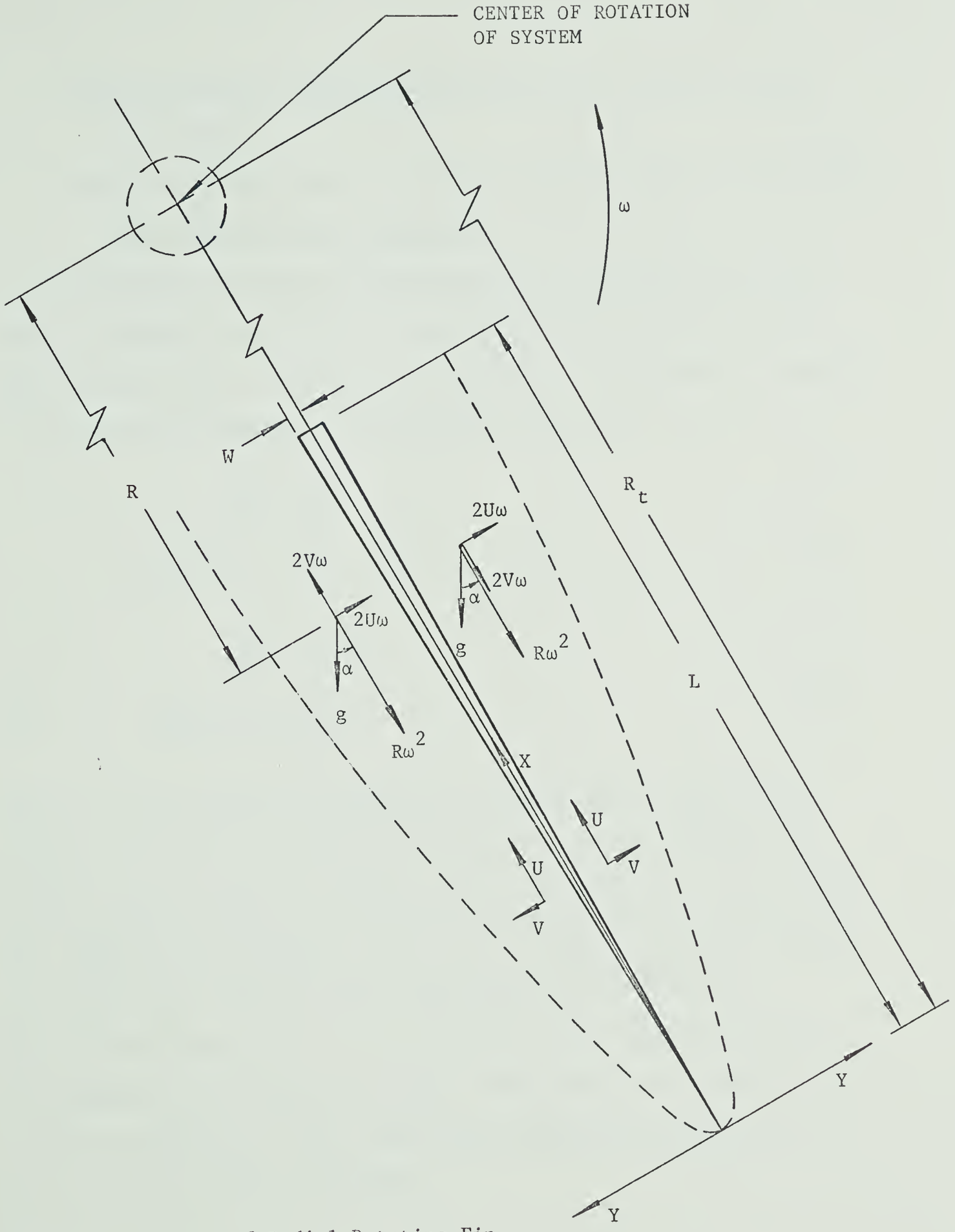

Figure 2.1 System of Radial Rotating Fin

(9) The mechanical work against the body force field is assumed to be small.

(10) The fin slenderness is so large that the effect of inclination and curvature become negligible.

Through the processes of normalization and ordering, it has been shown in appendix A that for air, the problem becomes quasi-steady at high rotating speed. By referring to equations (A.16)-(A.20) in appendix A, the governing equations in dimensionless form are

$$\frac{\partial u}{\partial x} + \frac{\partial v}{\partial y} = 0 \tag{2.1}$$

$$\frac{1}{Pr}\left(u\frac{\partial u}{\partial x} + v\frac{\partial u}{\partial y}\right) = \frac{\partial^2 u}{\partial y^2} + (1 - \gamma x)\phi \tag{2.2}$$

$$\frac{\partial p}{\partial y} = -2\lambda u\phi \tag{2.3}$$

and

$$u\frac{\partial \phi}{\partial x} + v\frac{\partial \phi}{\partial y} = \frac{\partial^2 \phi}{\partial y^2} \tag{2.4}$$

where $\lambda = -1$ or $+1$ for the trailing and leading faces, respectively. Equation (2.3) indicates that the Coriolis force merely induces the lateral pressure gradient in this problem. Since the pressure term has been suppressed from equation (2.2), one can find the pressure distribution without any difficulty once the profiles of u and ϕ are at hand. Hence equation (2.3) can be ignored in this problem unless one is interested in the pressure profile. Hereinafter, the problem treated is that of solving the other three partial differential equations with the associated boundary conditions:

$$
\begin{array}{lll}
x = 0 \ ; & u = 0 & \phi = 0 \\
y = 0 \ (x \geq 0) \ ; & u = v = 0 & \phi = \phi_0(x) \\
y = \infty \ ; & u = 0 & \phi = 0
\end{array}
\qquad (2.5)
$$

Looking at the overall problem of a fin heated at its root, the surface temperature $\phi_0(x)$ is normally fixed. There is no point in obtaining similarity solutions, even if there are any, of the boundary layer problem by forcing oneself to prescribe a specific form of this interfacial temperature. In other words, a scheme for obtaining more general results than similarity solutions is required.

The "local similarity" concept [17] suggests that the whole region can be discretized along the longitudinal direction into parallel levels. At each level, the integration is carried out laterally across the boundary layer while the longitudinal derivatives in the governing equations are approximated with finite differences. In this way, it is not necessary to specify the interfacial temperature $\phi_0(x)$ in any restricted form of x. On the contrary, ϕ_0 can be an arbitrary set of discrete values increasing monotonically from the tip. The flexibility of these discrete values is very advantageous to the problem of matching when the iterative method is applied in a numerical program as will be seen later.

2.1-2 LOCAL SIMILARITY TRANSFORMATION

A stream function $\psi(x,y)$ is defined by the relations

$$u = \frac{\partial \psi}{\partial y} \quad , \qquad v = - \frac{\partial \psi}{\partial x} \quad , \tag{2.6}$$

and equation (2.1) is automatically satisfied. In consequence of removing the singularity due to $\phi_0(0) \doteq \phi(0,0)$, see appendix B, the "local similarity" concept leads to the following transformation:

$$\xi = \gamma x \tag{2.7}$$

$$\eta = \gamma \frac{d}{d\xi}\left[\frac{4}{3\gamma}\int_0^{\xi} G_0{}^{1/3}(S)dS\right]^{1/4} y \tag{2.8}$$

$$f(\xi,\eta) = \left[\frac{4}{3\gamma}\int_0^{\xi} G_0{}^{1/3}(S)dS\right]^{-3/4} \psi(x,y) \tag{2.9}$$

$$\Phi(\xi,\eta) = G_0{}^{-1}(\xi)\ \phi(x,y) \tag{2.10}$$

where $$G_0(\xi) = \phi_0(x). \tag{2.11}$$

As outlined in appendix B, using equation (2.6) and the "local similarity transformation", equations (2.2) and (2.4) yield

$$\Pr\,(f''' + \Phi) + ff'' - \frac{2}{3}(f')^2 = -\frac{4}{3}\left[\frac{dG_0{}^{-1/3}(\xi)}{d\xi}\int_0^{\xi} G_0{}^{1/3}(S)dS\right](f')^2$$

$$+ \frac{4}{3}\left[G_0{}^{-1/3}(\xi)\int_0^{\xi} G_0{}^{1/3}(S)dS\right]\left(f'\frac{\partial f'}{\partial \xi} - f''\frac{\partial f}{\partial \xi}\right) + \Pr \xi \Phi \ , \tag{2.12}$$

and

$$\Phi'' + f\Phi' = -4\left[\frac{dG_0{}^{-1/3}(\xi)}{d\xi}\int_0^{\xi} G_0{}^{1/3}(S)dS\right] f'\Phi$$

$$+ \frac{4}{3}\left[G_0{}^{-1/3}(\xi)\int_0^{\xi} G_0{}^{1/3}(S)dS\right]\left(f'\frac{\partial \Phi}{\partial \xi} - \Phi'\frac{\partial f}{\partial \xi}\right), \tag{2.13}$$

where the primes denote partial differentiations with respect to η.

In the right-hand-sides of equations (2.12) and (2.13), each coefficient is a function of ξ, if the ξ-derivatives are replaced by finite differences, these two equations become ordinary differential equations for each specific value of ξ and a "local similarity" problem is in hand. Provided that the derivatives of f and Φ are finite and $\frac{dG_0}{d\xi}^{-1/3}$ is bounded at the leading edge, the right-hand-sides of equations (2.12) and (2.13) vanish as $\xi = 0$. With the associated boundary conditions:

$$\eta = 0 \quad ; \quad f = f' = \Phi - 1 = 0 \quad ,$$

$$\eta = \infty \quad ; \quad f' = \Phi = 0 \quad ,$$

there is no difficulty in starting the integration. The solution of these equations along $\xi = 0$ will give the "initial" values of this boundary layer problem.

2.2 CONDUCTION PROBLEM OF FIN

Heat transfer within a fin is demonstrated in appendix C to be a quasi-one-dimensional conduction problem when the Biot number (Bi) is much less than order one.

The basic notation and scheme of coordinates of this triangular fin problem are shown in figure (2.2).

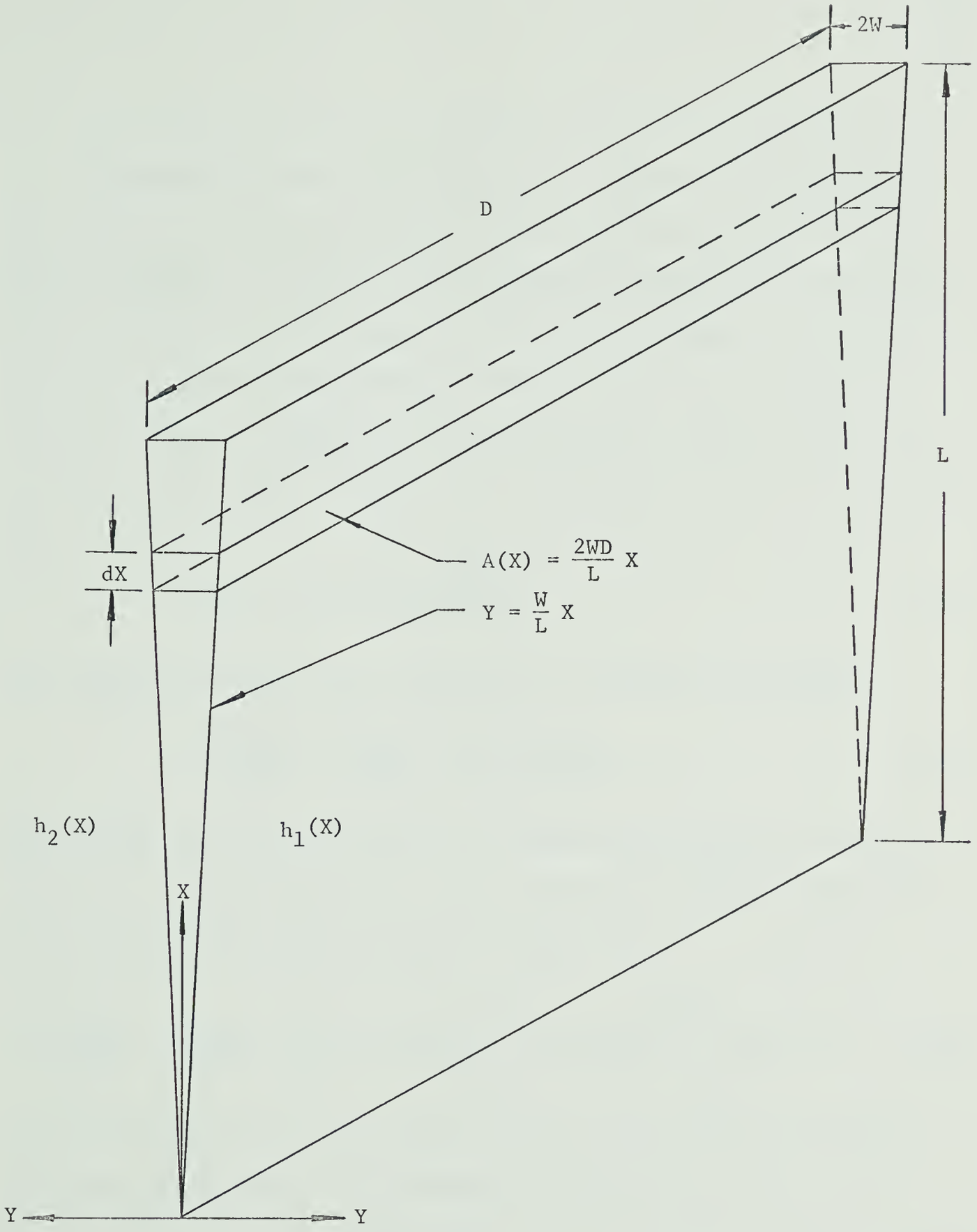

Figure 2.2 Dimensions of Triangular Fin

In addition to the assumption of Bi << O[1], it will be assumed that there is no heat generation in the fin and the properties of the fin are constant. From the order-of-magnitude procedure in the boundary layer problem, it is known that at high rotating speeds, the temperature as well as the velocity profiles of boundary layer flow are symmetric about the X-axis. Therefore, the convective heat transfer coefficients $h_1(X)$ and $h_2(X)$, shown in figure (2.2), are equal and can be represented by

$$h_1(X) = h_2(X) = \frac{-K_f \dfrac{\partial T(X,0)}{\partial Y}}{T_0(X) - T_\infty} \quad . \tag{2.14}$$

The temperature $T_0(X)$ of the triangular fin satisfies the equation

$$X \frac{d^2T_0(X)}{dX^2} + \frac{dT_0(X)}{dX} + \frac{L}{W}\frac{K_f}{K_s}\frac{\partial T(X,0)}{\partial Y} = 0 \quad . \tag{2.15}$$

Normalizing this equation with those characteristic values obtained in appendix A and introducing the "local similarity transformation" yield a nonlinear ordinary differential equation, i.e.

$$\xi \frac{d^2G_0(\xi)}{d\xi^2} + \frac{dG_0(\xi)}{d\xi} + \left[C\Phi'(\xi,0)\frac{d}{d\xi}\left(\frac{4}{3\gamma}\int_0^\xi {G_0}^{1/3}(S)dS\right)^{3/4}\right] G_0(\xi) = 0 \tag{2.16}$$

where $\Phi'(\xi,0)$ is one of the eiganvalues from the solution of the boundary value problem and C is a parameter, defined [12] as

$$C = \frac{L}{W}\frac{K_f}{K_s} Ra^{1/4} \quad . \tag{2.17}$$

It is clear that one of the boundary conditions for this second-order differential equation (2.16) is

$$G_0(\gamma) = 1$$

at the root of the fin. The other boundary condition needs more consideration. It is shown in appendix C that when the slenderness ratio $\frac{L}{W}$ is much larger than order one, either

$$G_0(0) = 0 \quad \text{or} \quad \frac{dG_0(0)}{d\xi} = 0$$

is a good approximation to the boundary condition at the tip. In view of the generality of the problem, it is undesirable to be constrained to the case of a very thin fin. A boundary condition which is also realistic to a triangular fin with smaller slenderness is required.

Equation (2.16) can be rewritten as

$$\frac{d}{d\xi}\left(\xi \frac{dG_0(\xi)}{d\xi}\right) + \left[C\Phi'(\xi,0) \frac{d}{d\xi}\left(\frac{4}{3\gamma}\int_0^{\xi} {G_0}^{1/3}(S)dS\right)^{3/4}\right] G_0(\xi) = 0 \qquad (2.18)$$

and it can be regarded as a first-order nonlinear equation in $\xi\frac{dG_0}{d\xi}$, and therefore one boundary condition on this variable is sufficient. Since $\xi\frac{dG_0}{d\xi}$ indicates the total amount of heat conducted across the fin section at a distance ξ from the tip, it tends to zero as the area of the cross-section becomes zero at the tip. Hence $\xi\frac{dG_0}{d\xi} = 0$ at the tip can be the boundary condition of equation (2.18). Once the solution of $\xi\frac{dG_0}{d\xi}$ is obtained, $G_0 = 1$ can be used as the boundary condition at the root for further integration in obtaining G_0.

2.3 MATCHING OF THE COUPLED CONDUCTION AND CONVECTION SYSTEMS

The whole problem has been shown to be governed by two boundary layer equations, (2.12) and (2.13), and one conduction equation, (2.18). All these three governing equations are mutually coupled. The interfacial heat flux between solid fin and fluid has been expressed in equation (2.14) and in succession equations (2.16) and (2.18) were formed. Hence the only interfacial matching left to be done is on the temperature, i.e., the assumed wall temperature $G_0(\xi)$ of the boundary layer problem must satisfy the conduction equation of the fin and its associated boundary conditions.

As was stated before, $G_0(\xi)$ is a fixed but unknown wall temperature, and therefore a logical way of solving this problem is to discretize the ξ-coordinate into certain levels and assume a set of values for $G_0(\xi)$ at these levels. These assumed values decrease monotonically from $G_0(\gamma) = 1$ to $G_0(0) \geq 0$. By means of this initial guess, the three aforementioned coupled equations can be solved to give a new set of values for $G_0(\xi)$. After comparison and modification, convergence of this interfacial temperature $G_0(\xi)$ to a unique distribution can be procured through an iterative method.

The numerical technique is too lengthy to be presented in this section and its details are described in appendix E: only the outlined procedures are given in sequence:

(1) With the initial set of $G_0(\xi)$ as an input to the boundary layer problem, equations (2.12) and (2.13) can be solved simultaneously at each ξ-level where finite difference approximations replace the ξ-derivatives. The integrations in the η-direction are carried out with a fourth-order Runge-Kutta method and convergence is obtained by means of the technique developed by Nachtsheim and Swigert [14].

(2) Once the boundary layer problem has been solved, the eiganvalues $\Phi'(\xi,0)$ at each level are known and can be substituted into equation (2.18). The bracketed group in this equation represents the convective heat transfer coefficient $h(G_0,\xi)$. In order to circumvent the non-linearity of this equation, the assumed $G_0(\xi)$ distribution is used in calculating this coefficient. A fourth-order Runge-Kutta method is then employed to integrate equation (2.18) from the root to give $G_0(\xi)$ and $\xi\frac{dG_0}{d\xi}$ at each level except the leading edge, because of a singularity. This latter difficulty is overcome when $G_0(\xi)$ is obtained by integrating equation (2.16) simultaneously with equation (2.18). The integration starts with the boundary condition $G_0(\gamma) = 1$ and a guessed value of $\xi\frac{dG_0}{d\xi}\Big|_{\xi=\gamma}$ which is gradually modified by means of a shooting method until the other boundary condition $\xi\frac{dG_0}{d\xi}\Big|_{\xi=0} = 0$ is satisfied within an error less than 10^{-5}.

(3) A new $G_0(\xi)$ is now obtained by halving the two most recent solutions and is substituted into the bracketed groups of equations (2.16) and (2.18) to calculate a new set of $h(G_0,\xi)$. The iteration continues until $G_0(\xi)$ has converged satisfactorily for the same input values of $\Phi'(\xi,0)$.

(4) This converged $G_0(\xi)$ is regarded as a better input to the boundary layer problem and the whole procedures starts all over again. Iteration between the conduction and convection systems stops when the normalized interfacial temperature $G_0(\xi)$ has converged at every point to within an error of less than 10^{-10}. Since the temperature distribution $G_0(\xi)$ is obtained and the interfacial heat flux is matched automatically, the problem is completely solved.

CHAPTER III

RESULTS AND DISCUSSION

Throughout the study, all the calculations are based on taking air as the fluid and 0.72 as its Prandtl number. By referring to the governing equations (2.12), (2.13), (2.16) or (2.18) and their associated boundary conditions, it is evident that C and γ are the principal parameters of this rotating radial fin problem. In this study, solutions are developed with four values of γ (0, 0.1, 0.2 and 0.3) and six values of C (0.01, 0.1, 1.0, 3.0, 5.0 and 10.0). Matched results can be separated into two parts: convection and conduction.

3.1 SOLUTIONS OF CONVECTION PROBLEM

In a boundary layer problem, interest most often rests in the velocity and temperature profiles of the fluid. In addition, the Nusselt number and fin effectiveness are also worth investigating from a heat transfer point-of-view.

3.1-1 DEPARTURE FROM SIMILARITY

Temperature and velocity profiles at three ξ levels along a rotating fin with $C = 1.0$ and $\gamma = 0.3$ are shown in figure (3.1). If similarity existed, all the velocity profiles would overlap, as would the temperature profiles. However, figure (3.1) shows that the departure from similarity is quite significant in velocity but not in temperature. Hence, considering the heat transfer rate from a rotating fin

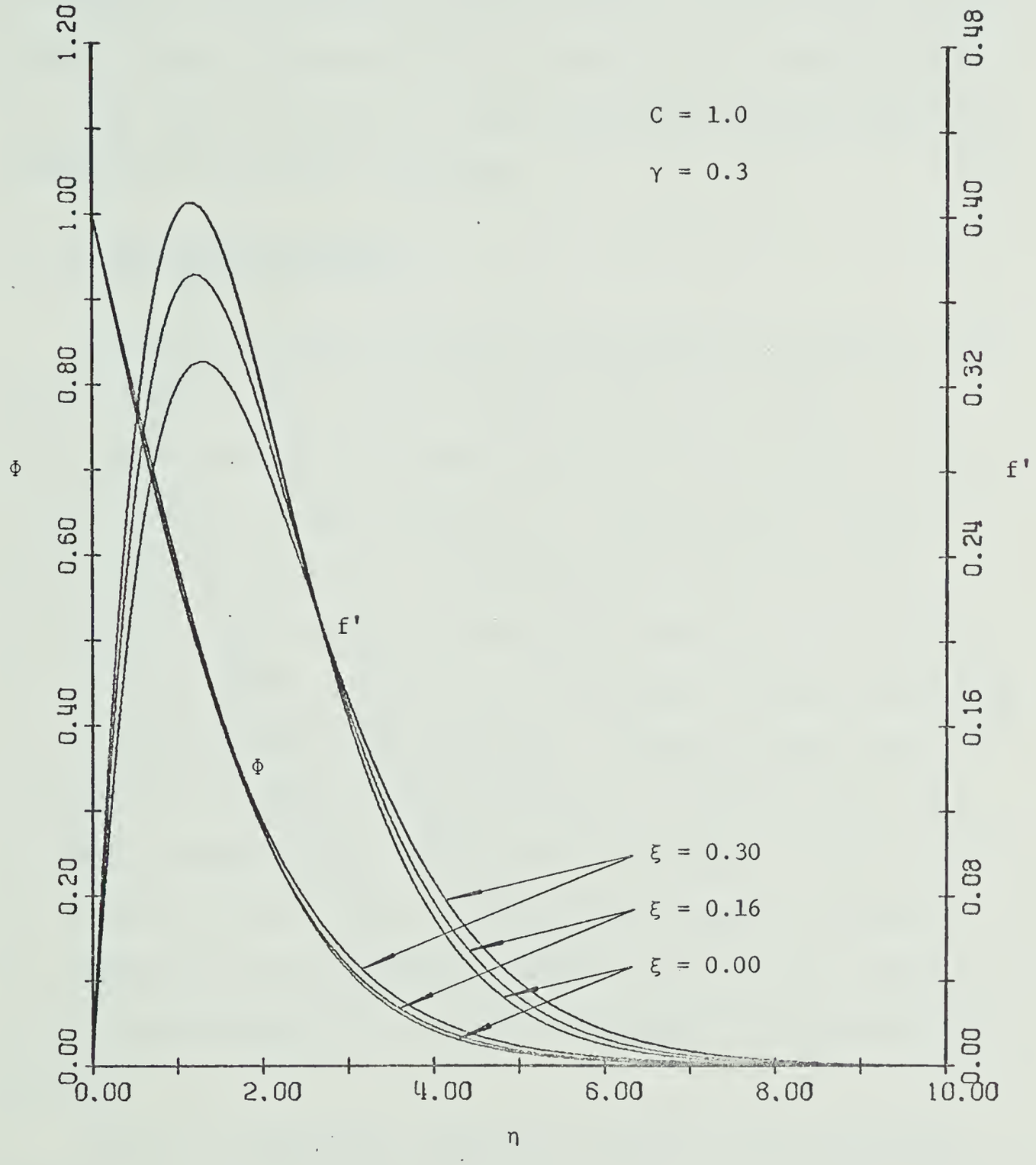

Figure 3.1 Departure from Similarity

with small γ, the similarity solution obtained locally at the leading edge provides a good approximation. This may not be suitable when γ is large, since the variation between temperature profiles appears to increase as ξ (through γ) increases.

3.1-2 EFFECT OF PARAMETER γ

Figure (3.2) shows the velocity and temperature profiles at the root of the fin, i.e., $x = 1.0$, for four values of γ with $C = 1.0$. It is obvious that the temperature profiles are less sensitive than velocity profiles to the variation of γ. Attention must be paid to the limiting case of $\gamma = 0$. As γ tends to zero, the body force approaches a constant value and the problem becomes that of a static fin. In other words, the case of $\gamma = 0$ simulates a downward-projecting fin in a gravitational force field [12]. Appendix D presents the formulation of the governing equations when $\gamma = 0$, and shows that non-similarity normally exists for this static fin problem. Only in the very special case when $C = 0$ and an isothermal surface is formed is the similarity solution possible. Since $C = 1.0$ is chosen in this figure, the presented profiles with $\gamma = 0$ are the local similarity solutions.

Again, the temperature profiles may deviate significantly from those with $\gamma = 0$ when the value of γ approaches unity; likewise for the velocity profiles.

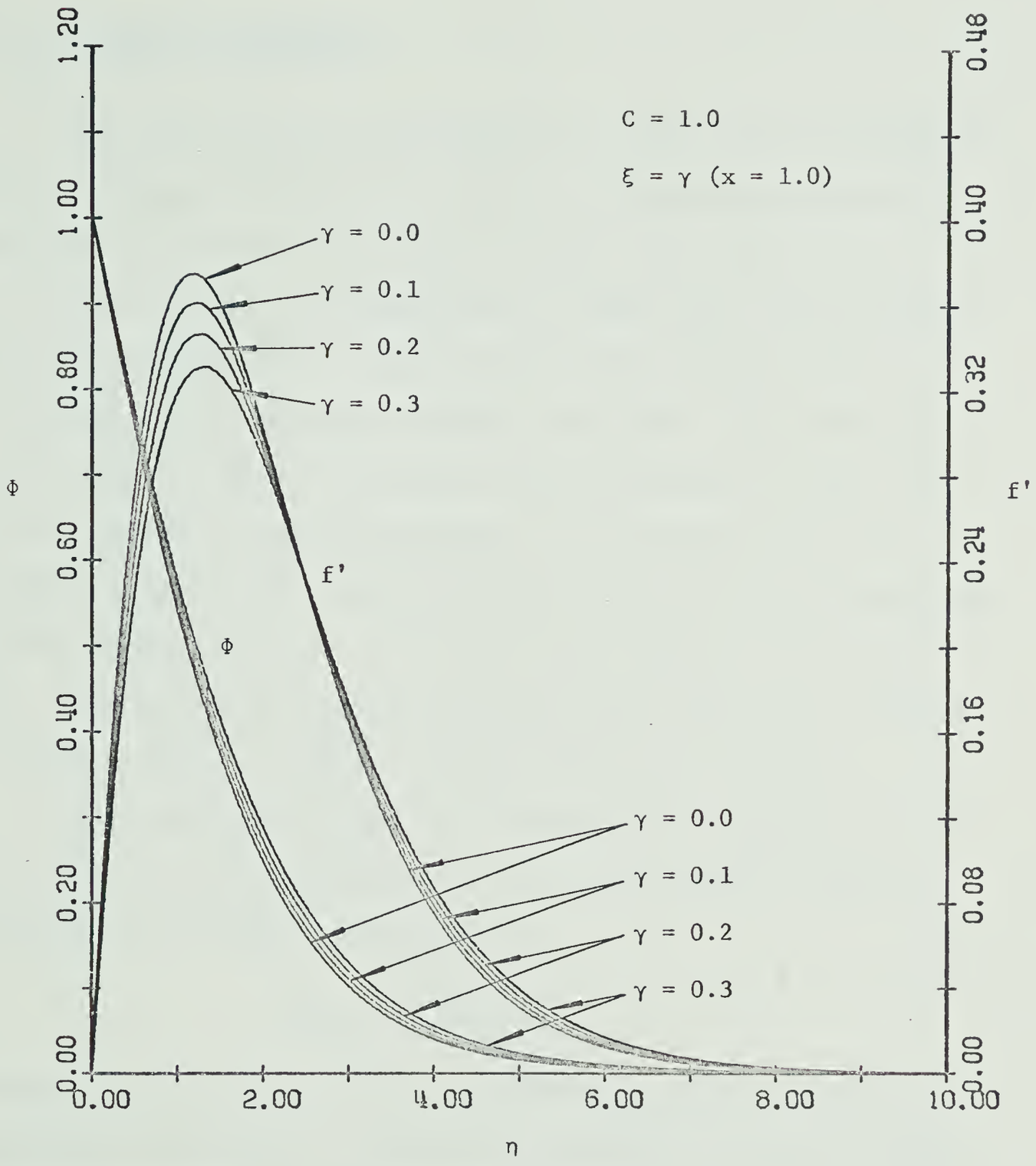

Figure 3.2 Effect of γ

3.1-3 EFFECT OF PARAMETER C

This effect has been investigated over three orders-of-magnitude for C. Salient changes in both velocity and temperature profiles at the root of the same fin are shown in figure (3.3), where $\gamma=0.3$. It can be seen that as the magnitude of C gets smaller, both profiles approach asymptotically to those for C=0: this evidently occurs in the vicinity of the presented profiles with C=0.01. Such asymptotic behavior is very useful in practice because whenever C is small, the result for C=0 is a good approximation. It is shown at the end of appendix D that the fin temperature $G_0(\xi)=1$ when C=0, and the matching problem no longer exists. Certainly, such a limiting solution for free convection from an isothermal surface takes less effort and time to attain, and is a convenient approximation when C is small.

It is worth noting again that the magnitude of parameter C depends on the fin slenderness, the conductivity ratio of fluid to solid and the Rayleigh number defined by

$$Ra = \frac{\beta R_t \omega^2 \Theta_r L^3}{\nu \kappa} .$$

Clearly, the variation of C may represent many possible situations. However, if all but one of the component parameters of C are regarded as fixed, the effect of each component parameter can be investigated separately through the effect of C. For example, it appears in figure (3.3) that the temperature profiles in the vicinity of the wall are more declivous for larger values of C. This behavior implies that the

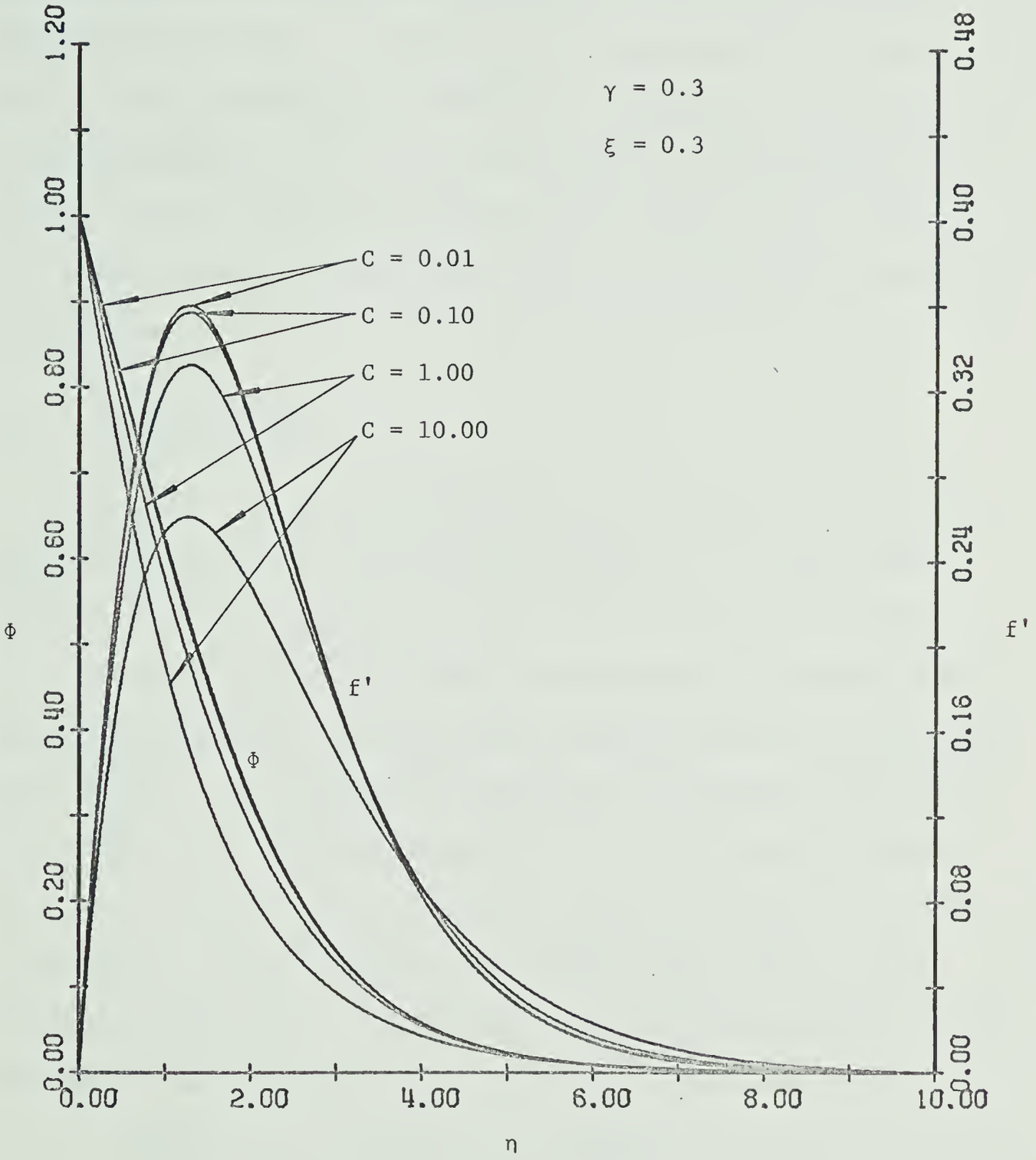

Figure 3.3 Effect of C

heat transfer can be increased by means of a longer fin, or with a good conductive fluid. In addition, this heat transfer can also increase with the temperature difference between the root and the surrounding fluid, or with the rotating speed. As C increases, it appears that the temperature boundary layer becomes thinner while the momentum boundary layer becomes thicker and the velocity profile flattens out.

3.1-4 NUSSELT NUMBER

It is well known that when free convection alone is considered, the Nusselt number for a vertical plate problem in a uniform gravitational field is a function of Grashof number and Prandtl number, e.g., reference [1]. In this study, consideration is extended to the interfacial temperature and heat flux matching problem in a centrifugal force field. It is reasonable to expect that the Nusselt number will be a function of additional parameters, which enter into the problem as a result of either the inclusion of conduction or the introduction of rotation. From the analysis, it is clear that C and γ are the additional parameters. Alternatively, the local Nusselt number at the root of the fin is defined as

$$Nu = \frac{h(L)\ L}{K_f} = \frac{-Ra^{1/4}}{\left[\frac{4}{3\gamma}\int_0^{\gamma} {G_0}^{1/3}(S)dS\right]^{1/4}} \frac{\partial\Phi(\gamma,0)}{\partial\eta} \quad . \tag{3.1}$$

Since in this study, both $G_0(\xi)$ and $\frac{\partial\Phi(\gamma,0)}{\partial\eta}$ are functions of γ and C

for air, one can assume that $Nu/Ra^{1/4}$ is a function of γ and C as well, i.e.,

$$Nu/Ra^{1/4} = F(C,\gamma).$$

The parameter $Nu/Ra^{1/4}$ is given as a function of C for various values of γ in figure (3.4). Just as predicted in section 3.1-4, the increase of C due to the variations of its "sub-parameters" can improve the heat transfer and hence increase the Nusselt number. A more interesting heat transfer relation appears in figure (3.5) where $Nu/Ra^{1/4}$ is plotted against γ at six different values of C. Least-squares lines, with a maximum error less than 1%, suggest that $Nu/Ra^{1/4}$ changes linearly with the parameter γ. Therefore, $Nu/Ra^{1/4}$ can be expressed by

$$\frac{Nu}{Ra^{1/4}} = F_1(C)-F_2(C)\gamma, \qquad (3.2)$$

where functions F_1 and F_2 increase with the parameter C. The magnitudes of F_1 and F_2 at six C levels are presented in table below:

C	F_1	F_2
0.01	0.389	0.116
0.10	0.401	0.126
1.00	0.484	0.178
3.00	0.573	0.205
5.00	0.623	0.214
10.00	0.696	0.228

TABLE I

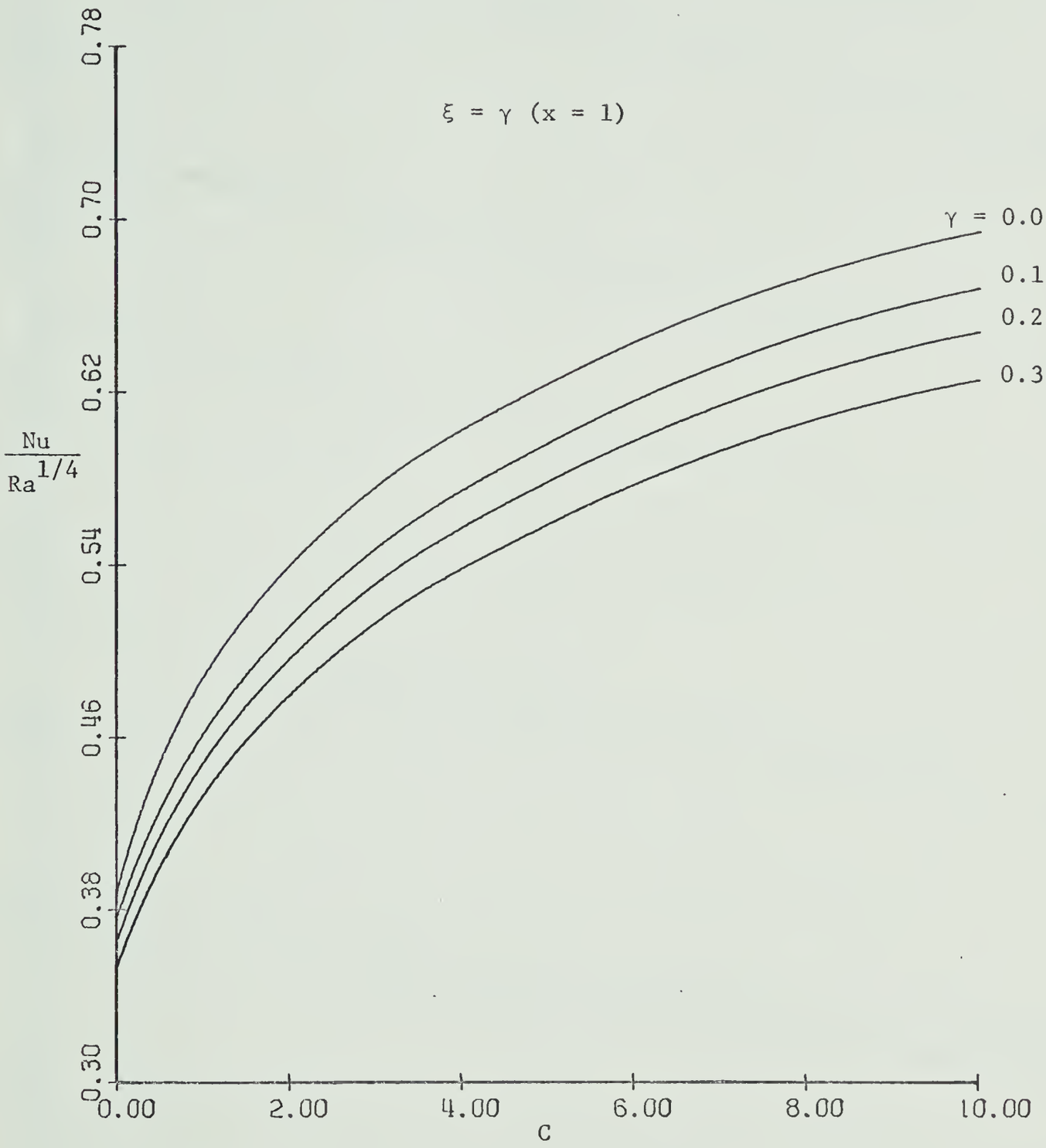

Figure 3.4 Heat Transfer Relation with γ as the Parameter

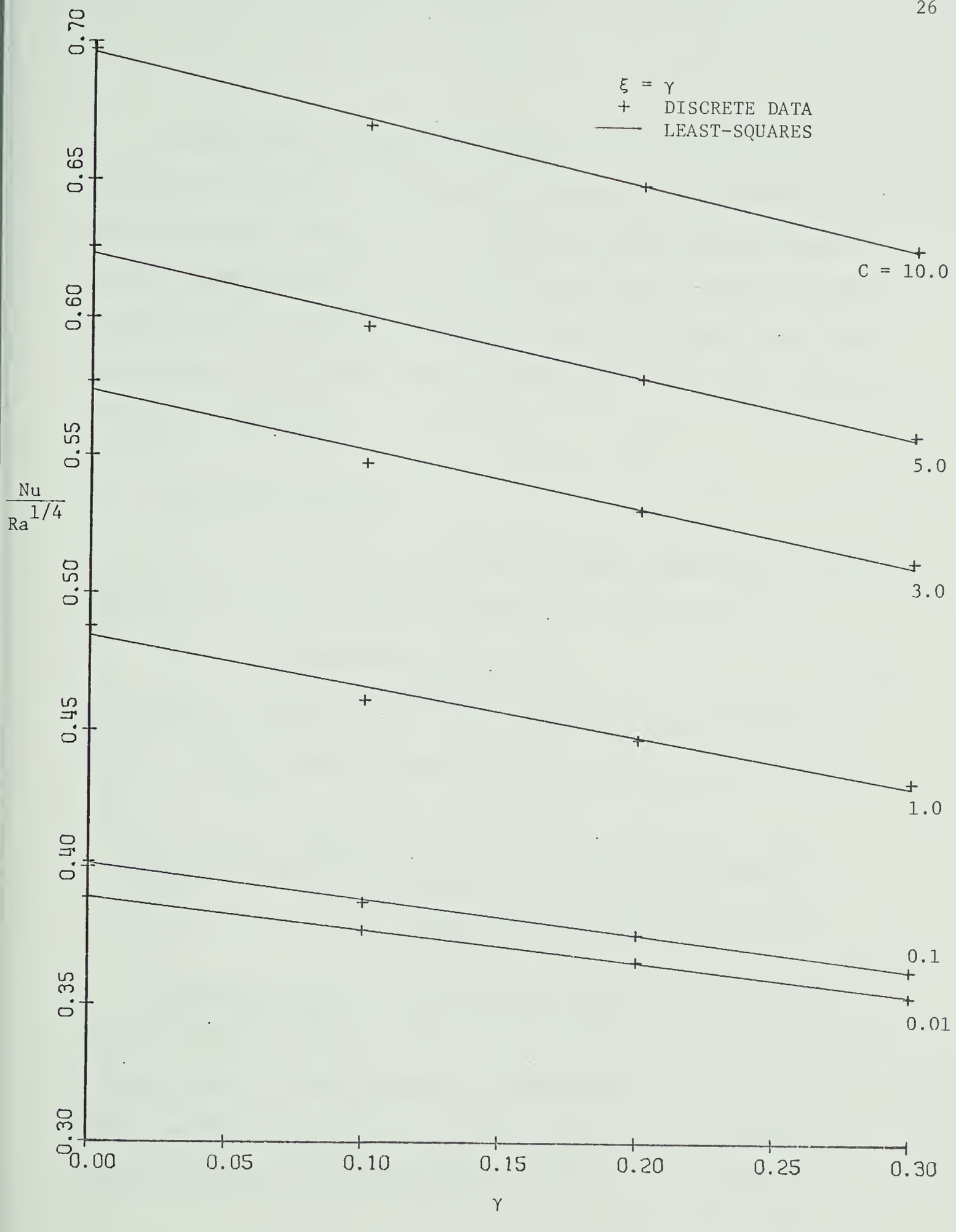

Figure 3.5 Heat Transfer Relation with C as the Parameter

Though values of $Nu/Ra^{1/4}$ for $\gamma>0.3$ were not obtained, one can confidently extrapolate the curves in figure (3.5): this would not have been said of figure (3.4). How far they can be extrapolated is certainly unknown, but they can not go beyond $\gamma=1$. Considering this limiting case of γ approaching unity, the extrapolations using table I and equation (3.2) always indicate non-negative heat transfer which is physically consistent.

3.1-5 FIN EFFECTIVENESS ε

The fin effectiveness for a heat transfer coefficient h varying along the fin surface has been defined in reference [12] as

$$\varepsilon = \int_0^L h(X)\theta_0(X)dX \Big/ h(L)\theta_r L \quad . \tag{3.3}$$

To express ε in terms of the normalized and transformed functions and variables, use is made of equations (2.7), (2.8), (2.10) and (2.11). Thus

$$\varepsilon = \frac{\left[\frac{4}{3\gamma}\int_0^\gamma G_0^{1/3}(\xi)d\xi\right]^{1/4}\int_0^\gamma G_0^{2}(\xi)\Phi'(\xi,0)\,\frac{d}{d\xi}\left[\frac{4}{3\gamma}\int_0^\xi G_0^{1/3}(S)dS\right]^{3/4}d\xi}{\Phi'(\gamma,0)} \quad . \tag{3.4}$$

Calculated values of ε for different ratios γ are plotted in figure (3.6) as a function of C. The approximate solution of reference [12] is also presented as a comparison to the static fin case when $\gamma\to 0$. It should be noted that no curve has intersected the coordinate of C=0: the minimum value of C used for each solid line

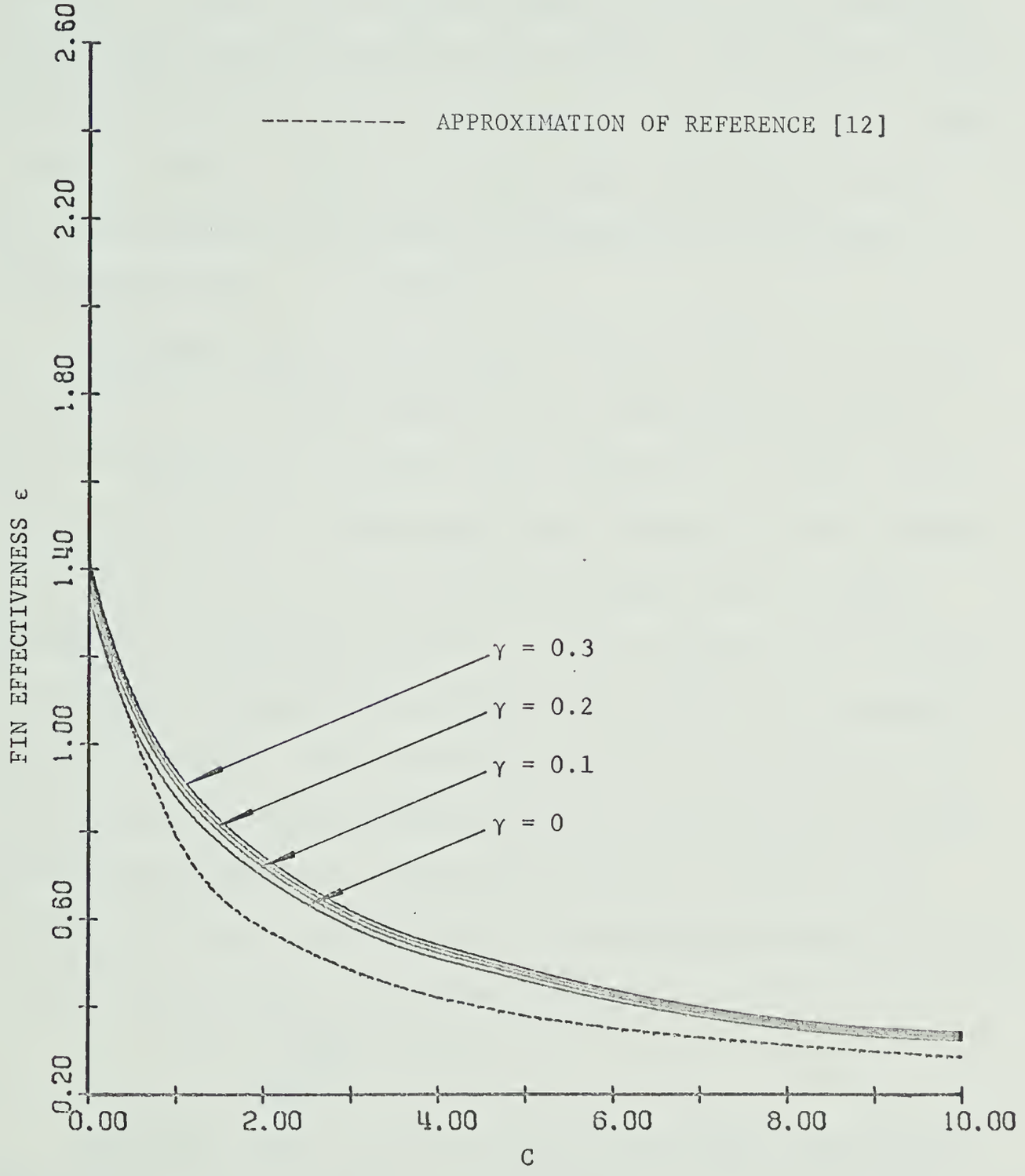

Figure 3.6 Fin Effectiveness

was 0.01. However, the fin effectiveness for C=0 can be predicted if the curves are extrapolated to the ordinate. The value of ε with C=0 is the fin effectiveness of an isothermal fin with $K_f = \infty$. This value of ε does not apply to the case where $K_s=0$ or $\theta_r=0$, since both the numerator and denominator of definition (3.3) vanish (appendix D); hence ε is undefined.

In figure (3.6), the effect of C is again shown to be greater than that of γ. At first glance, it may seem surprising that the fin effectiveness can be greater than unity when C is small. After the definition of ε is investigated more closely, it is not unreasonable to expect such a result. When C is small, the fin surface approaches an isothermal condition. In the definition (3.3), h(L) is no longer the maximum value of h(X) and the ratio ε can certainly be greater than unity. More convincing arguments can be obtained from the well known isothermal surface problem in a uniform gravitational field which simulates the case of γ=0 when C=0. By means of the ordinary similarity transformation for an isothermal surface [1,3,4,5], ε can be calculated from definition (3.3):

$$\varepsilon = \int_0^1 \frac{dx}{x^{1/4}} = \frac{4}{3} > 1.0 \quad .$$

Apparently, this is another check on the present study, since when the curve of γ=0 extends to the C=0 axis, it just meets this analytically obtained value of ε. As a matter of fact, the fin effectiveness ε of reference [12] is

$$\varepsilon = \frac{4}{5n+3}$$

where n is the index of the power law surface temperature distribution. An isothermal fin (C = n = 0) thus yields

$$\varepsilon = 4/3 \ .$$

That is, in this isothermal case, the predictions of both studies become coincident.

3.2 SOLUTIONS OF CONDUCTION EQUATION

As stated before, the interfacial heat flux between solid and fluid has been matched automatically in the formulation of the fin equation. Hence, only the interfacial temperature needs attention and investigation. Since the fin equation is of quasi-one-dimensional form as Bi<<O[1], its solutions are, in fact, the matched interfacial temperature profiles.

Figure (3.7) shows the salient effect of the parameter C on the matched surface temperature profile. One important point must be mentioned; as C approaches zero, the normalized wall temperature ϕ_0 becomes close to unity, this phenomenon strongly suggests that $\phi_0 = 1$ when C = 0. That is, the numerical results are once more supported by analysis. Another feature worth pointing out is that the surface temperature and its slope at the leading edge approach zero when C is large. Therefore, the ordinary boundary condition at the fin tip

$$\phi_0(0) = 0 \text{ or } \frac{d\phi_0(0)}{dx} = 0$$

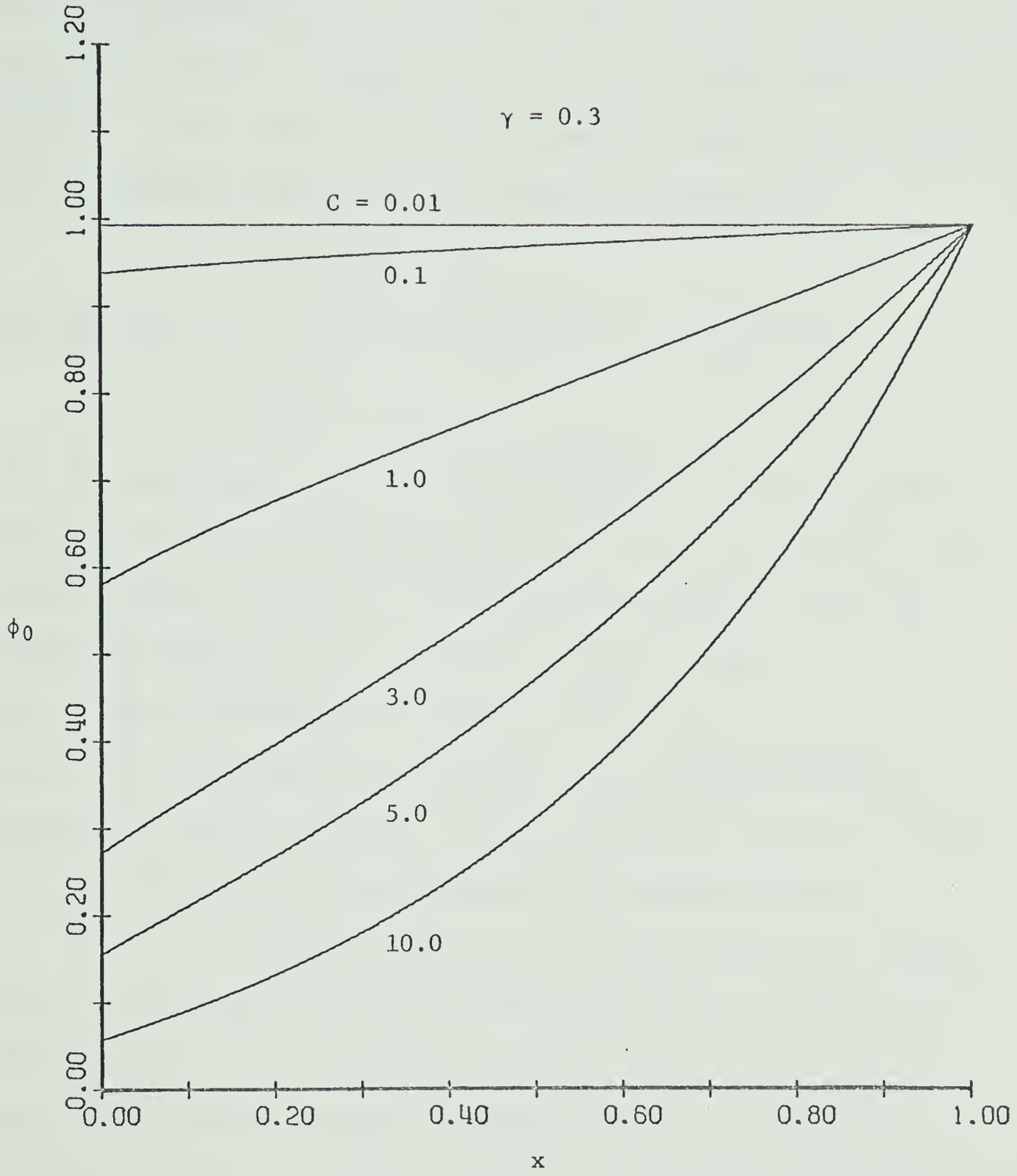

Figure 3.7 Effect of C on Interfacial Temperature

is a good approximation in the case of large C value: this is consistent with the predictions of appendix C, i.e., as $\frac{W}{L} << O[1]$, $\phi_0(0)=0$ and $\frac{d\phi_0(0)}{dx} = 0$. The consistency can be proved as follows. The validity of the quasi-one-dimensional fin equation is assumed when

$$Bi = \frac{hW}{K_s} << O[1].$$

Introduction of the normalized variables of appendix A gives

$$(\frac{W}{L})^2 C << O[1].$$

Now, the result shows that $\phi_0(0)=0$ and $\frac{d\phi_0(0)}{dx} = 0$ can be satisfied whenever $C >> O[1]$. This implies that $\frac{W}{L} << O[1]$. In fact, $\frac{W}{L} << O[1]$ is the necessary condition of the homogeneous boundary conditions $\phi_0(0)=0$ and $\frac{d\phi_0(0)}{dx} = 0$ for a conduction problem while $C >> O[1]$ is for a coupled problem of conduction and laminar free convection. Anyhow, in this problem if one intends to use the aforementioned homogeneous boundary condition, correct results can only be guaranteed when C is at least two orders-of-magnitude greater than unity.

In order to study the effect of γ on these interfacial temperatures, the profiles, based on the normalized variables x, for four different γ values are presented in figure (3.8) at four C levels. The profiles at each C level virtually coinside, and the maximum difference among them is less than 1%. This is a very interesting feature from the economic viewpoint, since even if the difference is not from the calculating errors, any normalized interfacial temperature

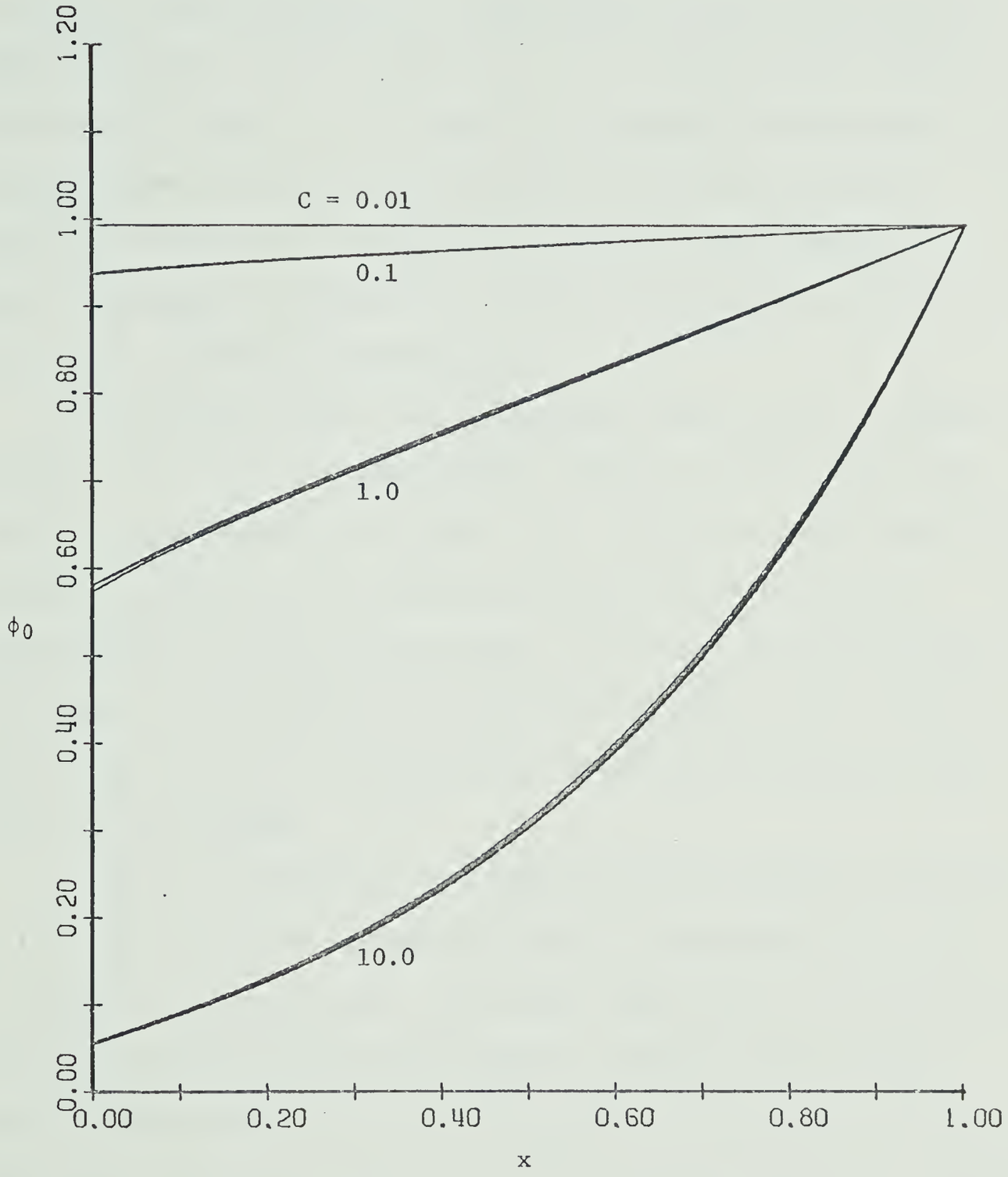

Figure 3.8 Effect of γ on Interfacial Temperature. Each Overlapped Curve Includes Four Curves for γ = 0, 0.1, 0.2, 0.3 .

for small γ can be considered as a good initial guessed profile for higher values of γ, for the same value of C. Experience shows that the larger the value of γ, the longer the computing time required; and the closer the initial guessed profile to the finally matched profile, the faster the convergent rate. Hence in such cases, a good initial guess can definitely cut down the computation required for a large γ value quite significantly.

The convergence rate of the interfacial temperature is indicated in figure (3.9) where two significantly different initial guesses, M1 and N1, were tested at C = 1.0 and γ = 0.2. After one loop of matching between the conduction and convection system, they gave very good approximations (M2 and N2 respectively) to the final converged profile. This figure not only reveals the fast matching ability of the technique used in this study, but also gives more confidence in convergence from "wild" initial guesses.

Finally, the possibility of approximating the similarity solution to the vertical surface convection problem is investigated at γ = 0.3 in figures (3.10) and (3.11). Both graphs suggest that the interfacial temperature profile $\phi_0(x)$ matched between conduction and convection generally bear neither the form of x^n nor e^{mx}. An exception to this occurs when C is small, where ϕ_0 is close to unity along the fin. Again, from a practical standpoint, the solution for an isothermal surface is a good approximation to that for small value of C. At least it can be a good initial guess to the problem when C is small.

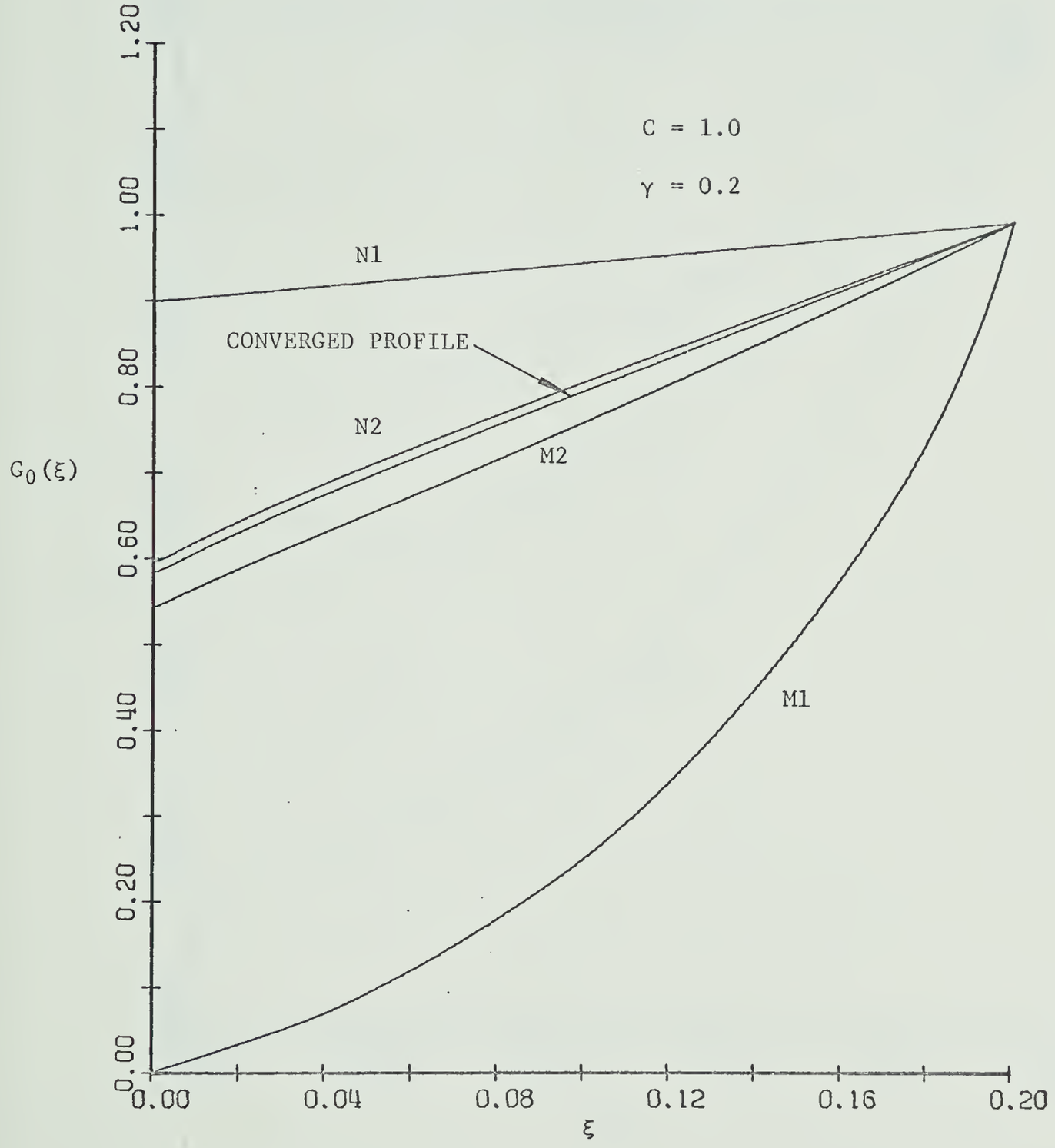

Figure 3.9 Rate of Convergence

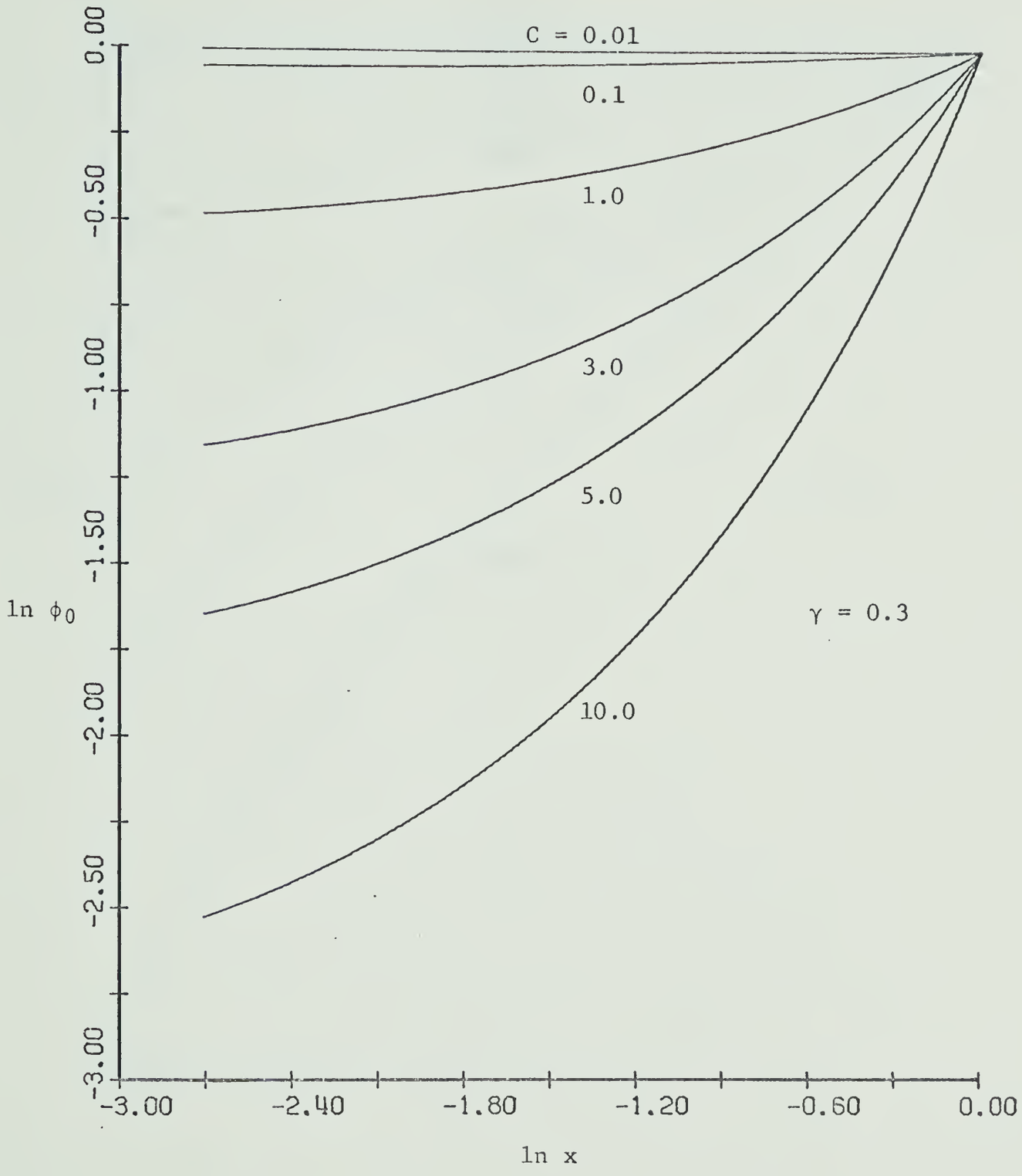

Figure 3.10 Interfacial Temperature Profiles for Checking the Possibility of Power Law Assumption, $\phi_0 = x^n$

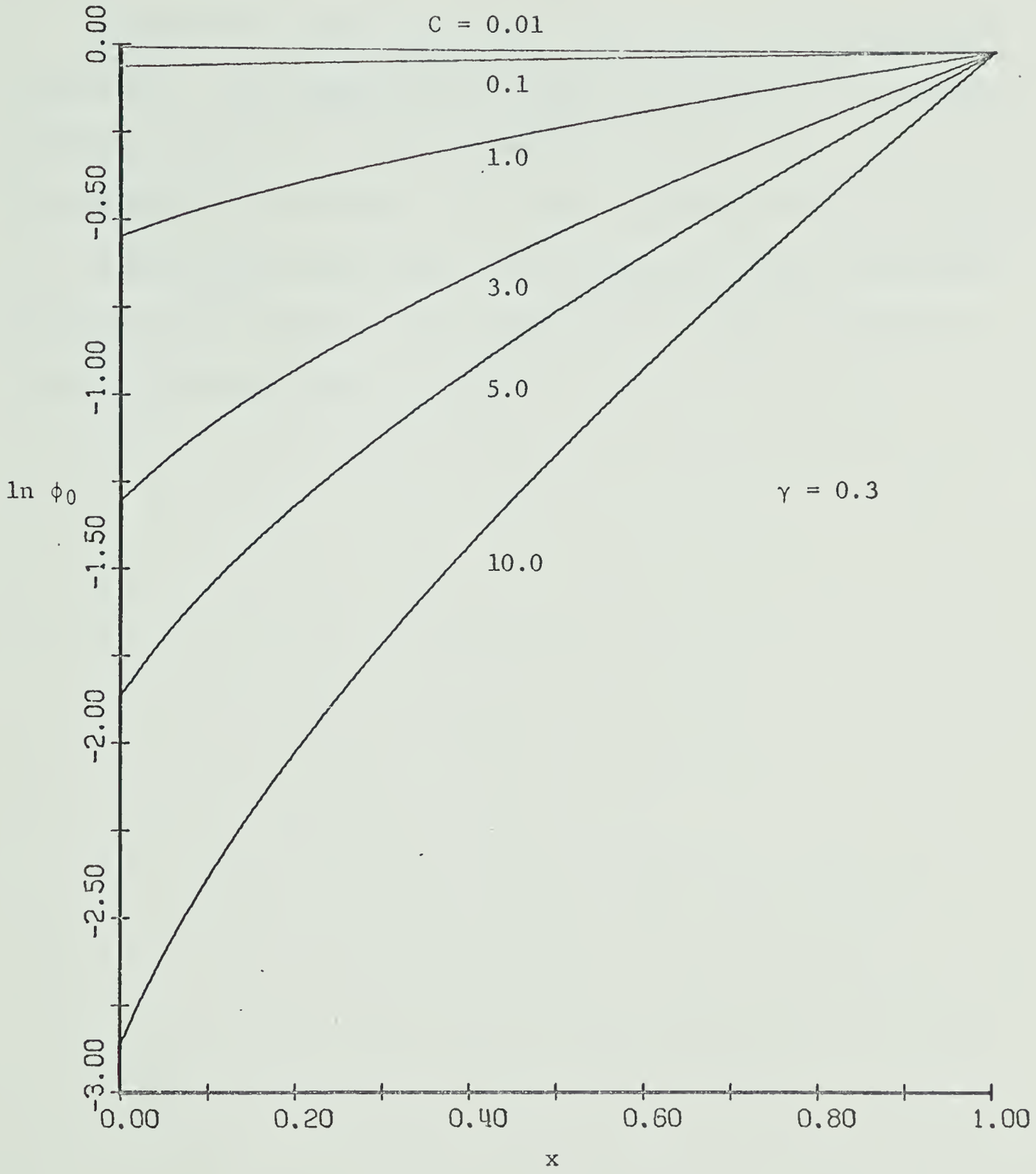

Figure 3.11 Interfacial Temperature Profiles for Checking the Possibility of Exponential Assumption, $\phi_0 = e^{mx}$

Figure (3.7) reveals that $\phi_0(0)$ tends to zero as the value of C increases. This suggests that a power law distribution of surface temperature might be a good approximation at large values of C. This is borne out by figure (3.11) which reveals that when the value of C is much greater than unity, the exponential surface temperature distribution e^{mx}, which is the asymptote for x^n when $n \to \infty$ [18], is a good approximation near the root.

CHAPTER IV

CONCLUSIONS AND RECOMMENDATIONS

4.1 CONCLUSIONS

The coupled problem of quasi-one-dimensional conduction and non-similarity convection for a heated triangular fin rotating together with surrounding air has been solved successfully and efficiently. The calculated functions and their derivatives being of order one indicates that the normalization procedure is valid. Although the simplified boundary layer equations (2.1)~(2.4), obtained by means of the order of magnitude method, require that all the dimensionless quantities $Ra^{-1/4}$, Fr^{-1}, $\beta\theta_r$, and Os should be much less than unity, a realistic example in appendix A has demonstrated that there is no conflict among these requirements.

The normalized governing equations indicate that when the angular velocity of the rotating system is high, the periodic effect of the gravitational force can be suppressed and the system can reach a quasi-static state. The Coriolis force is insignificant in the longitudinal direction along the fin, and only contributes to the pressure gradient in the lateral direction. This favorable feature not only simplifies the mathematical problem but also indicates symmetry of the boundary layer system about the fin.

A local similarity transformation with its coefficients being either constant or functions of the unprescribed interfacial temperature distribution has been developed so that the interface is free from the ordinary similarity restriction on the temperature profile; e.g., a power law assumption. This flexibility of the interfacial temperature makes the whole transformation suitable to the problem of interfacial matching. Analysis shows that only in the special case of an isothermal fin in a uniform gravitational field, can the traditional similarity transformation be applied to such a problem. Both transformations exhibiting the same forms in their coefficients can be regarded as a good check on this local similarity transformation.

The symmetry of the boundary layer systems on both sides of the rotating fin with large angular velocity permits the use of the quasi-one-dimensional equation for the conducting fin. It has been demonstrated in this study that the condition for a quasi-one-dimensional fin equation is $Bi << O[1]$. Again, an example shows that there is no conflict between this condition and any of the aforementioned four conditions in the convection problem. A new type of boundary condition with more generality for a tapered fin has been introduced at the tip of the fin. The traditional boundary condition, $T_w(0) = 0$ or $\frac{dT_w(0)}{dx} = 0$, is valid only when the parameter C of this problem is much greater than order one.

Truncation errors have been carefully controlled in the numerical approximations. After a preliminary test, the step size for integration in both the lateral and longitudinal directions were chosen, respectively,

to be 0.04 and 0.02, such that the eiganvalues, $\Phi'(\xi,0)$ and $f''(\xi,0)$, of the boundary layer problem were within an error of 1% of their asymptotic values, and with the computing time within a tolerable scale.

In the beginning, no guarantee could be made on the possibility and rate of convergence of interfacial temperature. More confidence was gained after several trials, as in figure (3.9), were conducted. When double precision is used, temperature can converge to consistency in five decimal places within 30 minute computation on an IBM 360/67 machine. The interfacial temperatures presented in this work have converged to sixteen decimal places. As a check on the numerical program, the total heat flux across the fin surfaces was compared with the heat flux applied at the root of the fin after each converged result was obtained. Comparisons of these values showed that the maximum discrepancy is of the order of 1%.

In addition to Prandtl number, two parameters, γ and C, appear in this study. The effect of the parameter γ was found to be smaller than that of C. When the parameter γ approaches zero, the problem becomes a static downward-projecting fin in a uniform gravitational field. Analysis has shown that the similarity solution only exists in the isothermal static fin problem, that is, when $C = 0$.

In fact, the isothermal fin result with $C = 0$ can also be extended to the problem in a centrifugal force field ($\gamma > 0$). The solutions of this work indicate a favorable feature for practical purposes, i.e., when C is small, solutions with $C = 0$ can represent a good approximation.

As one can see, the problem of matching no longer exists in the isothermal case C = 0 and the solution is much easier to obtain.

On studying the effects of γ and C on the local Nusselt number at the root of the fin, a linear relation between Nu and γ was obtained. i.e.

$$\frac{Nu}{Ra^{1/4}} = F_1(C) - F_2(C)\ \gamma\ .$$

The fin effectiveness as a function of parameter C were calculated at four γ values. The results for $\gamma = 0$ were compared with the solutions of reference [12]. If the calculated fin effectiveness for a static fin ($\gamma = 0$) is extended to C = 0 from the range of C in this study, it will match the analytical result for an isothermal static fin, i.e., $\varepsilon = 4/3$. This reveals that the solution of this work meets the solution of reference [12] in the isothermal case.

4.2 RECOMMENDATIONS

Firstly, experimental work is strongly suggested so that the results of this work can be compared with the physical evidence.

If time of computation were not a factor, it is worth trying the problem with γ larger than 0.3. The phenomenon in figure (3.8), that the normalized interfacial temperatures are almost independent of γ over its range of investigation, suggests that it can be a good initial guess to the problem for large γ, and the computing time on the matching can be reduced accordingly.

The order-of-magnitude procedure in this study refers to a fluid

with Prandtl number of order one and in the calculations, air with Pr = 0.72 has been considered as the fluid. One can carry out the same calculation for different fluids. If the Prandtl number is not of order one, a similar order-of-magnitude may be required, and different governing equations for the boundary layer problem may be formulated.

Further studies can be made either on the ultra-high rotating speed problem or in the problem with small angular velocity. The former will bring the heat dissipation and mechanical work against the large centrifugal force into the problem. The latter work will be much more complicated than the present one. When the angular velocity of the system is reduced, the Coriolis force will gradually increase in significance: this will results in an asymmetric boundary layer problem, and the quasi-one-dimensional conduction equation may no longer be applicable. When the angular velocity is reduced still further, the periodic effect of the gravitational field will give rise to an unsteady problem and the flow may then oscillate along the fin with each revolution. Finally, when the rotating speed tends to zero, it becomes a completely different problem of an inclined fin in a gravitational field.

REFERENCES

1. OSTRACH, S., "An Analysis of Laminar Free-Convection Flow and Heat Transfer About a Flat Plate Parallel to the Direction of the Generating Body Force, "NACA TR 1111, 1953.

2. SPARROW, E.M. and GREGG, J.L., "Laminar Free Convection From a Vertical Plate with Uniform Surface Heat Flux," Trans. ASME, Vol. 78, Feb. 1956, PP. 435-440.

3. SPARROW, E.M. and GREGG, J.L., "Similar Solutions for Free convection From a Nonisothermal Vertical Plate," Trans. ADME, Vol. 80, Feb. 1958, PP. 379-386.

4. YANG, K.T., "Possible Similarity Solutions for Laminar Free Convection on Vertical Plates and Cylinders," Journal of Applied Mechanics, Vol. 27, Trans. ADME, Series E, Vol. 82, No. 2, June 1960, PP. 230-236.

5. TAKHAR, H.S., "Free Convection from a Flat Plate," Journal of Fluid Mechanics, Vol. 34, Part1, 1968, PP. 81-89.

6. KREITH, F., "Convection Heat Transfer in Rotating Systems," Advances in Heat Transfer, Vol.5, 1968, PP. 129-251.

7. LEMLICH, R., "Natural Convection to Isothermal Flat Plate With a Spatially Nonuniform Acceleration," Ind. Eng. Chem. Fundamentals, Vol. 2, No. 2, May 1963, PP. 157-159.

8. LEMLICH, R. and STEINKAMP, J.S., "Laminar Natural Convection to an Isothermal Flat Plate With a Spatially Varying Acceleration," A.I.Ch.E. Journal, Vol. 10, No. 4, July 1964, PP. 445-447.

9. LEMLICH, R. and VARDI, J., "Steady Free Convection to a Flat Plate With Uniform Surface Heat Flux and Nonuniform Acceleration," Trans. ASME, Series C, Journal of Heat Transfer, Vol. 86, Nov. 1964, PP. 562-563.

10. CATTON, I., "Effect of a Gravity Gradient on Free Convection From a Vertical Plate," Chem. Eng. Progr. Symp. Ser., Vol. 64, No. 82, 1968, PP. 146-149.

11. MANOFF, M. and LEMLICH, R., "Free Convection to a Rotating Central Plate in Synchronously Rotating Surroundings With and Without Consideration of Coriolis Forces," A.I.Ch.E. Preprint 9 presented at the Eleventh National Heat Transfer Conference of A.I.Ch.E. and A.S.M.E., Minneapolis, Minnesota, August 3-6, 1969.

12. LOCK, G.S.H. and GUNN, J.C., "Laminar Free Convection From a Downward-Projecting Fin," Trans. ASME, Series C, Journal of Heat Transfer, Vol. 90, No. 1, Feb. 1968, PP. 63-70.

13. KELLEHER, M.D. and YANG, K.T., " A Steady Conjugate Heat Transfer Problem With Conduction and Free Convection," Applied Scientific Research, Vol. 17, 1967, PP. 249-269.

14. NACHTSHEIM, P.R. and SWIGERT, P., "Satisfaction of Asymptotic Boundary Conditions in Numerical Solution of Systems of Nonlinear Equations of Boundary-Layer Type," NASA-TN-D-3004, 1965.

15. IREY, R.K., "Errors in the One-Dimensional Fin Equation," Trans. ASME, Series C, Journal of Heat Transfer, Vol. 90, 1968, PP. 175-176.

16. HOLMAN, J.P., Heat Transfer, McGRaw-Hill Inc., 1968, PP. 199.

17. HAYDAY, A.A., BOWLUS, D.A., and McGRAW, R.A., "Free Convection From a Vertical Flat Plate With Step Discontinuities in Surface Temperature," Trans. ASME, Series C, Journal of Heat Transfer, Vol. 89, August 1967, PP. 244-250.

18. LOCK, G.S.H., "Steady Laminar Free Convection From Inclined, Arbitrarily Shaped Plane Surfaces," Trans. ASME, Series C, Journal of Heat Transfer, Vol. 84, 1964, PP. 669-673.

APPENDIX A

NORMALIZATION

Under the assumptions made in section 2.1-1, the governing equations of this rotating fin problem are:

$$\frac{\partial U}{\partial X} + \frac{\partial V}{\partial Y} = -\beta \left(\frac{\partial T}{\partial t} + U \frac{\partial T}{\partial X} + V \frac{\partial T}{\partial Y}\right), \tag{A.1}$$

$$\frac{\partial U}{\partial t} + U \frac{\partial U}{\partial X} + V \frac{\partial U}{\partial Y} = \frac{-1}{\rho} \frac{\partial P_d}{\partial X} + \nu \left(\frac{\partial^2 U}{\partial X^2} + \frac{\partial^2 U}{\partial Y^2}\right) + \beta \left[(R_t - X)\omega^2 + g \cos \alpha(t) + 2\lambda\omega V\right] (T - T_\infty), \tag{A.2}$$

$$\frac{\partial V}{\partial t} + U \frac{\partial V}{\partial X} + V \frac{\partial V}{\partial Y} = \frac{-1}{\rho} \frac{\partial P_d}{\partial Y} + \nu \left(\frac{\partial^2 V}{\partial X^2} + \frac{\partial^2 V}{\partial Y^2}\right) - \beta \left[Y\omega^2 - \lambda g \sin \alpha(t) + 2\lambda\omega U\right] (T - T_\infty), \tag{A.3}$$

and

$$\frac{\partial T}{\partial t} + U \frac{\partial T}{\partial X} + V \frac{\partial T}{\partial Y} = \kappa \left(\frac{\partial^2 T}{\partial X^2} + \frac{\partial^2 T}{\partial Y^2}\right) + \frac{2\nu}{c_p} \left[\left(\frac{\partial U}{\partial X}\right)^2 + \left(\frac{\partial V}{\partial Y}\right)^2\right] + \frac{\nu}{c_p} \left(\frac{\partial U}{\partial Y} + \frac{\partial V}{\partial X}\right)^2. \tag{A.4}$$

Introducing the following normalized variables into above equations:

$$u = \frac{U}{U_c}, \quad v = \frac{V}{V_c}, \quad x = \frac{X}{X_c}, \quad y = \frac{Y}{Y_c},$$

$$\tau = \frac{t}{t_c}, \quad p = \frac{P_d}{P_c} \quad \text{and} \quad \phi = \frac{T - T_\infty}{\Theta_c}$$

where subscript c indicates the corresponding characteristic values which will be determined later. The normalized equations are therefore

$$\left(\frac{U_c}{X_c}\right) \frac{\partial u}{\partial x} + \left(\frac{V_c}{Y_c}\right) \frac{\partial v}{\partial y} = -(\beta\Theta_c) \left[\left(\frac{1}{t_c}\right) \frac{\partial \phi}{\partial \tau} + \left(\frac{U_c}{X_c}\right) u \frac{\partial \phi}{\partial x} + \left(\frac{V_c}{Y_c}\right) v \frac{\partial \phi}{\partial y}\right], \tag{A.5}$$

$$\left(\frac{U_c}{t_c}\right)\frac{\partial u}{\partial \tau} + \left(\frac{U_c^2}{X_c}\right) u\,\frac{\partial u}{\partial x} + \left(\frac{V_c U_c}{Y_c}\right) v\,\frac{\partial u}{\partial y} = -\left(\frac{P_c}{\rho X_c}\right)\frac{\partial p}{\partial x}$$
$$+ \left(\frac{\nu U_c}{X_c^2}\right)\frac{\partial^2 u}{\partial x^2} + \left(\frac{\nu U_c}{Y_c^2}\right)\frac{\partial^2 u}{\partial y^2} + (\beta\omega^2 R_t \Theta_c)\,\phi - (\beta\omega^2 X_c \Theta_c)\,x\phi$$
$$+ (\beta g \Theta_c)\phi \cos\alpha(\tau) + (\beta\omega V_c \Theta_c)\,2\lambda v\phi \quad , \tag{A.6}$$

$$\left(\frac{V_c}{t_c}\right)\frac{\partial v}{\partial \tau} + \left(\frac{U_c V_c}{X_c}\right) u\,\frac{\partial v}{\partial x} + \left(\frac{V_c^2}{Y_c}\right) v\,\frac{\partial v}{\partial y} = -\left(\frac{P_c}{\rho Y_c}\right)\frac{\partial p}{\partial y}$$
$$+ \left(\frac{\nu V_c}{X_c^2}\right)\frac{\partial^2 v}{\partial x^2} + \left(\frac{\nu V_c}{Y_c^2}\right)\frac{\partial^2 v}{\partial y^2} - (\beta\omega^2 Y_c \Theta_c)\,y\phi$$
$$+ (\beta g \Theta_c)\,\lambda\phi \sin\alpha(\tau) - (\beta\omega U_c \Theta_c)\,2\lambda u\phi \quad , \tag{A.7}$$

and

$$\left(\frac{\Theta_c}{t_c}\right)\frac{\partial \phi}{\partial \tau} + \left(\frac{U_c \Theta_c}{X_c}\right) u\,\frac{\partial \phi}{\partial x} + \left(\frac{V_c \Theta_c}{Y_c}\right) v\,\frac{\partial \phi}{\partial y} = \left(\frac{\kappa\Theta_c}{X_c^2}\right)\frac{\partial^2 \phi}{\partial x^2}$$
$$+ \left(\frac{\kappa\Theta_c}{Y_c^2}\right)\frac{\partial^2 \phi}{\partial y^2} + \left(\frac{\nu U_c^2}{c_p X_c^2}\right) 2\left(\frac{\partial u}{\partial x}\right)^2 + \left(\frac{\nu V_c^2}{c_p Y_c^2}\right) 2\left(\frac{\partial v}{\partial y}\right)^2$$
$$+ \left(\frac{\nu U_c^2}{c_p Y_c^2}\right)\left(\frac{\partial u}{\partial y}\right)^2 + \left(\frac{\nu U_c V_c}{c_p X_c Y_c}\right) 2\,\frac{\partial u}{\partial y}\,\frac{\partial v}{\partial x} + \left(\frac{\nu V_c^2}{c_p X_c^2}\right)\left(\frac{\partial v}{\partial x}\right)^2 \quad . \tag{A.8}$$

If the system rotates at a constant high speed, the periodically changing effect of gravitational force can be suppressed in relation to the centrifugal force in equation (A.6). Hence, when the Froude number (Fr), defined as $R_t\omega^2/g$, is much greater than unity, and the boundary conditions are independent of time, the problem becomes steady after a

long period of time, i.e., t_c is large. In order to compare the coefficients of each normalized terms governing this quasi-steady problem, six characteristic values have to be obtained. Ab initio L and $T_r - T_\infty$ may be chosen as X_c and Θ_c respectively. The others have to be determined with reference to the physical characteristics of the system.

In equation (A.5), $\beta\Theta_c$ is normally small for free convection problems and the right-hand-side is therefore negligible, especially when t_c is large. Hence there are only two terms left and their coefficients must be of the same order of magnitude,

that is $$O\left[\frac{U_c}{L}\right] = O\left[\frac{V_c}{Y_c}\right] \quad .$$

For convenience it can be set

$$\frac{LV_c}{Y_c U_c} = 1 \quad . \tag{A.9}$$

Since the momentum boundary layer in free convection is manifest through the effect of viscosity in the presence of buoyancy, the coefficients of the largest viscosity term and the centrifugal force term in equation (A.6) can be set equal. Hence

$$\frac{\nu U_c}{\beta R_t \omega^2 (T_r - T_\infty) Y_c^2} = 1 \quad . \tag{A.10}$$

Assuming that advection and conduction in the energy equation (A.8) are equally important yields

$$\frac{U_c Y_c^2}{\kappa L} = 1 \quad . \tag{A.11}$$

From (A.9), (A.10) and (A.11), one can have

$$Y_c = L/Ra^{1/4} \quad ,$$

$$U_c = \kappa\, Ra^{1/2}/L \quad ,$$

and $$V_c = \kappa\, Ra^{1/4}/L$$

where the Rayleigh number, Ra, is defined as

$$Ra = \frac{\beta R_t \omega^2 (T_r - T_\infty) L^3}{\nu\kappa} \quad .$$

In the lateral momentum equation (A.7), the buoyancy effect of the gravitional force is suppressed by that of the Coriolis force when the rotating speed is high, hence the possible driving forces to cause the pressure gradient are the Coriolis force and the centrifugal force. In order to find which of them is more dominant, the magnitudes of these two terms should be compared. Their rotio is

$$\frac{U_c}{\omega Y_c} = \frac{\kappa}{\omega L^2} Ra^{3/4} = Pr^{-1}\, Ek\, Ra^{3/4} \quad .$$

If Prandtl number is of order one, the above ratio is generally much greater than unity as the rotating speed is high. Therefore, Coriolis force, $2u\phi$, gives rise to the lateral pressure gradient $\frac{\partial p}{\partial y}$, and it is convenient to set

$$P_c = \rho\omega Y_c U_c \beta\Theta_c \quad ,$$

i.e. $$P_c = \rho\kappa\omega\beta(T_r - T_\infty)\, Ra^{1/4} \quad .$$

Once the characteristic values are established, the normalized equations for this steady problem can be rewritten as

$$\frac{\partial u}{\partial x} + \frac{\partial v}{\partial y} = O[\beta(T_r - T_\infty)] << O[1] \ , \tag{A.12}$$

$$\frac{1}{Pr}\left(u\frac{\partial u}{\partial x} + v\frac{\partial u}{\partial y}\right) + \left[\beta(T_r - T_\infty)\ Ek^{-1}\ Ra^{-3/4}\right]\left(\frac{\partial p}{\partial x} - 2\lambda v\phi\right)$$
$$- \left[Ra^{-1/2}\right]\frac{\partial^2 u}{\partial x^2} - \frac{\partial^2 u}{\partial y^2} - (1 - \gamma x)\phi \leq O\left[Fr^{-1}\right] << O[1] \ , \tag{A.13}$$

$$\left[Ra^{-1/4}\right]\left(u\frac{\partial v}{\partial x} + v\frac{\partial v}{\partial y}\right) + \left[\beta\ (T_r - T_\infty)\ Ek^{-1}\ Ra^{-1/2}\right]\left(\frac{\partial p}{\partial y} + 2\lambda u\phi\right)$$
$$- \left[Ra^{-3/4}\right]\frac{\partial^2 v}{\partial x^2} - \left[Ra^{-1/4}\right]\left(\frac{\partial^2 v}{\partial y^2} - y\phi\right) \leq O\left[Fr^{-1}\right] << O[1] \ , \tag{A.14}$$

and

$$u\frac{\partial \phi}{\partial x} + v\frac{\partial \phi}{\partial y} = \left[Ra^{-1/2}\right]\frac{\partial^2 \phi}{\partial x^2} + \frac{\partial^2 \phi}{\partial y^2} + [Os]\left(\frac{\partial u}{\partial y}\right)^2$$
$$+ 2\left[Os\ Ra^{-1/2}\right]\left[\left(\frac{\partial u}{\partial x}\right)^2 + \frac{\partial u}{\partial y}\frac{\partial v}{\partial x} + \left(\frac{\partial v}{\partial y}\right)^2\right] + \left[Os\ Ra^{-1}\right]\left(\frac{\partial v}{\partial x}\right)^2 . \tag{A.15}$$

When air is the fluid, Prandtl number is of order one and the conditions that $Ra^{-1/4}$, Fr^{-1}, $\beta(T_r - T_\infty)$ and Os are all much less than unity, the boundary layer equations are simplified:

$$\frac{\partial u}{\partial x} + \frac{\partial v}{\partial y} = 0 \ , \tag{A.16}$$

$$\frac{1}{Pr}\left(u\frac{\partial u}{\partial x} + v\frac{\partial u}{\partial y}\right) = (1 - \gamma x)\ \phi + \frac{\partial^2 u}{\partial y^2} \ , \tag{A.17}$$

$$\frac{\partial p}{\partial y} = -2\lambda u\phi = O[10^{-1}] \ , \tag{A.18}$$

and

$$u\frac{\partial \phi}{\partial x} + v\frac{\partial \phi}{\partial y} = \frac{\partial^2 \phi}{\partial y^2} \ . \tag{A.19}$$

As an example, for a 6-inch aluminum fin, 12 inches from the center of rotation, rotating synchronously with air at 300 rpm, if

$(T_r - T_\infty)$ is 10° F, one will have $Fr^{-1} \simeq 0.02$, $\beta(T_r - T_\infty) \simeq 0.019$, $Os \simeq 2.2 \times 10^{-4}$, $Ra^{-1/4} \simeq 0.011$ and $(T_r - T_\infty)\, Ek^{-1}\, Ra^{-1/2} \simeq 0.1$.

In all cases, it is now clear that the nature of this quasi-steady problem is governed by the simultaneous equations (A.16), (A.17) and (A.19), while the separatable equation (A.18) can indicate the pressure distribution, if it is required, after the velocity and temperature profiles have been obtained.

The normalized boundary conditions associated with these simultaneous governing equations are

$x = 0$: $\quad u = 0$, $\quad \phi = 0$

$y = 0$ $(x \geq 0)$: $\quad u = 0$, $\quad v = 0$, $\quad \phi = \phi_0(x)$

$y = \infty$: $\quad u = 0$, $\quad \phi = 0$

where $\phi_0(x)$ is the temperature distribution along the fin surface.

APPENDIX B

LOCAL SIMILARITY TRANSFORMATION

The problem is to solve three partial differential equations, (A.16), (A.17) and (A.19), simultaneously. Introducing a stream function $\psi(x,y)$ defined by

$$u = \frac{\partial \psi}{\partial y} \qquad \text{and} \qquad v = -\frac{\partial \psi}{\partial x} \ , \tag{B.1}$$

equation (A.16) is automatically satisfied and the governing equations reduce into two partial differential equations:

$$Pr \frac{\partial^3 \psi}{\partial y^3} + \frac{\partial \psi}{\partial x}\frac{\partial \psi}{\partial y} - \frac{\partial \psi}{\partial y}\frac{\partial^2 \psi}{\partial x \partial y} + Pr\ (1 - \gamma x)\phi = 0 \ , \tag{B.2}$$

$$\frac{\partial^2 \phi}{\partial y^2} - \frac{\partial \psi}{\partial y}\frac{\partial \phi}{\partial x} + \frac{\partial \psi}{\partial x}\frac{\partial \phi}{\partial y} = 0 \ . \tag{B.3}$$

The corresponding boundary conditions become

$x = 0$; $\quad \frac{\partial \psi}{\partial y} = 0$, $\quad \phi = 0$,

$y = 0\ (x \geq 0)$; $\quad \psi = 0$, $\quad \frac{\partial \psi}{\partial y} = 0$, $\quad \phi = \phi_0(x)$,

$y = \infty$; $\quad \frac{\partial \psi}{\partial y} = 0$, $\quad \phi = 0$

where $\psi = 0$ at $y = 0$ is reasonable, since for boundary layer problems without mass transfer through the wall, it can always be arranged in this way that the stream function will be zero at the wall.

The ensuing effort is normally in finding a similarity solution for suitable form of $\phi_0(x)$. However, it is vital here to emphasize that $\phi_0(x)$ is an unknown temperature distribution along the fin surface. It is neither feasible nor desirable to assume that $\phi_0(x)$ will definitely fulfil the special power law requirement of similarity. Besides, whenever $\phi_0(0)$ is not zero, there is a singularity at the leading edge, i.e.,

$$\lim_{x\to 0} \phi_0(x) \neq \lim_{y\to 0} \phi(0,y) = 0 \ .$$

Hence, it is now necessary to seek a transformation, without prescribing the interfacial temperature $\phi_0(x)$, to remove this singularity. A transformation can be assumed in the form:

$$f(\xi,\eta) = \frac{\psi(x,y)}{F(x)} \ , \qquad \Phi(\xi,\eta) = \frac{\phi(x,y)}{\phi_0(x)} \ ,$$
$$\eta = H(x)\, I(y) \ , \qquad \text{and} \qquad \xi = K(x) \ . \tag{B.4}$$

where $\Phi(\xi,\eta)$ and $f(\xi,\eta)$ are two dependent variables in the new coordinate system corresponding to $\phi(x,y)$ and $\psi(x,y)$ respectively.

The present object is to define suitable functions, F(x), H(x), K(x) and I(y), to facilitate the numerical work. Substitution of the above transformation into equations (B.2) and (B.3) followed by rearrangement give

$$\Pr\left[(FH^3I_y)f''' + 3(FH^2I_yI_{yy})f'' + (FHI_{yyy})f'\right] + \Pr\left[(\phi_0)\Phi - (\gamma x\phi_0)\Phi\right]$$
$$+ \left[(FH^2F_xI_y^2)ff'' + (F^2HIH_xI_{yy} - FH^2F_xI_y^2 - F^2HH_xI_y^2)(f')^2\right.$$
$$\left. + (FHF_xI_{yy})ff'\right] = (F^2H^2K_xI_y^2)\left(f'\frac{\partial f'}{\partial \xi} - f''\frac{\partial f}{\partial \xi}\right) - (F^2HK_xI_{yy})f'\frac{\partial f}{\partial \xi} \ , \tag{B.5}$$

and

$$\left[(\phi_0 H^2 I_y{}^2)\Phi'' + (\phi_0 H I_{yy})\Phi'\right] + \left[(\phi_0 H F_x I_y) f\Phi' - (FH\phi_{0x} I_y) f'\Phi\right]$$

$$= (FH\phi_0 K_x I_y)\left(f'\frac{\partial \Phi}{\partial \xi} - \Phi'\frac{\partial f}{\partial \xi}\right) \qquad (B.6)$$

where the primes denote differentiations with respect to η; x and y derivatives are indicated with the subscripts. It should be noted that both equations have been arranged in such a way that any term dependent on ξ is kept on the righ-hand-side of the equation. This is the essential treatment of constructing a basis for "local similarity".

Since the highest derivative in the differential equation must not be eliminated, equations (B.5) and (B.6) can be simplified by dividing by $PrFH^3 I_y{}^3$ and $\phi_0 H^2 I_y{}^2$ respectively. Hence the coefficients of f''' and Φ'' become unity in the equations: thit is, the equations become

$$\left[f''' + 3\left(\frac{I_{yy}}{HI_y{}^2}\right)f'' + \left(\frac{I_{yyy}}{H^2 I_y{}^3}\right)f'\right] + \frac{1}{Pr}\left[\left(\frac{F_x}{HI_y}\right)ff''\right.$$

$$\left. + \left(\frac{FIH_x I_{yy}}{H^2 I_y{}^3} - \frac{E_x}{HI_y} - \frac{FH_x}{H^2 I_y}\right)f'^2 + \left(\frac{F_x I_{yy}}{H^2 I_y{}^3}\right)ff'\right] + \left[\left(\frac{\phi_0}{FH^3 I_y{}^3}\right)\Phi - \left(\frac{\gamma x \phi_0}{FH^3 I_y{}^3}\right)\Phi\right]$$

$$= \frac{1}{Pr}\left(\frac{FK_x}{HI_y}\right)\left(f'\frac{\partial f'}{\partial \xi} - f''\frac{\partial f}{\partial \xi}\right) - \frac{1}{Pr}\left(\frac{FK_x I_{yy}}{H^2 I_y{}^3}\right)f'\frac{\partial f}{\partial \xi}\,, \qquad (B.7)$$

and

$$\left[\Phi'' + \left(\frac{I_{yy}}{HI_y^2}\right)\Phi'\right] + \left[\left(\frac{F_x}{HI_y}\right)f\Phi' - \left(\frac{F\phi_{0x}}{H\phi_0 I_y}\right)f'\Phi\right] = \left(\frac{FK_x}{HI_y}\right)\left(f'\frac{\partial\Phi}{\partial\xi} - \Phi'\frac{\partial f}{\partial\xi}\right) . \tag{B.8}$$

The first and the second square-bracketed terms of equation (B.7) are related to viscous and inertia forces while the first and the second square-bracketed terms of equation (B.8) correspond to conduction and advection. The third square-bracketed term in equation (B.7) is the buoyancy effect.

It is important that in determining the four disposable functions, F(x), H(x), K(x) and I(y), the pitsfalls of eliminating the highest order derivatives in the physically significant brackets of equations (B.7) and (B.8) should be avoided and the singularity of the problem should be removed. Each disposable function can be determined either by directly defining it according to one's special purpose for solving the problem, or by equating a specific value to the parenthesized function group of any significant term in equations (B.7) or (B.8)

The normalization process implies that inertia force, viscous force, and buoyancy force terms are equally important in equation (A.17) and have to be retained in this problem. Besides, the advection terms must be as significant as the conduction term in equation (A.19). Thus, two parenthesized groups can be chosen and set to be two undefined non-zero constants C_1 and C_2:

$$\frac{F_x}{HI_y} = C_1 \ , \tag{B.9}$$

and

$$\frac{\phi_0}{FH^3 I_y^3} = C_2 \ . \tag{B.10}$$

Rearrangement of (B.9) yields

$$\frac{1}{H(x)} \frac{dF(x)}{dx} = C_1 \frac{dI(y)}{dy} = C_3 \ , \tag{B.11}$$

and hence,

$$I(y) = \frac{C_3}{C_1} y + C_4 \ .$$

Choosing $C_1 = C_3$ and $C_4 = 0$, $I(y)$ can be kept in the simplest form, i.e.,

$$I(y) = y \ . \tag{B.12}$$

From equations (B.10), (B.11) and (B.12),

$$\phi_0(x) = C_2 F(x) H^3(x) \ ,$$

$$H(x) = \frac{1}{C_1} \frac{dF(x)}{dx} \ ,$$

that is,

$$F(x)\left(\frac{dF(x)}{dx}\right)^3 = \frac{C_1^3}{C_2} \phi_0(x) \ .$$

Then from this,

$$F(x) = \left[\frac{4}{3} C_1 C_2^{-1/3} \int^x \phi_0^{1/3}(t)dt + \frac{4}{3} C_5\right]^{3/4} \tag{B.13}$$

and

$$H(x) = C_1 C_2^{-1/3} \phi_0^{1/3}(x) \left[\frac{4}{3} C_1 C_2^{-1/3} \int^x \phi_0^{1/3}(t)dt + \frac{4}{3} C_5 \right]^{-1/4} \qquad (B.14)$$

where t is the dummy variable.

Since the transformation is to remove the singularity which arises when $\lim_{x \to 0} \phi_0(x) \neq 0$ while $\lim_{y \to 0} \phi(0,y) = 0$, it is wished that this sigular point (0,0) in x - y plane can be transformed into a line in the new ξ-η plane, so that this sudden change at the singular point becomes smooth change along the line. This is fulfilled by setting

$$C_1 = C_2 = 1 \qquad \text{and} \qquad C_5 = \int^0 \phi_0^{1/3}(t)dt$$

in H(x). Hence F(x) and H(x) are simplified to be

$$F(x) = \left[\frac{4}{3} \int_0^x \phi_0^{1/3}(t)dt \right]^{3/4} \qquad (B.15)$$

and

$$H(x) = \frac{\phi_0^{1/3}(x)}{\left[\frac{4}{3} \int_0^x \phi_0^{1/3}(t)dt \right]^{1/4}} \quad . \qquad (B.16)$$

Substituting equations (B.12), (B.15), (B.16) in (B.7) and (B.8), and retaining those terms with coefficients which are functions of x on the right-hand-side of each equation, yields

$$\Pr(f''' + \Phi) + ff'' - \frac{2}{3}(f')^2 = \frac{-4}{3} \left[\frac{d\phi_0^{-1/3}(x)}{dx} \int_0^x \phi_0^{1/3}(t)dt \right] (f')^2$$

$$+ \frac{4}{3} \left[\frac{dK(x)}{dx} \phi_0^{-1/3}(x) \int_0^x \phi_0^{1/3}(t)dt \right] \left(f' \frac{\partial f'}{\partial \xi} - f'' \frac{\partial f}{\partial \xi} \right) + \Pr \gamma x \Phi \quad . \qquad (B.17)$$

and

$$\Phi'' + f\Phi' = -4\left[\frac{d\Phi_0^{-1/3}(x)}{dx}\int_0^x \phi_0^{1/3}(t)dt\right] f'\Phi$$

$$+ \frac{4}{3}\left[\frac{dK(x)}{dx}\phi_0^{-1/3}(x)\int_0^x \phi_0^{1/3}(t)dt\right]\left(f'\frac{\partial\Phi}{\partial\xi} - \Phi'\frac{\partial f}{\partial\xi}\right) . \qquad (B.18)$$

Since these transformed equations are now in ξ-η coordinates, those coefficients contained by brackets in equations (B.17) and (B.18) should be either constants or functions of ξ and η. The last term of equation (B.17) suggests that

$$\xi = K(x) = \gamma x . \qquad (B.19)$$

Hence,

$$\frac{dK(x)}{dx} = \gamma ,$$

and for a given function $G_0(\xi)$, if $G_0(\xi) = \phi_0(x)$ then

$$\frac{d\phi_0(x)}{dx} = \gamma\frac{dG_0(\xi)}{d\xi} \qquad \text{and} \qquad \int_0^x \phi_0(t)dt = \frac{1}{\gamma}\int_0^\xi G_0(S)dS ,$$

where $G_0(\xi)$ does not exhibit the same functional form as $\phi_0(x)$; it only implies that it is the same physical quantity but represented in different coordinate systems. By substitution, all the bracketed coefficients in equations (B.17) and (B.18) become functions of ξ. It is noteworthy that the salient merit of definition (B.19) not only transforms the equations completely into the (ξ,η) domain, but also saves a great deal of computing time. This is because γ is never

greater than one and the number of steps required in the approximation along ξ-direction is less for smaller γ. The detail will be discussed later.

Therefore, the definitions

$$\xi = \gamma x \ ,$$

$$\eta = \gamma \frac{d\left[\frac{4}{3\gamma}\int_0^{\xi} G_0{}^{1/3}(S)dS\right]^{3/4}}{d\xi} y \ ,$$

$$f(\xi,\eta) = \left[\frac{4}{3\gamma}\int_0^{\xi} G_0(S)^{1/3}dS\right]^{-3/4} \psi(x,y) \ , \tag{B.20}$$

$$\Phi(\xi,\eta) = G_0{}^{-1}(\xi)\ \phi(x,y) \ ,$$

and

$$G_0(\xi) = \phi_0(x) \ ,$$

transform governing equations into a new coordinate system of ξ and η, for which,

$$\mathrm{Pr}(f''' + \Phi) + ff'' - \frac{2}{3}(f')^2 = -\frac{4}{3}\left[\frac{dG_0(\xi)^{-1/3}}{d\xi}\int_0^{\xi} G_0(S)^{1/3}dS\right](f')^2$$

$$+ \frac{4}{3}\left[G_0(\xi)^{-1/3}\int_0^{\xi} G_0(S)^{1/3}dS\right]\left(f'\frac{\partial f'}{\partial \xi} - f''\frac{\partial f}{\partial \xi}\right) + \mathrm{Pr}\xi\Phi \tag{B.21}$$

and

$$\Phi'' + f\Phi' = -4\left[\frac{dG_0(\xi)^{-1/3}}{d\xi}\int_0^{\xi} G_0(S)^{1/3}dS\right] f'\Phi$$

$$+ \frac{4}{3}\left[G_0(\xi)^{-1/3}\int_0^{\xi} G_0(S)^{1/3}dS\right]\left(f'\frac{\partial \Phi}{\partial \xi} - \Phi'\frac{\partial f}{\partial \xi}\right) . \tag{B.22}$$

The associated boundary conditions in η-direction can easily be deduced from those of equations (B.3) and (B.4): whence

$$\eta = 0 ; \quad f = 0 , \quad f' = 0 , \quad \Phi = 1 ,$$
$$\eta = \infty ; \quad f' = 0 , \quad \Phi = 0 . \tag{B.23}$$

Provided that $\frac{dG_0^{-1/3}}{d\xi}$ is finite and the derivatives of f and Φ are bounded when $\xi = 0$, the right-hand-sides of equations (B.21) and (B.22) vanish completely at this leading edge. Hence the solution of the boundary layer equations,

$$Pr(f''' + \Phi) + ff'' - \frac{2}{3}(f')^2 = 0 \tag{B.24}$$

and

$$\Phi'' + f\Phi' = 0 , \tag{B.25}$$

and the boundary conditions of (B.23) give the boundary values along the line $\xi = 0$.

Although $G_0(\xi)$ is the temperature profile for each of the coupled heat transfer problems, it can be conceived of as an unknown but fixed input to the convection system of the fin problem. If $G_0(\xi)$ is "known", the coefficients on the right-hand-sides of equations (B.21) and (B.22) can be evaluated at each specific ξ-level. In the study of the boundary layer problem, most interest is placed in the variations of velocity and temperature in the lateral direction. Hence, whenever the first partial derivatives with respect to ξ are replaced with suitable approximations, equations (B.21) and (B.22) become two

coupled ordinary differential equations governing boundary layers at that specific ξ-level: this is the local similarity concept.

Several favorable features can then be seen from this "local similarity transformation":

(1) The definitions of the transformation (B.20) can be rewritten as:

$$\xi = \gamma x \ ,$$

$$\eta = \frac{G_0^{1/3}(\xi)}{\left[\frac{4}{3\gamma}\int_0^{\xi} G_0^{1/3}(S)dS\right]^{1/4}} y \ ,$$

$$\psi(x,y) = \left[\frac{4}{3\gamma}\int_0^{\xi} G_0^{1/3}(S)dS\right]^{3/4} f(\xi,\eta) \ ,$$

$$\phi(x,y) = G_0(\xi)\ \Phi(\xi,\eta)$$

and

$$\phi_0(x) = G_0(\xi) \ .$$

The singularity caused by $\phi_0(0) = G_0(0) \neq 0$ at the leading edge is obviously removed, after the point of discontinuity ($x = 0$, $y = 0$) has been expanded into the line $\xi = 0$ in the ξ-η plane. Along this line, $\Phi(0,\eta)$ changes from unity ($\eta = 0$) to zero ($\eta \to \infty$).

(2) As stated before, integration of equations (B.24) and (B.25) which are subjected to the boundary conditions (B.23) will give the supplemental boundary conditions along line $\xi = 0$. Hence, there is no difficulty in starting the numerical

integration of the boundary layer equations, (B.21) and (B.22), in the ξ-η plane.

(3) It is not subjected to the difficulty of deciding which similarity solution should be used, since no specific similarity restriction on the wall surface temperature is of concern in the transformation. This allows the possibility of matching the interfacial temperature $G_0(\xi)$ of such a coupled heat transfer problem of conduction and convection.

(4) In a boundary layer problem, comparatively less interest is taken along the longitudinal direction. This transformation introduced only first derivatives with respect to ξ,and this is very helpful in applying the local similarity concept.

(5) All the boundary conditions are properly transformed. Hence, there is no violation between the original and the transformed boundary values.

APPENDIX C

QUASI-ONE-DIMENSIONAL PROBLEM OF FIN

For the simplicity in studying the validity of the quasi-one-dimensional fin equation, a constant cross-section area and constant property circular fin will be assumed. The conduction heat transfer in the fin is governed by

$$R \frac{\partial^2 T_0(R,X)}{\partial X^2} + \frac{\partial}{\partial R}\left(R \frac{\partial T_0(R,X)}{\partial R}\right) = 0 \quad , \tag{C.1}$$ *

and the boundary conditions:

$$T_0(R,0) = T_r \quad , \quad \frac{\partial T_0(R,L)}{\partial X} + \frac{h}{K_s}[T_0(R,L) - T_\infty] = 0 \quad ,$$

$$T_0(0,X) = \text{finite} \quad , \quad \frac{\partial T_0(a,X)}{\partial R} + \frac{h}{K_s}[T_0(a,X) - T_\infty] = 0 \quad ,$$

where L and a are respectively the length and radius of the fin, while T_∞ and T_r indicate the ambient temperature and the temperature at the root of the fin.

After introducing the normalized geometric variables:

$$x = \frac{X}{L} \quad , \quad r = \frac{R}{a}$$

and a new temperature variable

$$\phi_0(x,r) = \frac{T_0(X,R) - T_\infty}{T_r - T_\infty}$$

the differential equation becomes

$$r \frac{\partial^2 \phi_0}{\partial x^2} + \frac{L^2}{a^2} \frac{\partial}{\partial r}\left(r \frac{\partial \phi_0}{\partial r}\right) = 0 \quad , \tag{C.2}$$

---

* In this appendix, X is the longitudinal displacement from fin root, and R is the radial distance from the axis of the circular fin.

which is subjected to the normalized conditions:

$$\phi_0(r,0) = 1 \quad , \quad \frac{\partial\phi_0(r,1)}{\partial x} = \frac{-hL}{K_s} \phi_0(r,1) \quad ,$$

$$\phi_0(0,x) = \text{finite} \ , \quad \frac{\partial\phi_0(1,x)}{\partial r} = \frac{-ha}{K_s} \phi_0(1,x) \quad .$$

Integrating equation (C.2) with respect to r from 0 to 1 and applying the last two boundary conditions give

$$\int_0^1 \frac{\partial^2\phi_0(r,x)}{\partial x^2} \, r \, dr - \frac{L^2h}{aK_s} \phi_0(1,x) = 0 \quad . \tag{C.3}$$

When ϕ_0 is independent of r, the problem is (by definition) one dimensional. When ϕ_0 is almost constant along the radial direction on each cross section of the fin, i.e.

$$\frac{\partial\phi_0}{\partial r} << O[1] \quad , \tag{C.4}$$

the approximations

$$\phi_0(1,x) \approx \phi_0(x) \qquad \text{and} \qquad \frac{\partial^2\phi_0(r,x)}{\partial x^2} \approx \frac{d^2\phi_0(x)}{dx^2}$$

may be used in equation (C.3) to produce the quasi-one-dimensional equation

$$\frac{d^2\phi_0}{dx^2} - \frac{2L^2h}{aK_s} \phi_0 = 0, \tag{C.5}$$

or in the original form

$$\frac{d^2T_0}{dX^2} - \frac{2h}{aK_s} (T_0 - T_\infty) = 0. \tag{C.6}$$

In other words, the necessary condition to construct the quasi-one-dimensional fin equation is

$$\frac{\partial \phi_0(r,x)}{\partial r} << O[1] \quad .$$

Moreover, since

$$\frac{\partial \phi_0(1,x)}{\partial r} = - \frac{ha}{K_s} \phi_0(1,x)$$

and $$\phi_0(1,x) = 1 \ ,$$

one can predict that

$$\frac{\partial \phi_0(r,x)}{\partial r} = O\left[\frac{ha}{K_s}\right] \quad . \tag{C.7}$$

Therefore, (C.4) and (C.7) infer that

$$Bi = \frac{ha}{K_s} << O[1] \tag{C.8}$$

is the necessary condition for the utility of equations (C.5) or (C.6). This conclusion was deduced numerically [15] when Irey checked the total amount of heat flux calculated from the quasi-one-dimensional fin equation with that of two dimensional Laplace equation. Irey concluded his results:

> "as far as the more significant variable, the total heat transfer, is concerned, the standard criteria of large length to diameter ratio is not only not of primary significance, it is almost irrelevent. Of far more significance is the ratio of interior to exterior resistance, the Biot number, and that only for small Biot

number is the one-dimensional solution a satisfactory approximation."

Hence, when Bi << O[1], the problem is governed by equations (C.6) and the boundary conditions which, in dimensional form are:

$$T_0(0) = T_r \qquad \text{and} \qquad \frac{dT_0(L)}{dX} + \frac{h}{K_s}\,[T_0(L) - T_\infty] = 0 \quad .$$

A related question that frequently arises concerns the condition at which the second boundary condition can be replaced by

$$T_0(L) = T_\infty \qquad \text{or} \qquad \frac{dT_0(L)}{dX} = 0 \quad . \tag{C.9}$$

Either approximation of (C.9) states that the heat transfer rate at the end of the fin is zero. Apparently, this is acceptable only when the total amount of heat dissipated at the end of the fin is comparatively small. Consider the situation when the heat transfer coefficient is constant, the expression for the total heat flux conducted away from fin is given by

$$Q = 2\pi ah \int_0^L [T_0(X) - T_\infty]\, dX + \pi a^2 h\, [T_0(L) - T_\infty]$$

$$= 2\pi aLh \int_0^1 \phi_0(x)dx + \pi a^2 h \phi_0(1) \quad ,$$

it can be seen that the approximation holds when

$$\frac{\pi a^2 h\, \phi_0(1)}{2\pi aLh \displaystyle\int_0^1 \phi_0(x)dx} << O[1] \quad ,$$

i.e.

$$\frac{a\phi_0(1)}{2L\int_0^1 \phi_0(x)dx} << O[1] \quad .$$

If ϕ_0 and x are normalized, this reduces to

$$\frac{a}{2L} << O[1] \quad .$$

In a word, if Bi << O[1] and $\frac{a}{L}$ << O[1], the fin system is approximately governed by the equation

$$\frac{d^2T_0(X)}{dX^2} - \frac{2h}{aK_s}[T_0(X) - T_\infty] = 0$$

and the associated boundary conditions

$$T_0(0) = T_r \quad \text{and} \quad T_0(L) = T_\infty \quad \left(\text{or } \frac{dT_0(L)}{dX} = 0\right) \quad .$$

In the study of conduction in a 6-inch triangular aluminum fin with 1/2-inch base width, the empirical data cited in reference [16] give

$$h = 0.29\left(\frac{\Delta T}{L}\right)^{1/4} \quad \frac{BTU}{hr\text{-}ft^2\text{-}F^\circ} \quad \text{for air}$$

and

$$K_s = 100 - 200 \quad \frac{BTU}{hr\text{-}ft\text{-}F^\circ} \quad \text{for aluminum,}$$

if $\Delta T = 100^\circ F$, the maximum Biot number of the problem is

$$Bi = \frac{Wh}{K_s} \simeq 5.4 \times 10^{-4} << O[1]$$

and the geometric ratio is

$$\frac{W}{L} \simeq 0.08 << O[1] \quad .$$

It is apparent that in this case, the quasi-one-dimensional conduction equation and the approximate boundary condition (C.9) are acceptable.

APPENDIX D

FORMULATION OF THE LIMITING CASE $\gamma = 0$

From appendix B, the similarity transformations are

$$\xi = \gamma x \quad ,$$

$$\eta = \frac{\phi_0^{1/3}(x)}{\left[\frac{4}{3}\int_0^x \phi_0^{1/3}(S)\,dS\right]^{1/4}} y \quad ,$$

$$\psi(x,y) = \left[\frac{4}{3}\int_0^x \phi_0^{1/3}(S)\,dS\right]^{3/4} f(\xi,\eta) \quad ,$$

and

$$\phi(x,y) = \phi_0(x)\,\Phi(\xi,\eta) \quad .$$

As $\gamma \to 0$, the variable $\xi \to 0$, a small modification of this transformation for this case is to set $\xi = x$, and then the boundary layer equations become

$$\Pr\,(f''' + \Phi) + ff'' - \frac{2}{3}(f')^2 = H_1(\phi_0)(f')^2 + H_2(\phi_0)\left(f'\frac{\partial f'}{\partial \xi} - f''\frac{\partial f}{\partial \xi}\right) + \Pr\,\gamma\xi\Phi \qquad (D.1)$$

and

$$\Phi'' + f\Phi' = 3H_1(\phi_0)f'\Phi + H_2(\phi_0)\left(f'\frac{\partial \Phi}{\partial \xi} + \Phi'\frac{\partial f}{\partial \xi}\right) \qquad (D.2)$$

where H_1 and H_2 are defined as

$$H_1(\phi_0) = -\frac{4}{3}\frac{d\phi_0^{-1/3}(x)}{dx}\int_0^x \phi_0^{1/3}(S)\,dS \qquad (D.3)$$

and

$$H_2(\phi_0) = \frac{4}{3}\,\phi_0^{-1/3}(x)\int_0^x \phi_0^{1/3}(S)\,dS \quad . \qquad (D.4)$$

It is obvious that as $\gamma \to 0$, the last term in equation (D.1) becomes zero while $H_1(\phi_0)$ and $H_2(\phi_0)$ may not vanish. Since $\xi = x$, $G_0(\xi) \equiv \phi_0(x)$, i.e. not only numerically equal but also of the same form. Thus as $\gamma \to 0$, equations (D.1) and (D.2) become

$$\Pr\,(f''' + \Phi) + ff'' - \frac{2}{3}(f')^2 = H_1(G_0)(f')^2 + H_2(G_0)\left[f'\frac{\partial f'}{\partial \xi} - f''\frac{\partial f}{\partial \xi}\right] \qquad (D.5)$$

and

$$\Phi'' + f\Phi' = 3H_1(G_0)f'\Phi + H_2(G_0)\left[f'\frac{\partial \Phi}{\partial \xi} - \Phi'\frac{\partial f}{\partial \xi}\right] , \qquad (D.6)$$

the transformed boundary conditions are

$$\eta = 0 ; \qquad f = f' = \Phi - 1 = 0$$

$$\eta = \infty ; \qquad f' = \Phi = 0,$$

and the solution of this boundary value problem at the leading edge will give the "initial" condition at $\xi = 0$. Similarly, the conduction in solid is governed by

$$\frac{d}{d\xi}\left(\xi \frac{dG_0(\xi)}{d\xi}\right) + C\Phi'(\xi,0)\frac{d\left[\frac{4}{3}\int_0^{\xi} G_0{}^{1/3}(S)dS\right]^{3/4}}{d\xi} G_0(\xi) = 0 \qquad (D.7)$$

with

$$\left(\xi \frac{dG_0(\xi)}{d\xi}\right)_{\xi=0} = 0 \qquad \text{and} \qquad G_0(1) = 1 \ .$$

Equations (D.5) and (D.6) indicate that in spite of the necessity of satisfying the above conduction equations and their associated

boundary conditions, the similarity solutions, if they exist, should also meet the following two conditions:

(1) function $H_1(G_0)$ should be independent of ξ, and

(2) either function $H_2(G_0)$ is zero everywhere or Φ and f are function of η only (with $H_2(G_0)$ bounded).

In the first case,

$$H_1(G_0) = -\frac{4}{3}\frac{dG_0^{-1/3}(\xi)}{d\xi}\int_0^{\xi} G_0^{1/3}(S)dS = A_1 \quad , \text{ say,} \tag{D.8}$$

and

$$H_2(G_0) = \frac{4}{3} G_0^{-1/3}(\xi)\int_0^{\xi} G_0^{1/3}(S)dS = 0 \ , \tag{D.9}$$

when condition (D.8) is integrated with respect to ξ, one can easily verify that $A_1 = \frac{4}{3}$ with the help of condition (D.9). Whereas, no wall temperature $G_0(\xi)$ can satisfy condition (D.9) and hence similarity solution is impossible in this case.

In the second case,

$$H_1(G_0) = -\frac{4}{3}\frac{dG_0^{-1/3}(\xi)}{d\xi}\int_0^{\xi} G_0^{1/3}(S)dS = A_2 \quad , \text{ say,} \tag{D.9a}$$

and

$$\Phi = \Phi(\eta) \qquad \text{and} \qquad f = f(\eta). \tag{D.10}$$

Condition (D.10) implies that those bracketed terms in equation (D.5) and (D.6) vanish automatically. Besides, in conduction equation (D.7),

$\Phi'(\xi,0)$ is no longer a function of ξ, i.e. $\Phi'(\xi,0) = \Phi'(0)$. Hence the possibility of similarity solutions relies on the satisfaction of (D.8) and the conduction problem.

It can be shown by substitution of the general power law surface temperature assumption, $G_0(\xi) = (a + b\xi)^n$, into the conduction part that only $G_0(\xi) = \xi^n$ may present similarity solution. If this power law assumption is made., then

$$H_1(G_0) = \frac{4n}{3(n + 3)}$$

and equation (D.7) becomes

$$n^2\xi^{n-1} + C\Phi'(0)\left(\frac{n + 3}{4}\right)^{1/4} \xi^{\frac{15n - 3}{12}} = 0 \ . \qquad \text{(D.11)}$$

The fact that this equation must be satisfied at every value of ξ between zero and unity requires that the power of ξ in both terms must be equal and then the sum of the two coefficients must be equated zero. Unfortunately, the first requirement yields $n = -3$ and with this value, not only can the second requirement not be satisfied but also the boundary condition at the tip of the fin is inadmissible. However, there is one special case for a similarity solution. When $n = 0$, i.e. an isothermal surface, and $C = 0$, equation (D.11) is always true and $H_1(G_0) = 0$. No conflict exists between conditions $n = 0$ and $C = 0$, on the contrary, the former is a consequence of the latter.

In chapter II, C is defined as

$$C = \frac{L}{W} \frac{K_f}{K_s} Ra^{1/4} \quad .$$

As far as a triangular fin is concerned, the slenderness $\frac{L}{W}$ will not likely be zero. The situations for C = 0 are therefore:

(1) $K_f = 0$, i.e. insulated fin surface, and obviously it will give rise to an uniformly heated body (n = 0), where $T = T_r$.

(2) $K_s = \infty$, although physically a solid with infinite thermal conductivity does not exist, it still can be conceived that such a perfect conductor will be an isothermal body under steady state condition.

(3) Ra = 0 due to $\theta_r = 0$. Apparently when $T_r = T_\infty$, the entire fin is of the same temperature T_∞.

In fact, the existence of an isothermal fin for C = 0 can be used when $\gamma \geq 0$. As C = 0, the conduction equation (D.7) reduces to

$$\frac{d}{d\xi}\left(\xi \frac{dG_0}{d\xi}\right) = 0 \quad .$$

After integration and using boundary condition

$$\left(\xi \frac{dG_0}{d\xi}\right)_{\xi=0} = 0 \quad ,$$

it yields

$$\frac{dG_0}{d\xi} = 0$$

one more integration and the isothermal profile is obtained following

the application of $G_0(\gamma) = 1$. Hence, when $C = 0$,

$$G_0(\xi) = 1.$$

It is evident that this solution is, in a sense, trivial. No matter whether $C = 0$ because of situation (1) or (3), no free convection can take place. However, it can be a good approximation to the solution for convective fin with very high conductivity in the solid. In addition to this practical usage, the behavior of the isothermal surface can be used as a way of checking the "local similarity transformation" of this study. When $G_0 = 1$ throughout the fin, the transformation becomes

$$\xi = x \,, \qquad \eta = \left(\frac{3}{4}\right)^{1/4} \frac{y}{x^{1/4}} \,,$$

$$f = \left(\frac{3}{4}\right)^{3/4} \frac{\psi}{x^{3/4}} \qquad \text{and} \qquad \Phi = \phi \,.$$

These are the same forms as were developed for the classical isothermal plate problem in references [1,3,4,5].

APPENDIX E

NUMERICAL TECHNIQUE

It has already been shown that this rotating fin problem is governed by the boundary layer equations;

$$\Pr(f''' + \Phi) + ff'' - \frac{2}{3}(f')^2 = F_1(G_0,\xi)(f')^2 + F_2(G_0,\xi)\left(f'\frac{\partial f'}{\partial \xi} - f''\frac{\partial f}{\partial \xi}\right) + \Pr\xi\Phi \ , \qquad (E.1)$$

$$\Phi'' + f\Phi' = 3F_1(G_0,\xi)f'\Phi + F_2(G_0,\xi)\left(f'\frac{\partial \Phi}{\partial \xi} - \Phi'\frac{\partial f}{\partial \xi}\right) \ , \qquad (E.2)$$

and the quasi-one-dimensional equation of conduction,

$$\frac{d}{d\xi}\left(\xi\frac{dG_0}{d\xi}\right) + F_3(G_0,\xi)G_0 = 0 \ , \qquad (E.3)$$

with the associated boundary conditions;

$$\left.\begin{aligned} \eta = 0 : &\quad f = f' = \Phi - 1 = 0 \ , \\ \eta = \infty : &\quad f' = \Phi = 0 \ , \end{aligned}\right\} \qquad (E.4)$$

and

$$\left.\begin{aligned} \xi = 0 : &\quad \xi\frac{dG_0}{d\xi} = 0 \ , \\ \xi = \gamma : &\quad G_0 = 1 \ , \end{aligned}\right\} \qquad (E.5)$$

provided that $\frac{dG_0}{d\xi}^{-1/3}$ is finite and the derivatives of f and Φ are bounded when $\xi = 0$. Functions F_1, F_2 and F_3 are defined as

$$F_1(G_0,\xi) = \frac{4}{3}\,G_0^{-4/3}(\xi)\,\frac{dG_0(\xi)}{d\xi}\int_0^{\xi} G_0^{1/3}(S)dS \ ,$$

$$F_2(G_0,\xi) = \frac{4}{3}\,G_0^{-1/3}(\xi)\int_0^{\xi} G_0^{1/3}(S)dS \ ,$$

and

$$F_3(G_0,\xi) = C\Phi'(\xi,0)\ \frac{d}{d\xi}\left[\frac{4}{3\gamma}\int_0^{\xi} G_0{}^{1/3}(S)dS\right]^{3/4} .$$

The complexity of these three coupled governing equations reveals that the analytic solution can not be procured by means of established mathematical techniques. A numerical method is hence considered as the most suitable scheme in solving this problem.

Apparently, the conduction equation is coupled with the boundary layer equations through F_1, F_2 and F_3 which are functions of the interfacial temperature distribution $G_0(\xi)$. Therefore, the matching problem between conduction and convection systems can be solved with a proper iterative routine searching for the true interfacial temperature $G_0(\xi)$.

From the standpoint of free convection alone, the surface temperature $G_0(\xi)$ can be regarded as the input of the problem. With a reasonable guessed profile $G_0(\xi)$ increasing from a positive value at $\xi = 0$ to unity at $\xi = \gamma$, the strongly coupled boundary layer equations can be solved using the concept of "local similarity".

As stated in appendix B, the problem of starting the integration is overcome by choosing the first ξ-level at the leading edge where both functions F_1 and F_2 vanish (as $\xi = 0$), and equations (E.1) and (E.2) become

$$Pr(f_1''' + \Phi_1) + f_1 f_1'' - \frac{2}{3}(f_1')^2 = 0 ,$$

and

$$\Phi_1'' + f_1\Phi_1' = 0 \ ,$$

where the subscript denotes the ordinal number of ξ-level.

The region is then divided into several equally spaced ξ-levels in order to have an easier estimation of the truncation errors of the approximations in ξ-direction. Besides, it can decrease the computing time and roundoff errors on evaluating the non-similar terms on the right-hand-sides of equations (E.1) and (E.2). Before the numerical work is applied to the successive ξ-levels, some numerical approximations of equally spaced interval with their associated truncation errors should first be introduced: if K is a function of the independent variable S, and ΔS is the step size, then

(1) two-point backward finite difference formula

$$\frac{\partial K_n}{\partial S} = \frac{1}{\Delta S}(K_n - K_{n-1}) + O\left[\frac{\Delta S}{2}\right] \ ,$$

(2) three-point backward finite difference formula

$$\frac{\partial K_n}{\partial S} = \frac{1}{2\Delta S}(3K_n - 4K_{n-1} + K_{n-2}) + O\left[\frac{\Delta S^2}{3}\right] \ ,$$

(3) central-difference method

$$\frac{\partial K_n}{\partial S} = \frac{1}{2\Delta S}(K_{n+1} - K_{n-1}) + O\left[\frac{\Delta S}{12}^2\right] \ ,$$

(4) two-point trapezoidal rule

$$\int_{S_{n-1}}^{S_n} K(t)dt = \frac{\Delta S}{2}(K_n + K_{n-1}) + O\left[\frac{\Delta S^3}{12}\right] \ ,$$

(5) Simpson's rule for even number of intervals, i.e. n = odd,

$$\int_0^{S_n} K(t)dt = \frac{\Delta S}{3} \sum_{m=3}^{n} (K_m + 4K_{m-1} + K_{m-2}) + O\left[\frac{\Delta S^4}{180}\right] ,$$

At the second ξ-level, two-point hackward finite difference is employed in representing the ξ-derivatives of f, f', and Φ, while $\frac{dG_0}{d\xi}$ is approximated with central-difference method. The integral of $G_0^{1/3}$ is substituted by the two-point trapezoidal rule. The ordinary differential equations to be integrated with respect to η at this level become

$$Pr(f_2''' + \Phi_2) + f_2 f_2'' - \frac{2}{3}(f_2')^2 = \frac{1}{9} G_2^{-4/3}(G_3 - G_1)(G_2^{1/3} + G_1^{1/3})(f_2')^2$$

$$+ \frac{2}{3}\left[1 + (G_1/G_2)^{1/3}\right]\left[(f_2')^2 - f_2'f_1' - f_2''f_2 + f_2''f_1\right] + Pr\xi_2\Phi_2 + O[\Delta\xi^2]$$

and

$$\Phi_2'' + f_2\Phi_2' = \frac{1}{3} G_2^{-4/3}(G_3 - G_1)(G_2^{1/3} + G_1^{1/3})f_2'\Phi_2$$

$$+ \frac{2}{3}\left[1 + (G_1/G_2)^{1/3}\right](f_2'\Phi_2 - f_2'\Phi_1 - \Phi_2'f_2 + \Phi_2'f_1) + O[\Delta\xi^2] \quad .$$

The ξ-derivatives of f, f' and Φ in the successive levels are approximated using the three-point backward finite difference. The central difference is still applied to $\frac{dG_0}{d\xi}$ throughout the remaining ξ-levels but the last one where $\frac{dG_0}{d\xi}$ is substituted by three-point backward finite difference. At each odd ξ-level (with an even number of intervals), the integral of $G_0^{1/3}$ is evaluated with simpson's rule, while at the even ξ-levels, the integral over the last interval

of ξ can be replaced by the two-point trapezoidal rule. Therefore, it is easy to show that if n is odd and $\xi_2 < \xi_n < \gamma$,

$$\Pr(f_n''' + \Phi_n) + f_n f_n'' - \frac{2}{3}(f_n')^2$$

$$= \frac{2}{27} G_n^{-4/3}(G_{n+1} - G_{n-1})\left[\sum_{m=3}^{n}(G_m^{1/3} + 4G_{m-1}^{1/3} + G_{m-2}^{1/3})\right](f_n')^2$$

$$+ \frac{2}{9} G_n^{-1/3}\left[\sum_{m=3}^{n}(G_m^{1/3} + 4G_{m-1}^{1/3} + G_{m-2}^{1/3})\right]\left[f_n'(3f_n' - 4f_{n-1}' + f_{n-2}')\right.$$

$$\left. - f_n''(3f_n - 4f_{n-1} + f_{n-2})\right] + \Pr\xi_n\Phi_n + O[\Delta\xi^3]$$

and

$$\Phi_n'' + f_n\Phi_n' = \frac{2}{9} G_n^{-1/3}(G_{n+1} - G_{n-1})\left[\sum_{m=3}^{n}(G_m^{1/3} + 4G_{m-1}^{1/3} + G_{m-2}^{1/3})\right] f_n'\Phi_n$$

$$+ \frac{2}{9} G_n^{-1/3}\left[\sum_{m=3}^{n}(G_m^{1/3} + 4G_{m-1}^{1/3} + G_{m-2}^{1/3})\right]\left[f_n'(3\Phi_n - 4\Phi_{n-1} + \Phi_{n-2})\right.$$

$$\left. -\Phi_n'(3f_n - 4f_{n-1} + f_{n-2})\right] + O[\Delta\xi^3] \quad .$$

If n is even,

$$\Pr(f_n''' + \Phi_n) + f_n f_n'' - \frac{2}{3}(f_n')^2$$

$$= \frac{2}{9} G_n^{-4/3}(G_{n+1} - G_{n-1})\left[\frac{1}{3}\sum_{m=3}^{n-1}(G_m^{1/3} + 4G_{m-1}^{1/3} + G_{m-2}^{1/3}) + \frac{1}{2}(G_n^{1/3} + G_{n-1}^{1/3})\right](f_n')^2$$

$$+ \frac{2}{3} G_n^{-1/3}\left[\frac{1}{3}\sum_{m=3}^{n-1}(G_m^{1/3} + G_{m-1}^{1/3} + G_{m-2}^{1/3})\right.$$

$$\left. + \frac{1}{2}(G_n^{1/3} + G_{n-1}^{1/3})\right]\left[f_n'(3f_n' - 4f_{n-1}' + f_{n-2}')\right.$$

$$\left. - f_n''(3f_n - 4f_{n-1} + f_{n-2})\right] + \Pr\xi_n\Phi_n + O[\Delta\xi^2]$$

and

$$\Phi_n'' + f_n\Phi_n' = \frac{2}{3} G_n^{-4/3}(G_{n+1} - G_{n-1})\left[\frac{1}{3}\sum_{m=3}^{n-1}(G_m^{1/3} + 4G_{m-1}^{1/3} + G_{m-2}^{1/3})\right.$$

$$\left. + \frac{1}{2}(G_n^{1/3} + G_{n-1}^{1/3})\right] f_n'\Phi_n + \frac{2}{3} G_n^{-1/3}\left[\frac{1}{3}\sum_{m=3}^{n-1}(G_m^{1/3} + 4G_{m-1}^{1/3} + G_{m-2}^{1/3})\right.$$

$$\left. + \frac{1}{2}(G_n^{1/3} + G_{n-1}^{1/3})\right]\left[f_n'(3\Phi_n - 4\Phi_{n-1} + \Phi_{n-2})\right.$$

$$\left. - \Phi_n'(3f_n - 4f_{n-1} + f_{n-2})\right] + O[\Delta\xi^2]$$

At the last ξ-level, $\xi = \gamma$ and $G_n = 1$, if n is odd,

$$Pr(f_n''' + \Phi_n) + f_n f_n'' - \frac{2}{3}(f_n')^2$$

$$= \frac{2}{27}(3 - 4G_{n-1} + G_{n-2})\left[\sum_{m=3}^{n}(G_m^{1/3} + 4G_{m-1}^{1/3} + G_{m-2}^{1/3})\right](f_n')^2$$

$$+ \frac{2}{9}\left[\sum_{m=3}^{n}(G_m^{1/3} + 4G_{m-1}^{1/3} + G_{m-2}^{1/3})\right]\left[f_n'(3f_n' - 4f_{n-1}' + f_{n-2}')\right.$$

$$\left. - f_n''(3f_n - 4f_{n-1} + f_{n-2})\right] + Pr\gamma\Phi_n + O[\Delta\xi^3]$$

and

$$\Phi_n'' + f_n\Phi_n' = \frac{2}{9}(3 - 4G_{n-1} + G_{n-2})\left[\sum_{m=3}^{n}(G_m^{1/3} + 4G_{m-1}^{1/3} + G_{m-2}^{1/3})\right] f_n'\Phi_n$$

$$+ \frac{2}{9}\left[\sum_{m=3}^{n}(G_m^{1/3} + 4G_{m-1}^{1/3} + G_{m-2}^{1/3})\right]\left[f_n'(3\Phi_n - 4\Phi_{n-1} + \Phi_{n-2})\right.$$

$$\left. - \Phi_n'(3f_n - 4f_{n-1} + f_{n-2})\right] + O[\Delta\xi^3],$$

and if n is even,

$$\mathrm{Pr}(f_n''' + \Phi_n) + f_n f_n'' + \frac{2}{3}(f_n')^2$$

$$= \frac{2}{9}(3 - 4G_{n-1} + G_{n-2})\left[\frac{1}{3}\sum_{m=3}^{n-1}(G_m^{1/3} + 4G_{m-1}^{1/3} + G_{m-2}^{1/3}) + \frac{1}{2}G_{n-1}^{1/3}\right](f_n')^2$$

$$+ \frac{2}{3}\left[\frac{1}{3}\sum_{m=3}^{n-1}(G_m^{1/3} + 4G_{m-1}^{1/3} + G_{m-2}^{1/3}) + \frac{1}{2}G_{n-1}^{1/3}\right]\left[f_n'(3f_n' - 4f_{n-1}' + f_{n-2}')\right.$$

$$\left. - f_n''(3f_n - 4f_{n-1} + f_{n-2})\right] + \mathrm{Pr}\gamma\Phi_n + O[\Delta\xi^2]$$

and

$$\Phi_n'' + f_n\Phi_n' = \frac{2}{3}(3 - 4G_{n-1} + G_{n-2})\left[\frac{1}{3}\sum_{m=3}^{n-1}(G_m^{1/3} + 4G_{m-1}^{1/3} + G_{m-2}^{1/3}) + \frac{1}{2}G_{n-1}^{1/3}\right]f_n'\Phi_n$$

$$+ \frac{2}{3}\left[\frac{1}{3}\sum_{m=3}^{n-1}(G_m^{1/3} + 4G_{m-1}^{1/3} + G_{m-2}^{1/3}) + \frac{1}{2}G_{n-1}^{1/3}\right]\left[f_n'(3\Phi_n - 4\Phi_{n-1} + \Phi_{n-2})\right.$$

$$\left. - \Phi_n'(3f_n - 4f_{n-1} + f_{n-2})\right] + O[\Delta\xi^2] \quad .$$

The coupled partial differential equations of the boundary layer problem have thus been replaced by a finite set of coupled ordinary differential equations with an error of $O[\Delta\xi^2]$. Boundary condition (E.4) indicates that it is a boundary value problem at each ξ-level. After the values of f'' and Φ' at $\eta = 0$ have been guessed, the integration with respect to η can be carried out with a fourth-order Runge-Kutta method. A scheme has to be set up to modify the initial

guesses of f'' and Φ until the boundary conditions $f' = 0$ and $\Phi = 0$ outside the boundary layer are satisfied.

A few trial runs have shown that the numerical integration is extremely sensitive to the initial guesses of f'' and Φ' at $\eta = 0$. The numerical routine is unstable if the guessed $f''(\xi,0)$ and $\Phi'(\xi,0)$ are not very close to their correct values. The iterative technique of Nachtcheim and Swigert [14] with a least-squares convergence criterion on satisfying the asymptotic boundary conditions has been adopted. Preliminary tests indicates that when the asymptotic boundary conditions are satisfied at $\eta = 2$ with a condition on mean square error being less than 10^{-5}, the numerical integration is always stable and convergence of $f''(\xi,0)$ and $\Phi'(\xi,0)$ can be assured with their initial guesses being 1.0 and -1.0 respectively. Using the converged $f''(\xi,0)$ and $\Phi'(\xi,0)$ as the initial guesses, the integration (following the same scheme) can subsequently be carried out to $\eta = 4$, 6, 8 and then 10 without any special difficulty in either the stability or the convergence of the numerical program. The only disadvantage of this technique is the time of computation, even with a IBM 360/67 high speed computer. For saving computing time, large step sizes for ξ and η with an acceptable accuracy are required. The truncation error of the coupled ordinary differential equations is shown to be of the order of $\Delta\xi^2$. In this study the step size $\Delta\xi$ is taken to be 0.02 so that the truncation error due to the "localization" of the problem is

less than one percent. Tests were conducted with different step sizes of η, and the converged $f''(\xi,0)$ and $\Phi'(\xi,0)$ were compared separately at two ξ-levels. The comparison suggested that a step size of 0.04 for the integration in η-direction can give an accuracy to these eiganvalues within an order of one percent.

This numerical solution of the boundary layer equations provides the values of $\Phi'(\xi,0)$ at each ξ-level for the initial guessed profile of $G_0(\xi)$. These values of $\Phi'(\xi,0)$ and $G_0(\xi)$ are substituted into the convective coefficient F_3 along the fin surface. By means of a fourth-order Runge-Kutta method, equation (E.3) can be integrated from the root with the boundary condition $G_0(\gamma) = 1$ and a guessed value of $\left(\xi\frac{dG_0}{d\xi}\right)_{\xi=\gamma}$ to give $\frac{dG_0}{d\xi}$ and $G_0(\xi)$ at each level, except the leading edge. When $\xi = 0$, the numerical integration of $\left(\frac{dG_0}{d\xi}\right)_{\xi=0}$ gives an infinite value of $G_0(0)$ since the integrand itself, obtained from $\left[\left(\xi\frac{dG_0}{d\xi}\right)_{\xi=0}\Big/\xi\right]_{\xi=0}$, is infinite. However, equation (E.3) can be re-written as

$$\xi\frac{d^2G_0}{d\xi^2} + \frac{dG_0}{d\xi} + F_3G_0 = 0 \ . \qquad \text{(E.6)}$$

Integration of this equation simultaneously with equation (E.3) using the Runge-Kutta method can respectively give the values of $G_0(\xi)$ and $\xi\frac{dG_0}{d\xi}$ at each level. A shooting method is then employed to modify the guessed value of $\left(\xi\frac{dG_0}{d\xi}\right)_{\xi=\gamma}$ until the other boundary condition, $\left(\xi\frac{dG_0}{d\xi}\right)_{\xi=0} = 0$ is satisfied to five decimal places.

Logically, this newly obtained $G_0(\xi)$ and the former $G_0(\xi)$ should give a better guessed input to the boundary layer system and the whole procedure is then iterated until $G_0(\xi)$ converges to the true temperature distribution. However, practical experience points out that the computing time in solving the boundary layer problem is much longer than the time on integrating the fin equations. Hence, it is better to refine $G_0(\xi)$ through the conduction equations as much as possible. When an improved $G_0(\xi)$, obtained from halving the lately obtained solution and the previous values of $G_0(\xi)$, is substituted into equations (E.3) and (E.6) to evaluate a new set of F_3 with the same values of $\Phi'(\xi,0)$, an iterative loop in integrating these two equations is formed. The finally converged $G_0(\xi)$ in this conduction loop is then used as the improved input of the boundary layer problem to generate another set values for $\Phi'(\xi,0)$. Such iteration between the conduction loop and the boundary layer problem continues until $G_0(\xi)$ converges at every ξ-level with an accuracy of ten decimal places.

In order to reduce the round-off error, double precision was used throughout the calculation. This requires a computing for a complete solution of about 30 minutes using an IBM 360/67 machine. Followed is the computer program used in this work:

```
C
C
C      PROGRAM FOR SOLVING COUPLED HEAT TRANSFER PROBLEM
C      OF CONDUCTION AND LAMINAR FREE CONVECTION OF A
C      HEATED TRIANGULAR FIN IN A CENTRIFUGAL FORCE FIELD
C
C
       EXTERNAL VI,TI,VII,TII,VIII,TIII
       REAL*8 GXJ(100),GXK(100),GXJ13(100),GXK13(100),
      1HEAT(100),HEAF(100),DIFSUM(100),GDO11,GDO21,
      2GDO31,GAMA43,H1I,F2I
       REAL*8 R13,R23,R14,R53,R43,SS,ST,SL,EI(100),
      1SIGMA(100),GXI13(100),DIF(100),RAT(100),GDI(100),
      2GDI1(100),GDII(100),GDII1(100),GAMA,CN,CL,GDK11,
      3GDK12,GDHH,GDHH1,GDK21,GDK22,GDK31,GDK32,GDK41,
      4GDK42,RESI,GDCOR,DI,DII,GX,GXO(100),GAMA3
       REAL*8 SF2(251),SF1(251),SF(251),SH1(251),SH(251),
      1SFOMI1(251),SF1MI1(251),SHOMI1(251),SH1MI1(251),
      2SFOMI2(251),SF1MI2(251),SHOMI2(251),SH1MI2(251),
      3GXI(100),XI(100),AC,BC,CC,DC,EC,FC,GC,HC,PR
       COMMON SF2,SF1,SF,SH1,SH,SFOMI1,SF1MI1,SHOMI1,
      1SH1MI1,SFOMI2,SF1MI2,SHOMI2,SH1MI2,PR,AC,BC,CC,
      2DC,EC,FC,GC,HC,GXI,XI,IX,I,J,KO,KOA,KOB,KOC,
      3KOD,KOE
       READ (5,100) KO,KOA,KOB,KOC,KOD,KOE
  100 FORMAT(' ',6I3)
       IJ=1
       IL=1
       R13=1.0DO/3.0DO
       R14=0.25DO
       R23=2.0DO/3.0DO
       R43=1.0DO+R13
       R53=1.0DO+R23
       LOOP=1
       ITERA=1
C
C      READ PARAMETER C (CN),PRANDTL NUMBER (PR),NUMBER
C      OF DISCRITIZED XI-LEVELS (NM),AND THE GUESSED
C      EIGANVALUES,F2I AND H1I,FOR EVERY XI-LEVEL
C
       READ (5,101) CN
  101 FORMAT (' ',D23.16)
       READ (5,102)  PR,F2I,H1I,NM
  102 FORMAT (' ',3D23.16, I4)
       SIGMA(1)=0.0
       DIF(1)=0.0DO
       RAT(1)=0.0DO
       NODD=NM/2*2-1
```

```
      IV=NODD+1
      MN=NM-1
C
C     READ THE INITIALLY GUESSED INTERFACIAL TEMPERATURE
C     DISTRIBUTION,GXI,AT EACH XI-LEVEL AND CALCULATE
C     THE COEFFICIENTS REQUIRED IN THE INTEGRATION OF
C     BOUNDARY LAYER EQUATIONS
C
      READ (5,103) GXI(1),XI(1)
  103 FORMAT (' ',2D23.16)
      DO 1 IZ=2,NM
      READ (5,103) GXI(IZ),XI(IZ)
      DIF(IZ)=XI(IZ)-XI(IZ-1)
      RAT(IZ)=DIF(IZ)/XI(IZ)
    1 CONTINUE
      GAMA=XI(NM)
      GAMA3=GAMA**3*R43
      GAMA43=R43/GAMA
    2 IK=1
      GXO(1)=GXI(1)
      GXI13(1)=GXI(1)**R13
      DO 3 IZ=2,NM
      GXO(IZ)=GXI(IZ)
      GXJ(IZ-1)=GXI(IZ-1)+(GXI(IZ)-GXI(IZ-1))/3.0D0
      GXK(IZ-1)=GXJ(IZ-1)+(GXI(IZ)-GXI(IZ-1))/3.0D0
      GXI13(IZ)=GXI(IZ)**R13
      GXJ13(IZ-1)=GXJ(IZ-1)**R13
      GXK13(IZ-1)=GXK(IZ-1)**R13
    3 CONTINUE
      DO 4 I=1,251
      SF1MI1(I)=0.0D0
      SF0MI1(I)=0.0D0
      SH1MI1(I)=0.0D0
      SH0MI1(I)=0.0D0
    4 CONTINUE
      SS=0.0D0
C
C     START SOLVING THE BOUNDARY LAYER PROBLEM WITH
C     SUBROUTINE "LOSIM" TO OBTAIN THE EIGANVALUES (EI)
C     AT EACH XI-LEVEL
C
      IX=1
      AC=R23
      BC=R43
      CALL LOSIM(F2I,H1I,VI,TI)
      EI(1)=H1I
      IX=2
      SIGMA(2)=(GXI13(2)+GXI13(1))*XI(2)/2.0D0
```

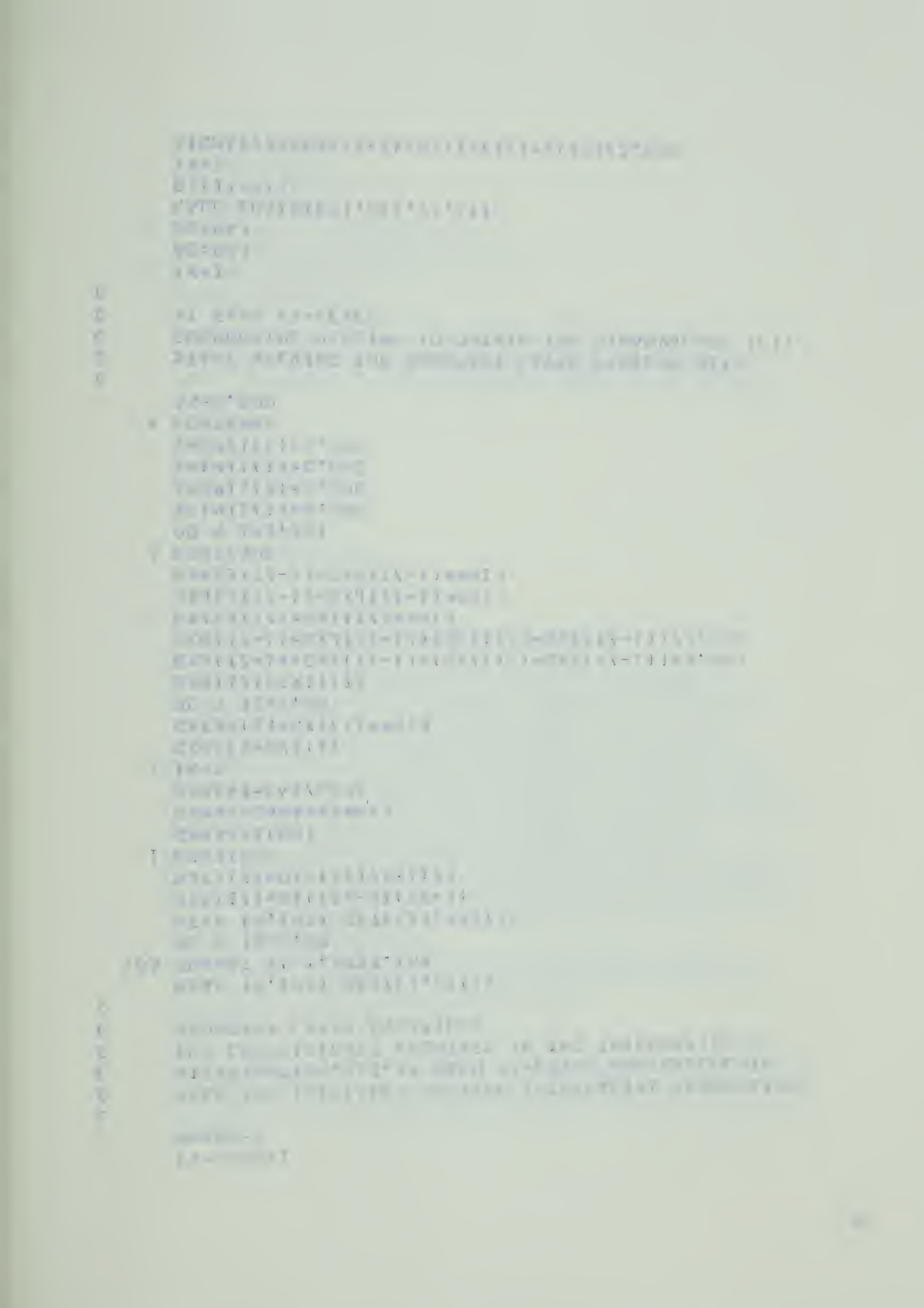

```
      AC=(2.0*(GXI(3)-GXI(1))/GXI(2)**R43/9.0D0+R43
     1/GXI13(2))*SIGMA(2)/XI(2)/PR+R23/PR
      CC=R43*SIGMA(2)/GXI13(2)/XI(2)/PR
      BC=CC+1.0D0/PR
      DC=1.0D0-XI(2)
      EC=AC*2.0D0
      HC=CC*PR
      GC=BC*PR
      FC=R23*(GXI(3)-GXI(1))*SIGMA(2)/GXI(2)**R43
     1/XI(2)+HC
      CALL LOSIM(F2I,H1I,VII,TII)
      EI(2)=H1I
      DO 5 IM=3,NODD,2
      SS=SS+(GXI13(IM-2)+4.0D0*GXI13(IM-1)+GXI13(IM))
     1/3.0D0
      SIGMA(IM)=SS*DIF(IM)
      BC=SS*R23/GXI13(IM)
      CC=1.0D0-XI(IM)
      EC=BC*(GXI(IM+1)-GXI(IM-1))/GXI(IM)
      AC=(EC+9.0D0*BC+2.0D0)/(3.0D0*PR)
      DC=AC*2.0D0
      IX=IM
      CALL LOSIM(F2I,H1I,VIII,TIII)
      EI(IM)=H1I
      IY=IM+1
      IF (IY .EQ. NM) GO TO 5
      ST=SS+(GXI13(IM)+GXI13(IM+1))/2.0D0
      SIGMA(IM+1)=ST*DIF(IM+1)
      BC=ST*R23/GXI13(IM+1)
      EC=BC*(GXI(IM+2)-GXI(IM))/GXI(IM+1)
      AC=(EC+9.0D0*BC+2.0D0)/(3.0D0*PR)
      CC=1.0D0-XI(IM+1)
      DC=AC*2.0D0
      IX=IM+1
      CALL LOSIM (F2I,H1I,VIII,TIII)
      EI(IM+1)=H1I
    5 CONTINUE
      IF (IV .EQ. NM) GO TO 6
      SL=SS+(GXI13(NM-2)+4.0D0*GXI13(NM-1)+GXI13(NM))
     1/3.0D0
      GO TO 7
    6 SL=SS+(GXI13(NM)+GXI13(NM-1))/2.0D0
    7 SIGMA(NM)=SL*DIF(NM)
      BC=SL*R23/GXI13(NM)
      EC=BC*(3.0D0-(4.0D0*GXI(NM-1)-GXI(NM-2))/GXI(NM))
      AC=(EC+9.0D0*BC+2.0D0)/(3.0D0*PR)
      CC=1.0D0-XI(NM)
      DC=2.0D0*AC
```

```
      IX=NM
      CALL LOSIM (F2I,H1I,VIII,TIII)
      EI(NM)=H1I
C
C     SOLVE THE CONDUCTION PROBLEM WITH A FOURTH-ORDER
C     RUNGE-KUTTA ROUTINE AND A SHOOTING METHOD. START
C     THE INTEGRATION FROM THE ROOT OF THE FIN WITH THE
C     BOUNDARY CONDITION GXI(NM)=1.0 AND A GUESSED VALUE
C     OF THE TOTAL HEAT TRANSFER,HEAT(NM),OF THE
C     OVERALL PROBLEM
C
      GDI(NM)=1.0D0
    8 HEAT(NM)=2.0D0
      DIFSUM(1)=(4.0D0*SIGMA(2)**0.75D0-SIGMA(3)
     1**0.75D0)/2.0D0/XI(2)
      DIFSUM(2)=SIGMA(3)**0.75D0/2.0D0/XI(2)
      DO 9 I=3,MN
      DIFSUM(I)=(SIGMA(I+1)**0.75D0-SIGMA(I-1)**0.75D0)
     1/2.0D0/XI(2)
    9 CONTINUE
      DIFSUM(NM)=(3.0D0*SIGMA(NM)**0.75D0-4.0D0
     1*SIGMA(NM-1)**0.75D0+SIGMA(NM-2)**0.75D0)
     2/2.0D0/XI(2)
   10 DO 11 IX=2,NM
      IR=NM+2-IX
      GDI1(IR)=HEAT(IR)/XI(IR)
      CL=CN*EI(IR)*DIFSUM(IR)*GAMA43**0.75D0
      GDO11=RAT(IR)*(GDI1(IR)+CL*GDI(IR))
      GDK11=DIF(IR)*CL*GDI(IR)
      GDK12=-DIF(IR)*GDI1(IR)
      GDHH=GDI(IR)+GDK12/3.0D0
      GDHH1=GDI1(IR)+GDO11/3.0D0
      CL=CN*GXK13(IR-1)*(EI(IR)-(EI(IR)-EI(IR-1))
     1/3.0D0)/(GAMA3*(SIGMA(IR-1)+(GXI13(IR-1)+4.0D0
     2*GXJ13(IR-1)+GXK13(IR-1))*DIF(IR)/9.0D0))**R14
      GDO21=DIF(IR)*(GDHH1+CL*GDHH)/(XI(IR)-DIF(IR)
     1/3.0D0)
      GDK21=DIF(IR)*CL*GDHH
      GDK22=-DIF(IR)*GDHH1
      GDHH=GDI(IR)+GDK22-GDK12/3.0D0
      GDHH1=GDI1(IR)+GDO21-GDO11/3.0D0
      CL=CN*GXJ13(IR-1)*(EI(IR-1)+(EI(IR)-EI(IR-1))
     1/3.0D0)/(GAMA3*(SIGMA(IR-1)+(GXJ13(IR-1)
     2+GXI13(IR-1))*DIF(IR)/6.0D0))**R14
      GDO31=DIF(IR)*(GDHH1+CL*GDHH)/(XI(IR)-DIF(IR)*R23)
      GDK31=DIF(IR)*CL*GDHH
      GDK32=-DIF(IR)*GDHH1
      GDHH=GDI(IR)-GDK22+GDK32+GDK12
```

```
      GDHH1=GDI1(IR)-GDO21+GDO31+GDO11
      CL=CN*EI(IR-1)*DIFSUM(IR-1)*GAMA43**0.75D0
      GDK41=DIF(IR)*CL*GDHH
      GDK42=-DIF(IR)*GDHH1
      GDI(IR-1)=GDI(IR)+(GDK12+3.0D0*(GDK22+GDK32)
     1+GDK42)/8.0D0
      HEAT(IR-1)=HEAT(IR)+(GDK11+3.0D0*(GDK21+GDK31)
     1+GDK41)/8.0D0
   11 CONTINUE
C
C     CHECK THE SATISFACTION OF THE BOUNDARY CONDITION
C     AT FIN TIP,HEAT(1)=0.0,AND THE CONVERGENCE OF GXI
C
      DI=HEAT(1)
      IF (DI .LT. 0.0D0) GO TO 19
      IF (DABS(DI) .GT. 1.0D-5)  GO TO 19
      DO 12 I=1,MN
      RESI=GXI(I)-GDI(I)
      IF (DABS(RESI) .LT. 1.0D-5) GO TO 12
      IJ=2
   12 CONTINUE
      IF (IJ .GT. 1) GO TO 24
   13 WRITE (6,104)
  104 FORMAT(10X,'GXI(IX)',14X,'XI(IX)',16X,'EI(IX)',
     113X,'IX',12X,' SIGMA(IX)',12X,' GXO(IX)')
      DO 14 IX=1,NM
      WRITE (6,105) GXI(IX),XI(IX),EI(IX),IX,SIGMA(IX),
     1GXO(IX)
  105 FORMAT (' ',3D23.16, I4, 2D23.16)
   14 CONTINUE
      WRITE (6,106) ITERA,LOOP
  106 FORMAT (' ITERATION= ',I6,' LOOP= ',I4)
C
C     CHECK THE MATCHING OF INTERFACIAL TEMPERATURE
C
      DO 15 I=1,MN
      RESI=GXI(I)-GXO(I)
      IF (DABS(RESI) .LT. 1.0D-5) GO TO 15
      IK=2
   15 CONTINUE
      DO 18 IX=1,NM
      GX=GXI(IX)
      IF (GX .GT. 1.0D-18) GO TO 17
      GXI(IX)=1.0D-18
      WRITE (7,103) GXI(IX), XI(IX)
      GO TO 18
   17 GXI(IX)=GX
      WRITE (7,103) GXI(IX), XI(IX)
```

```
   18 CONTINUE
      IK=1
      LOOP=LOOP+1
      IF (IK .GT. 1) GO TO 2
      KC=KO+1
      IF (KO .EQ. 2) GO TO 2
      WRITE (6,107)
  107 FORMAT(' PROBLEM IS SOLVED ')
      STOP
   19 ITERA=ITERA+1
C
C     OF THE TOTAL HEAT TRANSFER,HEAF(NM),SO THAT THE
C     THE TOTAL HEAT TRANSFER RATE,HEAF(NM),SO THAT THE
C     SHOOTING METHOD FOR MODIFYING THIS EIGANVALUE CAN
C     BE APPLIED
C
      GDII(NM)=1.0D0
      HEAF(NM)=HEAT(NM)*1.1D0
   20 DO 21 IX=2,NM
      IR=NM+2-IX
      GDII1(IR)=HEAF(IR)/XI(IR)
      CL=CN*EI(IR)*DIFSUM(IR)*GAMA43**0.75D0
      GDO11=RAT(IR)*(GDII1(IR)+CL*GDII(IR))
      GDK11=DIF(IR)*CL*GDII(IR)
      GDK12=-DIF(IR)*GDII1(IR)
      GDHH=GDII(IR)+GDK12/3.0D0
      GDHH1=GDII1(IR)+GDO11/3.0D0
      CL=CN*GXK13(IR-1)*(EI(IR)-(EI(IR)-EI(IR-1))
     1/3.0D0)/(GAMA3*(SIGMA(IR-1)+(GXI13(IR-1)+4.0D0
     2*GXJ13(IR-1)+GXK13(IR-1))*DIF(IR)/9.0D0))**R14
      GDO21=DIF(IR)*(GDHH1+CL*GDHH)/(XI(IR)-DIF(IR)
     1/3.0DC)
      GDK21=DIF(IR)*CL*GDHH
      GDK22=-DIF(IR)*GDHH1
      GDHH=GDII(IR)+GDK22-GDK12/3.0D0
      GDHH1=GDII1(IR)+GDO21-GDO11/3.0D0
      CL=CN*GXJ13(IR-1)*(EI(IR-1)+(EI(IR)-EI(IR-1))
     1/3.0DC)/(GAMA3*(SIGMA(IR-1)+GXJ13(IR-1)
     2+GXI13(IR-1))*DIF(IR)/6.0D0))**R14
      GDO31=DIF(IR)*(GDHH1+CL*GDHH)/(XI(IR)-DIF(IR)*R23)
      GDK31=DIF(IR)*CL*GDHH
      GDK32=-DIF(IR)*GDHH1
      GDHH=GDII(IR)-GDK22+GDK32+GDK12
      GDHH1=GDII1(IR)-GDO21+GDO31+GDO11
      CL=CN*EI(IR-1)*DIFSUM(IR-1)*GAMA43**0.75D0
      GDK41=DIF(IR)*CL*GDHH
      GDK42=-DIF(IR)*GDHH1
      GDII(IR-1)=GDII(IR)+(GDK12+3.0D0*(GDK22+GDK32)
```

```
     1+GDK42)/8.0D0
      HEAF(IR-1)=HEAF(IR)+(GDK11+3.0D0*(GDK21+GDK31)
     1+GDK41)/8.0D0
   21 CONTINUE
C
C     CHECK THE SATISFACTION OF THE BOUNDARY CONDITION
C     AT FIN TIP,HEAF(1)=0.0,AND THE CONVERGENCE OF GXI
C
      DII=HEAF(1)
      IF (DII .LT. 0.0D0) GO TO 37
      IF (DABS(DII) .GT. 1.0D-05) GO TO 37
   22 DO 23 IX=1,MN
      RESI=GXI(IX)-GDII(IX)
      IF (DABS(RESI) .LT. 1.0D-05) GO TO 23
      IL=2
   23 CONTINUE
      IF (IL .GT. 1) GO TO 29
C
C     FEED THE CONVERGED GXI OF CONDUCTION EQUATION BACK
C     TO THE BOUNDARY LAYER PROBLEM
C
      GO TO 13
C
C     IF GXI DOES NOT CONVERGE,GENERATE A NEW GXI AND
C     CALCULATE THE COEFFICIENTS  FOR THE NEW ITERATION
C     OF CONDUCTICN LOOP
C
   24 DO 27 IX=1,MN
      GX=(GDI(IX)+GXI(IX))/2.0D0
      IF (GX .GE. 1.0D-18) GO TO 25
      GXI(IX)=1.0D-18
      GO TO 26
   25 GXI(IX)=GX
   26 GXI13(IX)=GXI(IX)**R13
   27 CONTINUE
      DO 28 IX=2,NM
      GXJ(IX-1)=GXI(IX-1)+(GXI(IX)-GXI(IX-1))/3.0D0
      GXK(IX-1)=GXJ(IX-1)+(GXI(IX)-GXI(IX-1))/3.0D0
      GXJ13(IX-1)=GXJ(IX-1)**R13
      GXK13(IX-1)=GXK(IX-1)**R13
   28 CONTINUE
      IJ=1
      GO TO 34
   29 DO 32 IX=1,MN
      GX=(GDII(IX)+GXI(IX))/2.0D0
      IF (GX .GE. 1.0D-18) GO TO 30
      GXI(IX)=1.0D-18
      GO TO 31
```

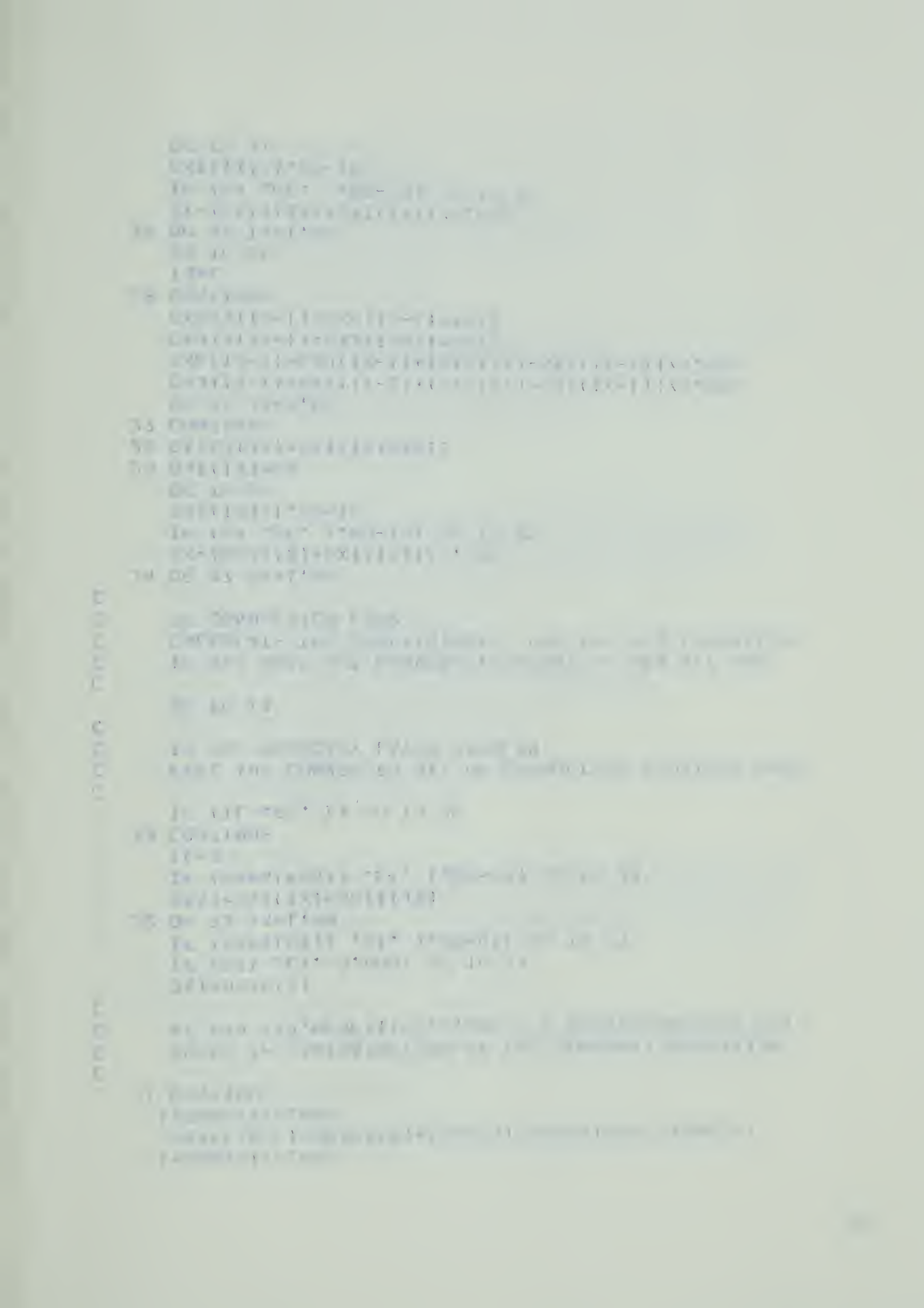

```
   30 GXI(IX)=GX
   31 GXI13(IX)=GXI(IX)**R13
   32 CONTINUE
      DO 33 IX=2,NM
      GXJ(IX-1)=GXI(IX-1)+(GXI(IX)-GXI(IX-1))/3.0D0
      GXK(IX-1)=GXJ(IX-1)+(GXI(IX)-GXI(IX-1))/3.0D0
      GXJ13(IX-1)=GXJ(IX-1)**R13
      GXK13(IX-1)=GXK(IX-1)**R13
   33 CONTINUE
      IL=1
   34 SIGMA(2)=(GXI13(2)+GXI13(1))*XI(2)/2.0D0
      DO 35 I=3,NODD,2
      SIGMA(I)=SIGMA(I-2)+(GXI13(I-2)+4.0D0*GXI13(I-1)
     1+GXI13(I))/3.0D0*DIF(I)
      SIGMA(I+1)=SIGMA(I)+(GXI13(I)+GXI13(I+1))/2.0D0
     1*DIF(I+1)
   35 CONTINUE
      IF (IV .EQ. NM) GO TO 36
      SIGMA(NM)=SIGMA(NM-2)+(GXI13(NM-2)+4.0D0
     1*GXI13(NM-1)+GXI13(NM))/3.0D0*DIF(NM)
   36 ITERA=ITERA+1
      GO TO 8
   37 DI=HEAF(1)-HEAT(1)
      IF (DABS(DI) .LT. 1.0D-20) GO TO 22
C
C     CALCULATE AN IMPROVED EIGANVALUE,HEAF(NM),BY MEANS
C     OF THE SHOOTING METHOD
C
      GDCOR=HEAT(NM)+(HEAT(NM)-HEAF(NM))/(HEAF(1)
     1-HEAT(1))*HEAT(1)
      HEAT(NM)=HEAF(NM)
      HEAF(NM)=GDCOR
      HEAT(1)=HEAF(1)
      ITERA=ITERA+1
      GO TO 20
      END
```

```
C
C
C     SUBROUTINE PROGRAM FOR INTEGRATING THE BOUNDARY
C     LAYER EQUATIONS WITH "LOCAL SIMILARITY" TECHNIQUE.
C     THE INTEGRATION IS ACCOMPLISHED USING A FOURTH-
C     ORDER RUNGE-KUTTA ROUTINE AND THE CONVERGENCE
C     IS BASED ON THE USE OF A LEAST-SQUARES METHOD
C
C
      SUBROUTINE LOSIM(F2I,H1I,FUNV,FUNT)
      REAL*8 SFOMI1(251),SF1MI1(251),SHOMI1(251),
     1SH1MI1(251),SFOMI2(251),SF1MI2(251),SHOMI2(251),
     2SH1MI2(251),F2(251),F1(251),F(251),H1(251),
     3H(251),SF2(251),SF1(251),SF(251),SH1(251),SH(251)
      REAL*8 F2M(4),F1M(4),H1M(4),HM(4),A2(4),A1(4),
     1GXI(100),XI(100),AC,BC,CC,DC,EC,FC,GC,HC,PR,
     2ERRDIF,AERRDI
      REAL*8 F2I,F1I,FI,H1I,HI,FF2,FF1,FF,HH1,HH,T,V,
     1K11,K12,K13,K14,K15,K21,K22,K23,K24,K25,K31,K32,
     2K33,K34,K35,K41,K42,K43,K44,K45,ERROR,ERRORO,
     3ERR,ERRAT,DEN,DF2,DH1,ETA,G,TEMP,VELO
      REAL O,P,Q,R,U,W,YS
      COMMON SF2,SF1,SF,SH1,SH,SFOMI1,SF1MI1,SHOMI1,
     1SH1MI1,SFOMI2,SF1MI2,SHOMI2,SH1MI2,PR,AC,BC,CC,
     2DC,EC,FC,GC,HC,GXI,XI,IX,I,J,KO,KOA,KOB,KOC,
     3KOD,KOE
      G=0.04DO
      ERRORO=0.ODO
      M=51
      HI=1.ODO
      FI=0.ODO
      F1I=0.ODO
   50 J=1
      N=M-1
C
C     START INTEGRATING THE BOUNDARY LAYER EQUATIONS
C
      F2(1)=F2I
      F1(1)=F1I
      F(1)=FI
      H1(1)=H1I
      H(1)=HI
      GO TO 53
   51 IF (J .GT. 2) GO TO 52
C
C     START INTEGRATING THE PERTURBATION EQUATIONS OF
C     THE BOUNDARY LAYER EQUATIONS (DUE TO THE VARIATION
C     OF EIGANVALUE F2I)
```

```
C
      F2(1)=1.0D0
      F1(1)=0.0D0
      F(1)=0.0D0
      H1(1)=0.0D0
      H(1)=0.0D0
      GO TO 53
   52 CONTINUE
C
C     START INTEGRATING THE PERTURBATION EQUATIONS OF
C     THE BOUNDARY LAYER EQUATIONS (DUE TO THE VARIATION
C     OF EIGANVALUE H1I)
C
      F2(1)=0.0D0
      F1(1)=0.0D0
      F(1)=0.0D0
      H1(1)=1.0D0
      H(1)=0.0D0
C
C     INTEGRATE THE EQUATION WITH A FOURTH-ORDER
C     RUNGE-KUTTA METHOD
C
   53 DO 54 I=1,N
      FF2=F2(I)
      FF1=F1(I)
      FF=F(I)
      HH=H(I)
      HH1=H1(I)
      CALL FUNV(V,FF2,FF1,FF,HH1,HH)
      CALL FUNT(T,FF2,FF1,FF,HH1,HH)
      K11=G*V
      K12=G*FF2
      K13=G*FF1
      K14=G*T
      K15=G*HH1
      FF2=F2(I)+K11/3.0D0
      FF1=F1(I)+K12/3.0D0
      FF=F(I)+K13/3.0D0
      HH=H(I)+K15/3.0D0
      HH1=H1(I)+K14/3.0D0
      CALL FUNV(V,FF2,FF1,FF,HH1,HH)
      CALL FUNT(T,FF2,FF1,FF,HH1,HH)
      K21=G*V
      K22=G*FF2
      K23=G*FF1
      K24=G*T
      K25=G*HH1
      FF2=F2(I)+K21-K11/3.0D0
```

```
      FF1=F1(I)+K22-K12/3.0D0
      FF=F(I)+K23-K13/3.0D0
      HH=H(I)+K25-K15/3.0D0
      HH1=H1(I)+K24-K14/3.0D0
      CALL FUNV(V,FF2,FF1,FF,HH1,HH)
      CALL FUNT(T,FF2,FF1,FF,HH1,HH)
      K31=G*V
      K32=G*FF2
      K33=G*FF1
      K34=G*T
      K35=G*HH1
      FF2=F2(I)-K21+K31+K11
      FF1=F1(I)-K22+K32+K12
      FF=F(I)-K23+K33+K13
      HH=H(I)-K25+K35+K15
      HH1=H1(I)-K24+K34+K14
      CALL FUNV(V,FF2,FF1,FF,HH1,HH)
      CALL FUNT(T,FF2,FF1,FF,HH1,HH)
      K41=G*V
      K42=G*FF2
      K43=G*FF1
      K44=G*T
      K45=G*HH1
      F2(I+1)=F2(I)+(K11+3.0D0*(K21+K31)+K41)/8.0D0
      F1(I+1)=F1(I)+(K12+3.0D0*(K22+K32)+K42)/8.0D0
      F(I+1)=F(I)+(K13+3.0D0*(K23+K33)+K43)/8.0D0
      H1(I+1)=H1(I)+(K14+3.0D0*(K24+K34)+K44)/8.0D0
      H(I+1)=H(I)+(K15+3.0D0*(K25+K35)+K45)/8.0D0
   54 CONTINUE
      IF (J .GT. 1) GO TO 56
      DO 55 I=1,M
      SF2(I)=F2(I)
      SF1(I)=F1(I)
      SF(I)=F(I)
      SH(I)=H(I)
      SH1(I)=H1(I)
   55 CONTINUE
   56 F1M(J)=F1(M)
      F2M(J)=F2(M)
      HM(J)=H(M)
      H1M(J)=H1(M)
      J=J+1
      IF (J .GT. 3) GO TO 57
      GO TO 51
C
C     CHECK THE MEAN SQUARE ERROR
C
   57 O=F1M(1)**2
```

```
      P=F2M(1)**2
      Q=HM(1)**2
      R=H1M(1)**2
      ERROR=O+P+Q+R
      IF (ERROR .LT. 1.0D-10) GO TO 58
      ERR=(ERROR-ERRORO)/ERROR
      ERRAT=DABS(ERR)
      GO TO 59
   58 ERRAT=0.0D0
      ERR=0.0D0
   59 ERRDIF=ERROR-ERRORO
      AERRDI=DABS(ERRDIF)
      IF (M .EQ. 101) GO TO 61
      IF (M .EQ. 151) GO TO 63
      IF (M .EQ. 201) GO TO 65
      IF (M .EQ. 251) GO TO 67
      IF (ERROR .LT. 1.0D-05) GO TO 60
      IF (AERRDI .LT. 1.0D-05) GO TO 60
      IF (ERRAT .GT. 1.0D-05) GO TO 68
   60 ERRORO=0.0D0
      M=101
      GO TO 69
   61 IF (ERROR .LT. 1.0D-05) GO TO 62
      IF (AERRDI .LT. 1.0D-05) GO TO 62
      IF (ERRAT .GT. 1.0D-05) GO TO 68
   62 ERRORO=0.0D0
      M=151
      GO TO 69
   63 IF (ERROR .LT. 1.0D-05) GO TO 64
      IF (AERRDI .LT. 1.0D-05) GO TO 64
      IF (ERRAT .GT. 1.0D-05) GO TO 68
   64 ERRORO=0.0D0
      M=201
      GO TO 69
   65 IF (ERROR .LT. 1.0D-05) GO TO 66
      IF (AERRDI .LT. 1.0D-05) GO TO 66
      IF (ERRAT .GT. 1.0D-05) GO TO 68
   66 ERRORO=0.0D0
      M=251
      GO TO 69
   67 IF (ERRAT .LT. 1.0D-10) GO TO 70
      IF (ERROR .LT. 1.0D-10) GO TO 70
      IF (AERRDI .LT. 1.0D-10) GO TO 70
   68 ERRORO=ERROR
C
C     GENERATE AN IMPROVED SET OF EIGANVALUES F2I AND
C     H1I
C
```

```
   69 A1(1)=F1M(1)*F1M(2)+HM(1)*HM(2)+F2M(1)*F2M(2)
     1+H1M(1)*H1M(2)
      A1(2)=F1M(2)**2+HM(2)**2+F2M(2)**2+H1M(2)**2
      A1(3)=F1M(2)*F1M(3)+HM(2)*HM(3)+F2M(2)*F2M(3)
     1+H1M(2)*H1M(3)
      A2(1)=F1M(1)*F1M(3)+HM(1)*HM(3)+F2M(1)*F2M(3)
     1+H1M(1)*H1M(3)
      A2(2)=A1(3)
      A2(3)=F1M(3)**2+HM(3)**2+F2M(3)**2+H1M(3)**2
      DEN=A1(2)*A2(3)-A1(3)*A2(2)
      DF2=A1(1)*A2(3)-A1(3)*A2(1)
      DH1=A1(2)*A2(1)-A1(1)*A2(2)
      F2I=F2I-DF2/DEN
      H1I=H1I-DH1/DEN
      GO TO 50
   70 F2I=SF2(1)
      H1I=SH1(1)
C
C     IF THE CONVERGED SOLUTION OF THE OVERALL PROBLEM
C     IS OBTAINED,PUNCH THE DATA OF THE BOUNDARY LAYER
C     PROFILES AT THOSE SPECIFIED XI-LEVELS OF KOA,KOB,
C     KOC,KOD,AND KOE
C
      DO 72 I=1,M,2
      IE=I-1
      ETA=G*DFLOAT(IE)
      IF (IX .EQ. KOA) GO TO 71
      IF (IX .EQ. KOB) GO TO 71
      IF (IX .EQ. KOC) GO TO 71
      IF (IX .EQ. KOD) GO TO 71
      IF (IX .EQ. KOE) GO TO 71
      GO TO 72
   71 IF (KO .EQ. 1) GO TO 73
      WRITE (6,200) IX,GXI(IX),XI(IX)
  200 FORMAT (' IX=',I4,'  GXI=',D23.16,' XI=' D23.16)
      WRITE (6,203)
  203 FORMAT('0           ETA',8X,'F',14X,'F1',13X,
     1'F2',13X,'H',14X,'H1')
      TEMP=SH(I)
      VELO=SF1(I)
      W=SNGL(TEMP)
      U=SNGL(VELO)
      YS=SNGL(ETA)
      WRITE (7,204) U,W,YS
  204 FORMAT (' ',3E13.6)
      WRITE (6,205)  ETA,SF(I),SF1(I),SF2(I),SH(I),
     1SH1(I)
  205 FORMAT (' ',4X,F10.4,5E15.8)
```

```
 72 CONTINUE
    WRITE (6,206) ERROR,ERRAT,AERRDI
206 FORMAT(' ERROR=',D23.16,' ERRAT= ',D23.16,
   1' AERRDI= ',D23.16)
 73 DO 74 I=1,M
    SF1MI2(I)=SF1MI1(I)
    SFOMI2(I)=SFOMI1(I)
    SH1MI2(I)=SH1MI1(I)
    SHOMI2(I)=SHOMI1(I)
    SF1MI1(I)=SF1(I)
    SFOMI1(I)=SF(I)
    SH1MI1(I)=SH1(I)
    SHOMI1(I)=SH(I)
 74 CONTINUE
    RETURN
    END
```

```
C
C
C      FUNCTION SUBROUTINE OF EQUATION OF MOTION AND ITS
C      PERTURBATION EQUATION(J>1) AT THE FIRST XI-LEVEL
C
C
       SUBROUTINE   VI(V,FF2,FF1,FF,HH1,HH)
       REAL*8 FF2,FF1,FF,HH1,HH,V
       REAL*8 SF2(251),SF1(251),SF(251),SH1(251),SH(251),
      1SFOMI1(251),SF1MI1(251),SHOMI1(251),SH1MI1(251),
      2SFOMI2(251),SF1MI2(251),SHOMI2(251),SH1MI2(251),
      3GXI(100),XI(100),AC,BC,CC,DC,EC,FC,GC,HC,PR
       COMMON SF2,SF1,SF,SH1,SH,SFOMI1,SF1MI1,SHOMI1,
      1SH1MI1,SFOMI2,SF1MI2,SHOMI2,SH1MI2,PR,AC,BC,CC,
      2DC,EC,FC,GC,HC,GXI,XI,IX,I,J,KO,KOA,KOB,KOC,
      3KOD,KOE
       IF (J .GT. 1) GO TO 81
       V=(AC*FF1*FF1-FF2*FF)/PR-HH
       RETURN
   81  V=(BC*FF1*SF1(I)-FF2*SF(I)-FF*SF2(I))/PR-HH
       RETURN
       END
```

```
C
C
C      FUNCTION SUBROUTINE OF ENERGY EQUATION AND ITS
C      PERTURBATION EQUATION(J>1) AT THE FIRST XI-LEVEL
C
C
       SUBROUTINE   TI(T,FF2,FF1,FF,HH1,HH)
       REAL*8 FF2,FF1,FF,HH1,HH,T
       REAL*8 SF2(251),SF1(251),SF(251),SH1(251),SH(251),
      1SFOMI1(251),SF1MI1(251),SHOMI1(251),SH1MI1(251),
      2SFOMI2(251),SF1MI2(251),SHOMI2(251),SH1MI2(251),
      3GXI(100),XI(100),AC,BC,CC,DC,EC,FC,GC,HC,PR
       COMMON SF2,SF1,SF,SH1,SH,SFOMI1,SF1MI1,SHOMI1,
      1SH1MI1,SFOMI2,SF1MI2,SHOMI2,SH1MI2,PR,AC,BC,CC,
      2DC,EC,FC,GC,HC,GXI,XI,IX,I,J,KO,KOA,KOB,KOC,
      3KOD,KOE
       IF (J .GT. 1) GO TO 82
       T=-FF*HH1
       RETURN
   82  T=-FF*SH1(I)-HH1*SF(I)
       RETURN
       END
```

```
C
C
C      FUNCTION SUBROUTINE OF EQUATION OF MOTION AND ITS
C      PERTURBATION EQUATION(J>1) AT THE SECOND XI-LEVEL
C
C
       SUBROUTINE  VII(V,FF2,FF1,FF,HH1,HH)
       REAL*8 FF2,FF1,FF,HH1,HH,V
       REAL*8 SF2(251),SF1(251),SF(251),SH1(251),SH(251),
      1SFOMI1(251),SF1MI1(251),SHOMI1(251),SH1MI1(251),
      2SFOMI2(251),SF1MI2(251),SHOMI2(251),SH1MI2(251),
      3GXI(100),XI(100),AC,BC,CC,DC,EC,FC,GC,HC,PR
       COMMON SF2,SF1,SF,SH1,SH,SFOMI1,SF1MI1,SHOMI1,
      1SH1MI1,SFOMI2,SF1MI2,SHOMI2,SH1MI2,PR,AC,BC,CC,
      2DC,EC,FC,GC,HC,GXI,XI,IX,I,J,KO,KOA,KOB,KOC,
      3KOD,KOE
       IF (J .GT. 1) GO TO 83
       V=AC*FF1*FF1-BC*FF*FF2+CC*(SFOMI1(I)*FF2
      1-SF1MI1(I)*FF1)-DC*HH
       RETURN
   83  V=EC*FF1*SF1(I)-BC*(FF*SF2(I)+FF2*SF(I))+CC
      1*(SFOMI1(I)*FF2-SF1MI1(I)*FF1)-DC*HH
       RETURN
       END
```

```
C
C
C      FUNCTION SUBROUTINE OF ENERGY EQUATION AND ITS
C      PERTURBATION EQUATION(J>1) AT THE SECOND XI-LEVEL
C
C
       SUBROUTINE  TII(T,FF2,FF1,FF,HH1,HH)
       REAL*8 FF2,FF1,FF,HH1,HH,T
       REAL*8 SF2(251),SF1(251),SF(251),SH1(251),SH(251),
      1SFOMI1(251),SF1MI1(251),SHOMI1(251),SH1MI1(251),
      2SFOMI2(251),SF1MI2(251),SHOMI2(251),SH1MI2(251),
      3GXI(100),XI(100),AC,BC,CC,DC,EC,FC,GC,HC,PR
       COMMON SF2,SF1,SF,SH1,SH,SFOMI1,SF1MI1,SHOMI1,
      1SH1MI1,SFOMI2,SF1MI2,SHOMI2,SH1MI2,PR,AC,BC,CC,
      2DC,EC,FC,GC,HC,GXI,XI,IX,I,J,KO,KOA,KOB,KOC,
      3KOD,KOE
       IF (J .GT. 1) GO TO 84
       T=FC*FF1*HH-GC*FF*HH1+HC*(SFOMI1(I)*HH1
      1-SHOMI1(I)*FF1)
       RETURN
   84  T=FC*(FF1*SH(I)+HH*SF1(I))-GC*(HH1*SF(I)+FF
      1*SH1(I))+HC*(SFOMI1(I)*HH1-SHOMI1(I)*FF1)
       RETURN
       END
```

```
C
C
C      FUNCTION SUBROUTINE OF EQUATION OF MOTION AND ITS
C      PERTURBATION EQUATION(J>1) AT THE I-TH XI-LEVEL
C      WHERE I>2
C
C
       SUBROUTINE VIII(V,FF2,FF1,FF,HH1,HH)
       REAL*8 FF2,FF1,FF,HH1,HH,V
       REAL*8 SF2(251),SF1(251),SF(251),SH1(251),SH(251),
      1SFOMI1(251),SF1MI1(251),SHOMI1(251),SH1MI1(251),
      2SFOMI2(251),SF1MI2(251),SHOMI2(251),SH1MI2(251),
      3GXI(100),XI(100),AC,BC,CC,DC,EC,FC,GC,HC,PR
       COMMON SF2,SF1,SF,SH1,SH,SFOMI1,SF1MI1,SHOMI1,
      1SH1MI1,SFOMI2,SF1MI2,SHOMI2,SH1MI2,PR,AC,BC,CC,
      2DC,EC,FC,GC,HC,GXI,XI,IX,I,J,KO,KOA,KOB,KOC,
      3KOD,KOE
       IF (J .GT. 1) GO TO 85
       V=AC*FF1*FF1-(BC*(FF1*(4.0D0*SF1MI1(I)-SF1MI2(I))
      1+FF2*(3.0D0*FF-4.0D0*SFOMI1(I)+SFOMI2(I)))
      2+FF*FF2)/PR-CC*HH
       RETURN
   85  V=DC*FF1*SF1(I)-(BC*(FF1*(4.0D0*SF1MI1(I)
      1-SF1MI2(I))+FF2*(3.0D0*SF(I)-4.0D0*SFOMI1(I)
      2+SFOMI2(I))+3.0D0*FF*SF2(I))+SF(I)*FF2+FF*SF2(I))
      3/PR-CC*HH
       RETURN
       END
```

```
C
C
C      FUNCTION SUBROUTINE OF ENERGY EQUATION AND ITS
C      PERTURBATION EQUATION(J>1) AT THE I-TH XI-LEVEL
C      WHERE I>2
C
C
       SUBROUTINE TIII(T,FF2,FF1,FF,HH1,HH)
       REAL*8 FF2,FF1,FF,HH1,HH,T
       REAL*8 SF2(251),SF1(251),SF(251),SH1(251),SH(251),
      1SFOMI1(251),SF1MI1(251),SHOMI1(251),SH1MI1(251),
      2SFOMI2(251),SF1MI2(251),SHOMI2(251),SH1MI2(251),
      3GXI(100),XI(100),AC,BC,CC,DC,EC,FC,GC,HC,PR
       COMMON SF2,SF1,SF,SH1,SH,SFOMI1,SF1MI1,SHOMI1,
      1SH1MI1,SFOMI2,SF1MI2,SHOMI2,SH1MI2,PR,AC,BC,CC,
      2DC,EC,FC,GC,HC,GXI,XI,IX,I,J,KO,KOA,KOB,KOC,
      3KOD,KOE
       IF (J .GT. 1) GO TO 86
       T=EC*FF1*HH-FF*HH1+BC*(FF1*(3.0D0*HH-4.0D0
      1*SHOMI1(I)+SHOMI2(I))-HH1*(3.0D0*FF-4.0D0
      2*SFOMI1(I)+SFOMI2(I)))
       RETURN
    86 T=EC*(FF1*SH(I)+HH*SF1(I))-FF*SH1(I)-HH1*SF(I)
      1+BC*(FF1*(3.0D0*SH(I)-4.0D0*SHOMI1(I)+SHOMI2(I))
      2+3.0D0*HH*SF1(I)-HH1*(3.0D0*SF(I)-4.0D0*SFOMI1(I)
      3+SFOMI2(I))-3.0D0*FF*SH1(I))
       RETURN
       END
```